

Establishment of an *in vitro* test strategy for
orally inhaled drug products

Dissertation
zur Erlangung des Grades
des Doktors der Naturwissenschaften
der Naturwissenschaftlich-Technischen Fakultät
der Universität des Saarlandes

von

Julia Katharina Metz

Saarbrücken

2021

Tag des Kolloquiums: 24. September 2021

Dekan: Prof. Dr. Jörn Erik Walter

Berichterstatter: Prof. Dr. Claus-Michael Lehr
Prof. Dr. Marc Schneider

Vorsitz: Prof. Dr. Rolf W. Hartmann

Akad. Mitarbeiter: Dr. Britta Diesel

Die vorliegende Arbeit entstand im Zeitraum von Mai 2017 bis April 2021 unter Anregung und Anleitung von Herrn Prof. Dr. Claus-Michael Lehr am Lehrstuhl für Biopharmazie und Pharmazeutische Technologie an der Universität des Saarlandes in Kooperation mit der PharmBioTec Research & Development GmbH, Abteilung Drug Delivery.

Für meine Familie

∞

“What I tell everyone, and I really do for myself is, I have a long-run dream, which is I want to work on stuff that I think matters.”

Sheryl Sandberg, Facebook executive, author, and activist

Table of Content

I Summary	VII
II Zusammenfassung.....	VIII
III Index of Abbreviations	IX
1 Introduction	1
1.1 Overview of the most common lung diseases	1
1.2 Development of orally inhaled drug formulations	2
1.3 Regulatory requirements for safety assessment for pharmaceuticals and chemicals	5
1.4 <i>In vitro</i> systems for orally inhaled drug products in research and industry	9
References	16
2 Aims of the thesis	23
3 Major outcomes of the thesis – Extended summary	24
4 Results: Original publications	27
4.1 Combining MucilAir™ and Vitrocell® Powder Chamber for the In Vitro Evaluation of Nasal Ointments in the Context of Aerosolized Pollen.....	27
4.2 Safety Assessment of Excipients (SAFE) for Orally Inhaled Drug Products	40
4.3 Modulating the Barrier Function of Human Alveolar Epithelial (hAELVi) Cell Monolayers as a Model of Inflammation	69
5. Discussion.....	93
5.1 Complexity of an <i>in vitro</i> system has (still) no influence on an officially accepted alternative method	93
5.2 An AOP-based approach is the most reliable way to perform an <i>in vitro</i> safety assessment	95
References	98
6 Conclusion and Perspectives	100
7 Scientific Output.....	102
8 Curriculum Vitae	104
9 Acknowledgments	105

I Summary

This thesis describes and evaluates three animal experiment free approaches for the safety and efficacy assessment of pulmonary drug formulation in the pre-clinical phase.

In the first approach the complex cell culture system MucilAir™ was exposed to pollen through the Vitrocell® Powder Chamber to simulate *in vitro* an allergic reaction and predict drug safety. However, cytokine response was not sufficient, and the setup has to be optimized for safety studies. Two *in vitro* setups were further developed for estimating drug safety and inflammatory response. For safety studies, an *in vitro* model should predict human data by using approved FDA excipient concentrations. From these excipients the *in vitro* IC50 was determined with pulmonary cell lines and ranked in the thus established SAFE classification. Consequently, SAFE allows for predicting human safety data by *in vitro* testing.

For estimating potential inflammatory reactions located in the respiratory area, the alveolar cell line hAELVi was exposed to the pro-inflammatory cytokines TNF- α and IFN- γ . Similar to an inflammatory *in vivo* reaction, a loss of epithelial barrier function was observed. Furthermore, the anti-inflammatory response to hydrocortisone of the stimulated model underlines its potential for *in vitro* drug testing.

The described *in vitro* models are a promising tool for replacing animal experiments, whereby their standardization and validation are future challenges according to recognized guidelines.

II Zusammenfassung

Diese Arbeit beschreibt und bewertet drei tierversuchsfreie Ansätze zur Sicherheits- und Wirksamkeitsbewertung von Inhalativa in der präklinischen Phase.

Im ersten Ansatz wurde das Zellsystem MucilAir™ durch die Vitrocell® Powder Chamber Pollen ausgesetzt, um *in vitro* eine allergische Reaktion zu simulieren. Die Zytokinreaktion war jedoch nicht ausreichend und der Aufbau muss für Sicherheitsstudien optimiert werden. Folglich wurden zwei *in vitro* Modelle entwickelt, um die Arzneimittelsicherheit und Entzündungsreaktion abzuschätzen. Für eine Sicherheitsbewertung sollte ein *in vitro* Modell Humandaten unter Verwendung von FDA-Hilfsstoffkonzentrationen vorhersagen. Aus diesen Hilfsstoffen wurde der *in vitro* IC50 Wert für Lungenzellen bestimmt und in die etablierte *SAFE*-Klassifikation eingestuft. *SAFE* ermöglicht so die Vorhersage von Humandaten durch *in vitro* Tests. Zur Bewertung von Entzündungen wurden hAELVi Zellen den Zytokinen TNF- α und IFN- γ ausgesetzt. Ähnlich wie bei einer entzündlichen *in vivo* Reaktion wurde ein Verlust der epithelialen Barrierefunktion beobachtet. Darüber hinaus unterstreicht die entzündungshemmende Reaktion des Modells auf Hydrocortison sein Potenzial für eine *in vitro* Sicherheitsbewertungen von potenziellen Wirkstoffen.

Die etablierten *in vitro* Modelle bieten einen vielversprechenden Ansatz, um Tierversuche zu ersetzen, wobei ihre Standardisierung und Validierung künftige Herausforderungen zur Aufnahme in anerkannten Richtlinien darstellen.

III Index of Abbreviations

ADME	Absorption, distribution, metabolism, excretion
ALI	Air liquid interface
ALI	Acute Lung Injury
AM	Alveolar macrophages
AO	Adverse outcome
AOP	Adverse outcome pathway
API	Active pharmaceutical ingredient
ARDS	Acute Respiratory Distress Syndrome
AT1	Pulmonary alveolar type I cell
AT2	Pulmonary alveolar type II cell
BaP	Benzopyrene
BASC	Bronchoalveolar stem cells
BMC	Benchmark concentration
CBF	Cilia beating frequency
CFD	Computational fluid dynamics
CLSM	Confocal laser scanning microscope
COPD	Chronical obstructive pulmonary disease
COVID-19	Coronavirus Disease 2019
CRO	Contract research organisation
CTA	Clinical trial application
DPI	Dry powder inhaler
DPRA	Direct Peptide Reactivity Assay
DSMZ	German Collection of Microorganisms and Cell Cultures GmbH
EC	European Commission
ECHA	European Chemical Agency
EURL ECVAM	European Union Reference Laboratory for alternatives to animal testing
EMA	European medicines Agency
ERS	European Respiratory Society
EU	European Union
FDA	U.S. Food and Drug Administration
GHS	Globally Harmonized System of Classification, Labelling and Packaging of Chemicals
GIVIMP	Guidance Document on Good In Vitro Method Practices
GLP	Good-Laboratory-Practice
GMP	Good Manufacturing Practice
GOLD	Global Initiative for Chronic Obstructive Lung Disease
hAELVi	human Alveolar Epithelial Lentivirus immortalized
hAEpC	Human alveolar primary cells
HPMEC	Human pulmonary microvascular endothelial cells
HC	Hydrocortisone
hPSC	Human pluripotent stem cells
IC50	Half maximal inhibitory concentration
ICCVAM	Interagency Coordinating Committee on the Validation of Alternative Methods
ICH	International Council for Harmonisation of Technical Requirements for Pharmaceuticals for Human Use

IL-6	Interleukin-6
IL-8	Interleukin-8
IND	Investigational new drug
INF-γ	Interferon gamma
IVIVC	<i>in vitro-in vivo</i> correlation
KE	Key event
LLI	Liquid-liquid interface
LLNA	Local lymph node assay
LOAEC	Lowest observed adverse effect concentration
LOAEL	Lowest observed adverse effect level
LPS	Lipopolysaccharides
MDI	Metered dose inhaler
MDM	Monocyte derived macrophages
MIE	Molecular initiating event
MTT	3-(4,5-dimethylthiazol-2-yl)-2,5-diphenyltetrazolium bromide
NDA	New drug application
NICEATM	Interagency Center for the Evaluation of Alternative Toxicological Methods
No.	Number
NOAEC	No observed adverse effect concentration
NOAEL	No observed adverse effect level
NP	Nanoparticle
NTP	National Toxicology Program
OECD	Organization for Economic Co-operation and Development
PADDOCC	Pharmaceutical Aerosol Deposition Device on Cell Cultures
PAHs	Polycyclic aromatic hydrocarbons
P_{app}	Apparent Permeability
PBPK	Physiologically- based pharmacokinetic
QSAR	Quantitative Structure-Activity Relationship
REACH	Registration, Evaluation, Authorisation and Restriction of Chemicals
SAAOP	Society for the Advancement of Adverse Outcome Pathways
SAFE	Safety Assessment of Excipients
SEM	Scanning electron microscopy
SPECT	Single-photon emission computed tomography
TEER	Transepithelial electrical resistance
TG	Test guideline
TIMES	Tissue metabolism simulator
TNF-α	Tumor necrosis factor alpha
US	United States
VPC	Vitrocell® Powder Chamber
WHO	World Health Organization

1 Introduction

State of the art - lung *in vitro* tools applied in research and industry

1.1 Overview of the most common lung diseases

According to the World Health Organisation (WHO) chronic obstructive pulmonary disease and lower respiratory infections occupied 3rd and 4th place, respectively, of the most common causes of death worldwide.¹ The lethality of patients suffering from lung diseases will rise in the future due to the COVID-19 pandemic.² The most relevant lung disorders are summarized in Figure 1, divided into four main categories: 1) acute lung diseases e.g., pneumonia and influenza; 2) chronic inflammatory diseases, e.g. chronic obstructive pulmonary disease (COPD) and asthma; 3) occupational lung disorders, such as various forms of lung fibrosis, and 4) parenchymal lung diseases, mostly related to immune disorders.³

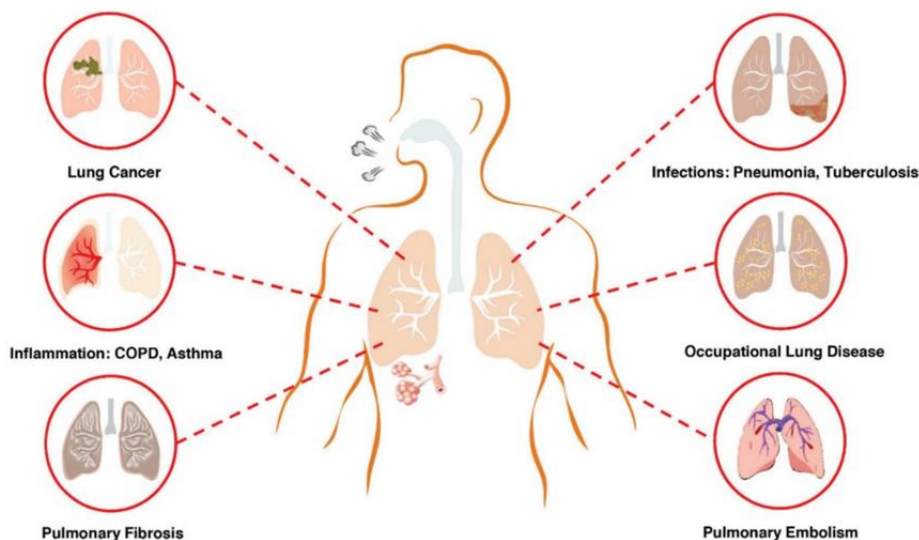


Figure 1: Overview of the most common lung diseases.

Lung diseases can be categorized into four main classes according to the lung region affected. The main categories of adult lung diseases are 1) acute diseases, e.g., pneumonia, influenza after infections; 2) chronic inflammatory diseases, e.g., chronic obstructive pulmonary disease (COPD), asthma; 3) occupational lung disorders, e.g., pulmonary fibrosis, and 4) parenchymal lung diseases, e.g., immune-related lung diseases. Other classes are lung cancer, tuberculosis, and various subtypes of pneumonia.^{3,4} Reprinted from: Shrestha et al. 'Lung-on-a-chip: the future of respiratory disease models and pharmacological studies', copyright © 2020 critical reviews in biotechnology, Taylor & Francis.

Chronic lung complications are a cause of underlying diseases mostly because of previous acute lung failures such as infections.⁵ Chronic lung conditions such as asthma and COPD are mainly triggered by allergies and an increased inflammatory response due to air contaminations, e.g. cigarette smoke and noxious gases.^{6,7} Acute lung diseases such as pneumonia are caused by lower respiratory tract infections of bacteria or viruses⁸ resulting mostly in acute lung injury (ALI) or acute respiratory distress syndrome (ARDS) depending on the symptom severity.^{9–11}

This diversity of lung diseases leads to an enormous range of treatment options. For example, in the 'Guidelines for the management of adult lower respiratory tract infections' the European Respiratory Society (ERS) listed various antibiotic treatment options, e.g., amoxicillin or tetracyclines, depending on the degree and type of infection and recommended that vaccination is suitable for risk prevention.¹² The Global Initiative for Chronic Obstructive Lung Disease (GOLD) compiled a list with medical formulations and typical doses for the pharmacological treatment of COPD. Next to inhalable corticosteroids, anticholinergics, beta₂-agonists, and various combinations can be applied via metered dose inhaler (MDI) or dry powder inhaler (DPI) to COPD patients.^{13,14}

Apart from these classic pharmacological treatments, innovative therapies, especially for the cure of ARDS due to the spread of COVID-19, are on their way for regulatory approval. At the end of 2019, Silva *et al.* discussed that personalized medicine can offer targeted therapies including coordinated treatments for the individual patient's biochemical and physiological reconstitution during ARDS.¹⁵ In addition, cell therapies with (embryonic) stem cells promise *in vivo* a reconstitution of damaged lung epithelial cells during ALI/ARDS and innovative gene therapies can influence protein expression responsible for the regulation of inflammatory signalling pathways.¹⁶ A lot of active pharmaceutical ingredients (API) with potential ARDS treatment options are currently in the pre-clinical phase of drug development. Examples of such APIs are common anti-coagulants with effects against vascular dysfunction, immunomodulatory pleiotropic and pathway specific consequences (e.g., Elafin and anti-INF- γ therapies), and anti-viral agents such as Remdisivir and Favipiravir which have been heavily promoted in their development process as treatment for ARDS during the COVID-19 pandemic in 2020.¹⁷ A further example for an innovative ARDS treatment is the hormone therapy based on PEG-adrenomedullin submitted as an orphan drug approval by Bayer AG Pharmaceuticals with indication for ARDS in clinical phase II.^{18,19} These drug developments and approvals are essential for new therapeutic options to treat the above-mentioned lung diseases. Nevertheless, only a few drug candidates pass the long and financially risky drug development process to achieve official approval.²⁰ The reasons for the high failure rate are described in the following section.

1.2 Development of orally inhaled drug formulations

As soon as a potent drug candidate has been identified, several development phases must be passed through. Often, the development process starts with a chemical optimization of the ac-

tive substance molecule, which serves to improve the physicochemical and biological characteristics to achieve an increased efficacy (lead compound optimization).²¹ In the pre-clinical phase the targeted compound is tested mainly in short-and long term animal studies for toxicology and disease-modifying effects.²² A first goal of this testing is the identification of the no-observed-adverse-effect levels (NOAELs) which specify the initial dose for starting the clinical phase I.^{22,23} If there are no safety concerns after the pre-clinical phase, the developing company can submit an approval for investigatory new drug (IND) to the US Food and drug administration (FDA) or clinical trial application (CTA) by the European Medicines Agency (EMA).²⁴ After authorisation has been obtained from the IND or CTA, respectively, the clinical trials start. With an increasing number of participants in the clinical phase, the safety and efficacy of the IND is evaluated in humans until the data situation allows for the preparation of a new drug application (NDA) which is then sent to the FDA or EMA. An independent advisory committee of the agency will discuss the results of the NDA and decide if the drug promises good treatment options for the patients.^{23,25} During the final drug approval phase in Europe the different national committees can sometimes also be involved in the ultimate approval decision.²⁵ Occasionally, the regular drug approval process can be accelerated due an emergency, like during the COVID-19 pandemic, where the BioNTech/Pfizer vaccine received approval after 10 months, compared to an average of 15 years or longer in the regular approval process.²⁶ Moreover, drug approval processes can be changed when it comes to the approval of orphan drugs including a reduced clinical phase II in 4 years compared to 6 years for standard approvals.^{25,27,28} Figure 2 summarizes the drug development process which must be passed for a final FDA approval.

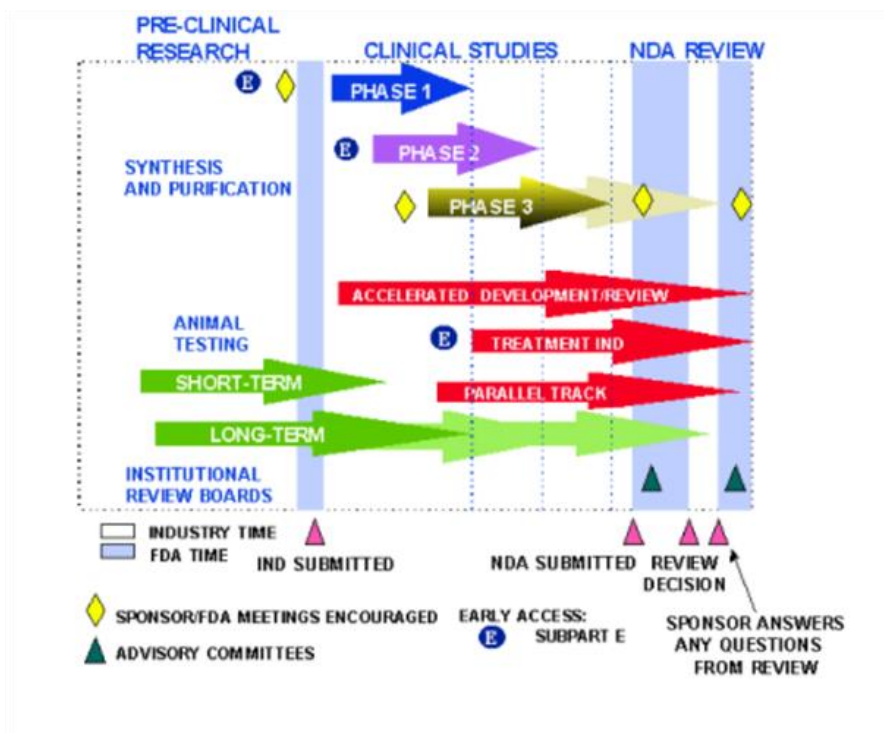


Figure 2: Overview of the drug development and approval process of new drugs by the FDA.

An investigational new drug (IND) undergoes during their development various phases of pre-clinical research and clinical studies. After a successful synthesis and purification, the IND will be tested in the pre-clinical phase for their efficacy and safety by inter alia short- and long-term animal studies followed by an official IND submission. Passing the three phases of clinical studies, the advisory committees decide for an approval of the drug product.²³ Reprinted from: 'New Drug Development and Review Process', copyright © 2020 FDA homepage, <https://www.fda.gov/drugs/cder-small-business-industry-assistance-sbia/new-drug-development-and-review-process>, accessed 01/03/2021.

A key element during the drug development process is the IND application, which is crucial for the start of clinical studies in humans. It stands to reason that potential safety issues of a new drug should be clarified in advance. This is done in IND enabling studies which cover the pre-clinical safety assessment by a complete description of the pharmacodynamics- and kinetics (ADME properties), safety pharmacology, reproductive and developmental toxicity, as well as genotoxicity studies.²⁹ The FDA provides various forms which must be submitted for IND application. One of the most important forms is the FDA 1571 Title 21, Code of Federal Regulations (CFR) Part 312 including a detailed description of the data situation in the pre-clinical evaluation.^{29–32} To ensure FDA acceptance of the data integrated in an IND application internationally accepted good laboratory and manufacturing practice (GLP/GMP) and quality guidelines from the 'Organisation for Economic Co-operation and Development' (OECD) and the 'International Council for Harmonisation of Technical Requirements for Pharmaceuticals for Human Use' (ICH) should be met.^{33–35}

1.3 Regulatory requirements for safety assessment for pharmaceuticals and chemicals

The ICH, a consortium of key players from regulatory authorities and pharmaceutical industries, has established standards on quality, safety, efficacy, and also provides the multidisciplinary guidelines, all of which help to unify the international drug development process.³⁶ These guidelines ensure that adequate data quality can be guaranteed, which makes a successful drug approval more likely. The ICH guidance document M3 (R2), for example, describes in detail the required data for the pre-clinical evaluation of pharmaceuticals to support subsequent clinical trials.^{37,38} Safety assessments do not only play an essential role during drug approvals, they are also important in the registration and market authorization of chemicals and, consequently, their commercial distribution and industrial processing.³⁹ Sufficient data is important in order to obtain a European market approval for chemicals. Therefore, the European Union's REACH regulation ((EC) 1907/2006) legally regulates the market and safety of chemicals since 2007. According to the slogan: 'no data, no market', chemical manufacturers must provide all necessary data for a detailed safety evaluation for the product that they want to release to the market.⁴⁰ The best way for a uniform evaluation of the product is to adhere to certain guidelines. Relating thereto, the OECD, an international association with 36 member states aiming for the reduction of economic, political, and environmental complications through standardized procedures, is responsible for the development of such guidelines.⁴¹ The internationally accepted OECD guidelines include the (bio)safety assessment of chemicals and the protection of the environment and human health. This collection of guidelines for the testing of chemicals is divided into 5 sections, (1) physical-chemical properties; (2) effects on biotic systems; (3) environmental fate and behaviour; (4) health effects and (5) other test guidelines.⁴² The 4th section of chemical testing, which deals with health effects, is relevant for this dissertation and will be discussed below in more detail. In this selection of guidelines, 80 OECD regulations describe suitable methods for identifying potential health risks of the substances under test. For example, the (acute) toxicity, genotoxicity, neurotoxicity, sensitization and corrosion effects of the test substance are addressed *in vitro* and *in vivo* studies depending on the organ affected.⁴³ Many *in vitro* assays are officially accepted, especially the *in vitro* skin evaluations, such as the skin sensitization test (No. 442 C-E) and the *in vitro* skin irritation test (No. 439), and also many *in vitro* genotoxicity tests, as the mammalian cell micronucleus test (No. 487). However, no *in vitro* method for the inhalative safety assessment is yet recommended by the OECD. Consequently, the required data must be generated by animal experiments. The official guidelines for the applied *in vivo* methods are No. 403, 433 and 436, reporting the acute toxicity, and the

guidelines No. 412 and 413, analysing the sub-acute and sub-chronical effects to the lung after substance exposure (Table 1).

Table 1: OECD Guidelines for the inhalative safety assessment of chemicals performed by *in vivo* studies. TG No.: Test guideline number; LC50: Lethal concentration; GHS: Globally Harmonized System; BMC: Benchmark concentration; NOAEC: No observed adverse effect concentration; LOAEC: Lowest observed adverse effect concentration.

TG No.	Indication	Aim	Instruments	Reference
Acute Toxicity				
403	Acute inhalation toxicity, 4 h	LC50	Inhalation chamber (nose-only, whole-body)	[44]
433	Fixed Concentration Procedure, 4 h	Evident toxicity	Inhalation chamber (head/nose-only, whole-body)	[45]
436	Acute Toxic Class (ATC) method, 4 h	Fixed concentrations, step wise to GHS	Inhalation chamber (head-only, nose-only, snout-only)	[46]
Sub-acute Toxicity				
412	repeated dose inhalation toxicity, 28-day study	quantitative risk assessments BMC, NOAEC, LOAEC	Inhalation chamber (head-only, nose-only, snout-only)	[47]
Sub-chronic Toxicity				
413	sub-chronic inhalation toxicity, 90-day study	quantitative risk assessments BMC, NOAEC, LOAEC	Inhalation chamber (head-only, nose-only, snout-only)	[48]

In order to adequately comply with the law and, thus, ensure safety for humans and the environment, animal experiments cannot be avoided.⁴⁹ Animal experiments are essential, especially for the inhalation safety assessment, because, as mentioned above, no alternative methods are available of yet.⁵⁰

Animal experiments are very expensive, in some cases ethically unacceptable, and they often produce results that are not valid enough to predict potential safety issues in humans.^{51,52} In 2011, 1.3 billion € were spent on animal experiments for the safety assessment of chemicals in total, whereby the acute inhalation toxicity is calculated with 13.85 million € and sub-chronic toxicity studies with 61.95 million €. ⁵³ Next to these considerable costs the predictivity of animal experiments is called into question by numerous studies. Only 71% of two-species studies can predict the human toxicity studies⁵⁴ resulting in a 89% failure rate of new drugs after human clinical trials.⁵¹ Reasons for this low predictivity are physiological differences between the spe-

cies that lead to, among other things, diverse metabolism functions, varied microbiome constitutions, altered gene expression profiles and differently expressed disease phenotypes.⁵⁴ In response to these limitations of animal experiments, the demand for suitable *in vitro* methods is increasing. The preference of animal-free research was expressed for the first time in 1959 by Russel and Burch, who, in their publication ‘The Principles of Humane Experimental Technique’, proclaimed the Three Rs principle to refine, reduce and replace animal experiments.⁵⁵ These principles have not lost their validity, legitimacy and importance to this day and have established themselves as a fundamental ethical concept in science.⁵⁶ As a result of the implementation of the Three Rs principle, Figure 3 highlights the increasing demand of *in vitro* assays in the pharma industry. Goh *et al.* calculated all *in vitro* assays performed in the main three fields genotoxicity, safety pharmacology and ADME of pre-clinical studies from three pharma companies and three contract research organisations (CRO) in the years 1980 to 2013 with the result that the percentage of performed *in vitro* assays in the pharma industry has increased by a remarkable 20% since 2012.⁵⁷

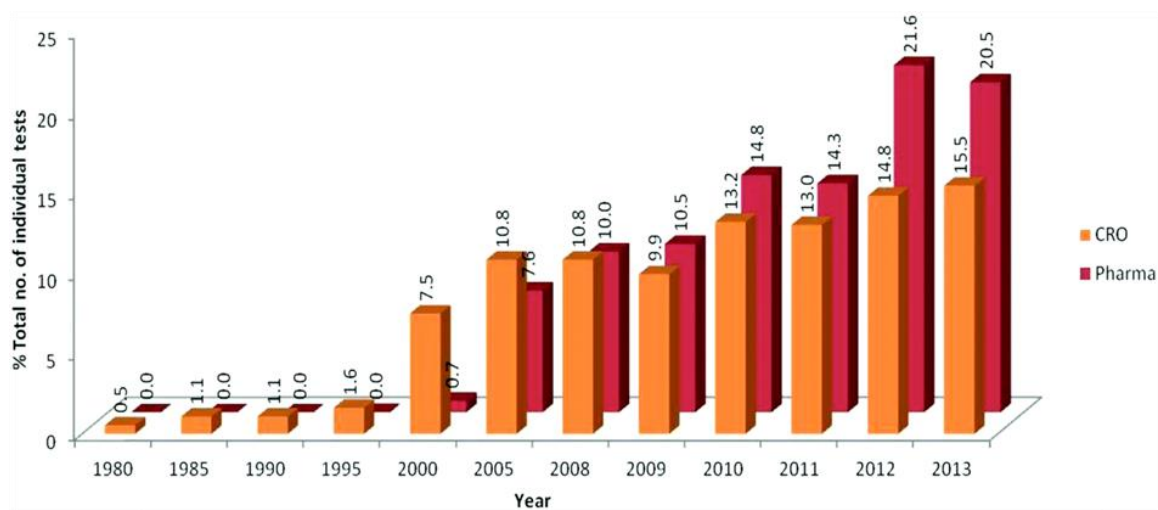


Figure 3: Increasing number of *in vitro* tests from 1980 – 2013 in three CRO (contract research organisations) and three pharma companies. The total amount of performed *in vitro* tests per year was normalised to the amount of all *in vitro* test applied from 1980 – 2013 and multiplied by 100 to obtain the percentage. Reprinted from: Goh *et al.* ‘Development and use of *in vitro* alternatives to animal testing by the pharmaceutical industry 1980-2013’; copyright © 2015 Oxford University Press.⁵⁷

There is also increasing public pressure to reduce animal testing. A prime example of such a successful political implementation is the development of the *in vitro* safety assessment of chemicals, especially for toxicological studies, in the cosmetics industry.⁵⁸ The regulation (EC) No 1223/2009 of the European Parliament and of the Council, which came into force on November 30, 2009, states that animal experiments for testing finished cosmetics are forbidden by law.^{59,60} This law exerts pressure on research and industry to focus on developing alternative methods for testing. On December 12, 2013, the European Union Reference Laboratory for

Alternatives to Animal Testing (EURL ECVAM) recommended the Direct Peptide Reactivity Assay (DPRA) testing to evaluate potential skin sensitizers.⁶¹ The methods for *in vitro* evaluation of skin sensitizer was expanded to the cell-based assays KeratinoSens™, LuSens, h-CLAT, (m)MUSST showing a better predictivity to human data.⁶² Urbisch *et al.* show that *in silico* methods as the QSAR (Quantitative structure–activity relationship) Toolbox and TIMES (tissue metabolism simulator) were more reliable to identify skin sensitizer in comparison to the *in vivo* LLNA (local lymph node assay).⁶³ In 2018, the ECHA (European Chemical Agency) recommended how to use the established *in vitro* skin sensitizing methods within the safety assessment to meet the REACH regulation according the OECD guidelines 442 C-E.⁶⁴ Although the *in vitro* assays for examining the skin sensitizer were successfully established in guidelines, no officially OECD recommendations are available for most other parts of toxicological studies of chemicals such as orally inhaled substances. To steer this development towards the development of applicable animal-free alternatives, the OECD published the 'Guidance Document on Good In Vitro Method Practices (GIVIMP)' in 2018. In these guidelines detailed recommendations regarding the most important aspects of an *in vitro* assay are made, including, for example, quality considerations, devices, test systems and reporting of the results.⁶⁵ These requirements are important to consider during the development of new *in vitro* test systems for the safety assessment of orally inhalable substances and drugs. Following these requirements, an effective and targeted establishment for the development of an officially recognized guideline can succeed. The state of the art in research and industry in developing a valid alternative method for the safety assessment of orally inhaled substances will be summarized below.

1.4 *In vitro* systems for orally inhaled drug products in research and industry

For an *in vitro* simulation of the lungs, countless well-established test systems are available. They differ in their complexity from simple monolayer 2D cultures to mixed cultures (co-cultures), 3D cultures and overly complex co-cultures with more than three cell types. The costs

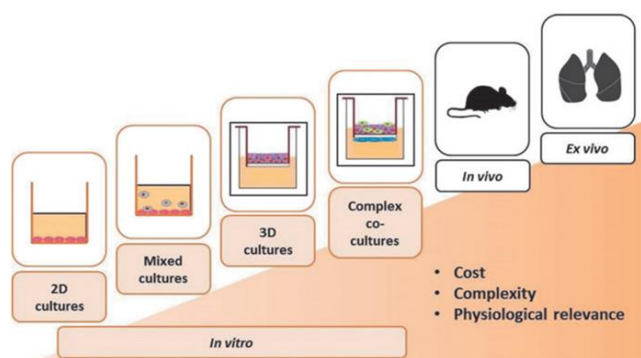


Figure 4: Overview of available *in vitro* models of the respiratory system starting from simple 2D cultures to *ex vivo* models. With the increase in complexity, the costs rise, but also the physiological relevance. Reprinted from Lacroix *et al.* 'Air-Liquid Interface *In Vitro* Models for Respiratory Toxicology Research: Consensus Workshop and Recommendations', copyright 2018 Applied *In Vitro* Toxicology.⁶⁶

of these test systems increase but the physiological relevance grows as well (Figure 4). But none of the test systems is validated under permitted guidelines recommended from the OECD or ICH.⁶⁶ A complete validation of an applicable *in vitro* method implies a successful transfer from research to industry.^{66,67} The coordination of this validation process is carried out by the US Interagency Coordinating Committee on the Validation of Alternative Methods (ICCVAM)⁶⁸ and, for the European Union, by the EURL ECVAM.⁶⁹ In the ECVAM status report from 2019, only two alternatives for respiratory *in vitro* alternatives are reported: 1) the *in vitro* system ALIsens, which should replace the respiratory LLNA assay, and 2) undergoing validation at the time of publication, the EpiAirway™ system, a reconstructed human lung epithelium for detecting acute inhalation toxicity studies.⁷⁰

The question arises why, so far, only a few lung *in vitro* systems and simulations were established in research and industry. The main challenges for the development of *in vitro* methods are the simulation of the human respiratory physiology, the dosimetry of inhaled particles and mechanism of acute toxicity including the adverse outcome pathways (AOP).⁷¹ Figure 5 A describes the airflow of inhaled gas particles, whereby a very abrupt and spontaneous directional change with increased deposition by impaction and sedimentation appears in the upper airways. The mild deposition forms diffusion and electrostatic interaction are present in the alveoli. The flow of inhaled gases depends on the diameter of the airway, in other words, larger airways result in a higher turbulence, and a laminar flow occurs in smaller animals considering the same velocity.^{71,72} Figure 5 B illustrates the concentration of inhaled particles on their way through the respiratory system. The concentration of the particle is decreased stepwise by their interaction with the tissue barriers mucus and epithelial layer and the diffusion and metabolism from the basal cells and the submucosa in the blood. The transport of particles and gas is mainly

dependent on convection, diffusion, absorption, dissolution, and possible chemical reactions.^{71,73}

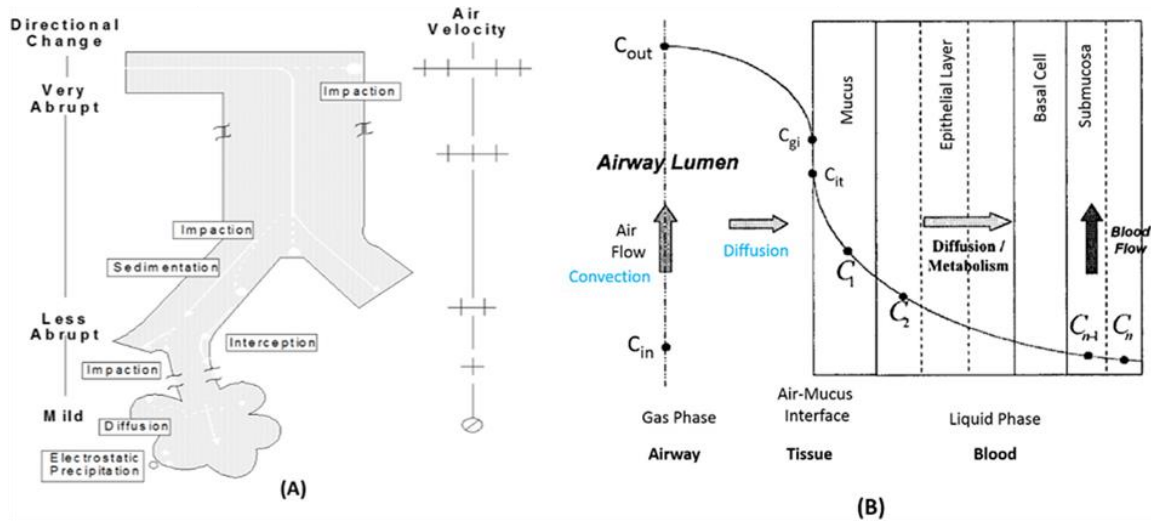


Figure 5: Illustration of complex physiological parameters and deposition mechanisms of potential inhaled substance deposition in the lung. (A) The airflow coming from the upper airways underlies spontaneous direction changes and an increased speed. The particle deposition is mainly characterized by impaction and sedimentation and in the alveoli by diffusion and electrostatic precipitation with mild directional changes at low air velocity. (B) Concentration depended on change of an inhaled chemical in gas phase by passing the sections (Airway, lung tissue, and blood). C_{in} = concentration of inhaled gas, C_{out} = concentration of exhaled gas if no metabolism took place, C_{gi}/C_{it} = concentration of gas at the interface to mucus/epithelial layer, C_1/C_2 = concentration in mucus/epithelial cells, C_{n-1}/C_n = concentration in submucosa/blood. Adapted from: Clippinger et al. 'Alternative approaches for acute inhalation toxicity testing to address global regulatory and non-regulatory data requirements: An international workshop report', copyright © 2018 The Authors. Published by Elsevier Ltd., original published from Bogdanffy et al. 1999 and US EPA 1994.^{71–73}

In addition to the physiological parameters and the deposition mechanism of substances in the alveolar space, the cellular constitution and the interactions of various cell types are also difficult to simulate *in vitro*. The alveolar region consists of two epithelial cell types: alveolar type 1 (AT1) cells which, together with capillary endothelial cells, form the air blood barrier, and alveolar type 2 (AT2), the surfactant producing cells.⁷⁴ In the upper alveoli, the protein as well as mucus producing club (clara cells) and goblet cells are located.⁷⁵ Next to these cells, alveolar macrophages, two types of mast cells, fibroblasts (lipofibroblasts, myofibroblasts, alveolar fibroblasts) are responsible for a functional human alveolus.^{76,77} The lungs of humans and mice differ in their respective number of pulmonary lobes (mice have only one on the left side), and in the constitution of the bronchioalveolar duct junction where mainly club and bronchioalveolar stem cells (BASC, involved in injury-induced cellular plasticity) are present (Figure 6).⁷⁶

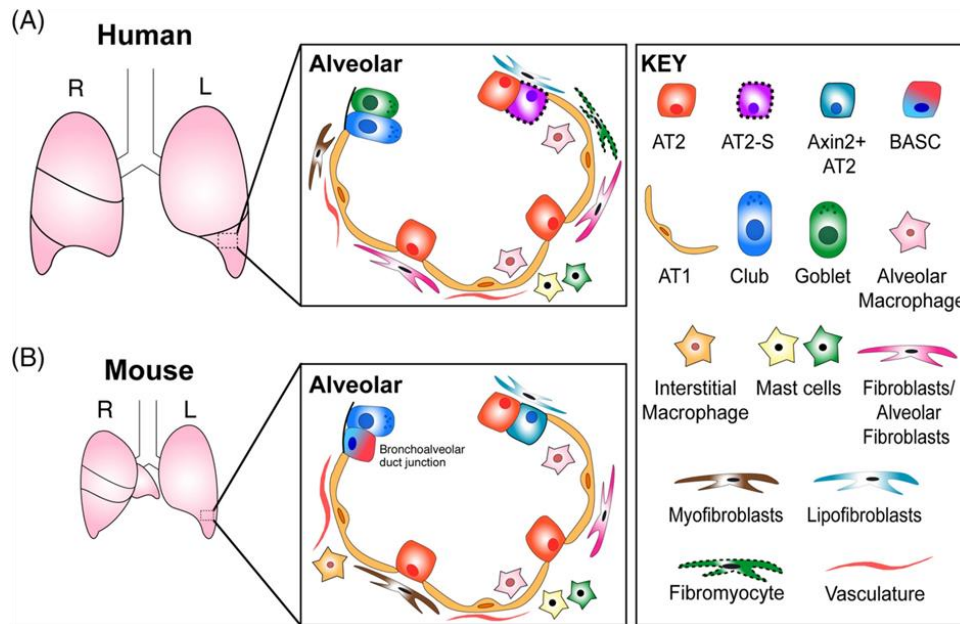


Figure 6: Cellular composition of human (A) and mouse (B) lung with their corresponding cell types.

(A) Structure of human lung. The grown human lung consists of two epithelial cell types: alveolar type 2 (AT2) surfactant producing cells and the alveolar type 1 (AT1) cells which are responsible for the gas exchange, forming the air blood barrier. In the upper alveoli, club and goblet cells are located. Next to these cells, alveolar macrophages, two types of mast cells, fibroblasts (lipofibroblasts, myofibroblasts, alveolar fibroblasts) are responsible for a functional human alveolus. (B) Structure of mouse alveoli. The alveolar region consists of two subsets of AT2 cells (Axin2+ AT2) with high stem cell activity. The epithelium between the bronchioles and the alveoli is named bronchoalveolar duct junction and consist of bronchoalveolar stem cells (BASCs); the basal cells are limited to the trachea and the bronchi. Cells with no complete border are not fully confirmed. Adapted from: Evans and Lee 'Alveolar wars: The rise of *in vitro* models to understand human lung alveolar maintenance, regeneration, and disease', © 2020 The Authors. *STEM CELLS TRANSLATIONAL MEDICINE* published by Wiley Periodicals LLC on behalf of AlphaMed Press.⁷⁶

Despite this challenge of intricacy, *in vitro* lung models have evolved through several stages of development over the past few years. Table 2 summarizes *in vitro* models with increased complexity predominantly of the deep lung area. The list starts with simple monolayer cultures of available epithelial cell lines, like Calu-3, A549, the human alveolar primary cells (hAEPc) with Type II and Type I characteristics and the hAELVi (human alveolar lentivirus immortalized) cells.⁷⁸⁻⁸⁵ However, the predictability for *in vivo* outcomes of frequently used monolayer cells of *in vitro* lung models, especially the simulation of kinetic absorption and permeation, is still up for discussion.⁸⁶ To increase the predictability, epithelial cells can be co- or even triple cultivated with immune cells (THP-1, monocyte derived macrophages (MDM)) and human pulmonary microvascular endothelial cells (HPMEC) to simulate the air-blood barrier.⁸⁷⁻⁹² Because the lung is constituted of many cellular and non-cellular (mucus, surfactant) barriers, whose spatial arrangement is essential for a functioning lung physiology, lung organoids were developed. Organoids are defined as 3D *in vitro* tissue structures simulating a complete *in vivo* organ.^{93,94} Most organoids were cultivated in a Matrigel matrix and are mostly generated from hPSC (human pluripotent stem cells).⁹⁵⁻⁹⁸ The main limitation of organoids is the low standardisation of cell cultivation due to the complicated differentiation protocols with countless

variations, which causes high costs.⁹⁹ Lung-on-a-chip models provide the cell cultivation in a microfluidic device. With a dynamic flow for media transport a simulation of the function and exposure scenarios of the different lung areas is possible depending on the integrated cell types. However, this technology is still in its infancy.^{4,100–102} A further development of complex *in vitro* lung systems are the 3D tissue cultures, which are commercially available, for example from MatTek and Epithelix. These systems include ciliated cells, goblet cells with a mucus layer and basal cells in the variant for the upper airways (MucilAir™, Epithelix) or the lower airways (SmallAir™, Epithelix), mucuciliary epithelium on fibroblasts (EpiAirway, MatTek), or the 3D constitution of alveolar epithelial cells, fibroblasts and alveolar endothelial cells (Epi-Alveolar™, MatTek).^{103–106} The overall advantage of these ready-to-use systems is the high degree of standardization which is demonstrated by their presence in the ECVAM validation process (EpiAirway™) as mentioned above.⁷⁰ Further advantages of these systems are the individual user adaption through various cells (e.g. immune cells), the availability of diseased models as well as the combination with innovative exposure systems.¹⁰⁷ One of the most renowned manufacturers of exposure systems for inhalation toxicology is VITROCELL® Systems. These VITROCELL® devices can expose airborne particles or chemicals (gases, mixtures, NPs) to many formats of cell cultures cultivated in liquid-liquid interface (LLI) or in air-liquid interface (ALI).¹⁰⁸ In 2019, Kooter *et al.* investigated asthma patients' increased sensitivity to copper oxide nanoparticle aerosols using the MucilAir™ (Epithelix) and a VITROCELL® exposure system. They observed a changed response of the model in a diseased state after NP exposure in comparison to the healthy cells by performing a transcriptomic analysis.¹⁰⁹ This experimental set up tries to simulate the particle concentration in the atmosphere more realistically than the calculation of particle concentration in dilution (LLI).¹¹⁰ Nevertheless, there are still limitations to the advanced complex exposure experiments, such as technical restrictions to simulating the highest dose of airborne particles and substances compared with surrounding contaminant concentration.¹¹¹ Future challenges for the standardisation of physiologically relevant exposure systems with ALI cell cultures are the validation of *in vitro* to *in vivo* outcomes, simulation of chronic exposure and the evaluation of the dosimetry (gas versus particles) to identify the exact NOAEL/LOAEL.^{111,112} These challenges were discussed during an international workshop with respiratory toxicology experts in 2018, which evaluated the necessary conditions and set-up for an *in vitro* test system for respiratory safety assessment aiming the ECVAM validation. During the discussion, the main question arose as to which results can be validated to which endpoints regarding, for ex-

ample, respiratory irritation, sensitization, or inflammation. The problem being that no standardisation of the established *in vitro* methods is possible, and, most critically, *in vitro* models are not compared to human clinical data and only correlated to animal data.⁶⁶ Based on these challenges, further experimental approaches and additional data will result from this thesis, which are required for the improvement and optimization of the respiratory *in vitro* models. This contributes to the target achievement of a valid *in vitro* test system and a wide-reaching implementation of the Three Rs principle in research and industry.

Table 2: Examples of *in vitro* systems with increasing complexity, simulating mainly the deep lung area, categorized in monolayer, co-culture, triple-culture, organoids, lung-on-a-chip models and 3D tissue models.

Abbreviations: AT I/AT II: alveolar epithelial cells type I/II; LLC: Liquid-liquid conditions; ALI: Air-liquid conditions, ATCC: American type culture collection; DSMZ: German Collection of Microorganisms and Cell Cultures; PADDOCC: Pharmaceutical Aerosol Deposition Device On Cell Cultures; hAELVi: human alveolar epithelial lentivirus immortalized; hAEpC: human alveolar epithelial cells; hPSCs: human pluripotent stem cells; hPAEC: human Pulmonary Artery Endothelial Cells AM: Alveolar macrophages; MDM: monocyte derived macrophages; MDDC: monocyte derived dendritic cells; NPs: nanoparticles; MWCNTs: Multi-walled carbon nanotubes; FACS: Fluorescence activated cell sorting; PAHs: polycyclic aromatic hydrocarbons; CBF: cilia beating frequency.

	Title of <i>in vitro</i> system	Cultivation/ Exposure system	Short description	Commercially available	Reference
Monolayer	Rat AT I epithelial cells	LLC	Barrier function > 1000 $\Omega \cdot \text{cm}^2$	No	[78]
	Human lung adenoma carcinoma cells A549 (AT II like)	ALI, Transwell™	Endocytic ability, cytochrome P450, permeability of proteins/substances	Yes (ATCC, DSMZ)	[79,80]
	Human alveolar primary cells AT II	LLC	Barrier function > 2000 $\Omega \cdot \text{cm}^2$, permeability	No	[81]
	Human alveolar primary cells AT I	ALI, PADDOCC	Isolated from human lung, Permeability, viability	No	[82]
	hAELVi cells	ALI, Transwell™	Immortalized cell line, barrier properties > 1000 $\Omega \cdot \text{cm}^2$, permeability	Yes (InSCREENex)	[83,84]
	ALI-iAEC2	ALI, Transwell™	Stem cell derived, wound healing, barrier properties > 200 $\Omega \cdot \text{cm}^2$	No	[85]
Co-Culture	Primary rat AT II cells and fibroblasts	LLC, Transwell™	Isolated from rat lung, transport studies	No	[87]
	Primary human alveolar cells (AT I like) + AM	ALI, Transwell™, PADDOCC	Barrier properties < 1000 $\Omega \cdot \text{cm}^2$, deposition NPs, inflammation	No	[88,89]
	hAELVi + THP-1M	ALI, Transwell™, Aeroneb® Lab nebulizer	Permeability, barrier properties > 1000 $\Omega \cdot \text{cm}^2$, cytotox of NPs	No	[90]
Triple-culture	Triple culture A549/ 16HBE14o/ hAEpC + MDM + MDDC	LLC, Transwell™	Comparison to primary cells hAEpC, barrier properties A549 > 200 $\Omega \cdot \text{cm}^2$, 16HBE14o/ hAEpC > 1000 $\Omega \cdot \text{cm}^2$	No	[91]
	NCI-H441 cells + HPMEC-ST1.6R cells + THP-1M	ALI, Transwell™	Permeability, barrier properties < 100 $\Omega \cdot \text{cm}^2$, Inflammation (IL-8)	No	[92]

	Title of <i>in vitro</i> system	Cultivation/ Exposure system	Short description	Commercially available	Reference
Organoids	Generated from hPSCs (lung bud)	Matrigel	Histology, differentiation marker, fluorescence microscopy	No	[⁹⁵]
	Mice AT II, human AT II	Matrigel	Histology, differentiation marker, immunofluorescence, FACS	No	[⁹⁶]
	Human AT II	Matrigel	Histology, differentiation marker, fluorescence microscopy, virus exposition	No	[⁹⁷]
	hPAEC, A549, Calu-3	Culture membrane, ALI	Immunofluorescence, viability, microscopy	No	[⁹⁸]
Lung-on-a-chip	Calu-3	Chip device	Cigarette smoke, Viability, mucus staining, Permeability, inflammation	No	[¹⁰⁰]
	16HBE14o- cells + pHPAEC + pHUVEC	Chip device, dynamic exposure	Permeability, viability, inflammation, immunofluorescence	No	[¹⁰¹]
	Primary hAECs, neutrophils	Chip device, dynamic exposure	Permeability, immunofluorescence, adhesion, SEM/TEM, inflammation, gene expression	No	[¹⁰²]
3D Tissue models	MucilAir™	ALI, Transwell™	PAHs exposure, viability, gene expression, barrier properties $> 500 \Omega \cdot \text{cm}^2$,	Yes (Epithelix)	[¹⁰³]
	SmallAir™	ALI, Transwell™	Histology, CBF, no mucus production, barrier properties $> 300 \Omega \cdot \text{cm}^2$,	Yes (Epithelix)	[¹⁰⁴]
	EpiAirway™	ALI, Transwell™, Vitrocell 12/12 Exposure System	Methyl iodide vapor exposures, viability, GC-MS	Yes (MatTek)	[¹⁰⁵]
	EpiAlveolar™ + MDM	ALI, Transwell™, Vitrocell Cloud	MWCNTs exposure, immunofluorescence, TEM, barrier properties $> 1000 \Omega \cdot \text{cm}^2$, viability, inflammation	Yes (MatTek)	[¹⁰⁶]

References

1. World Health Organization. The top 10 causes of death. 2020. <https://www.who.int/news-room/fact-sheets/detail/the-top-10-causes-of-death>. Accessed January 2, 2021.
2. World Health Organization. WHO reveals leading causes of death and disability worldwide: 2000-2019. 2020. <https://www.who.int/news/item/09-12-2020-who-reveals-leading-causes-of-death-and-disability-worldwide-2000-2019>. Accessed January 3, 2021.
3. Speizer FE, Horton S, Batt J, Slutsky AS. Chapter 35. Respiratory Diseases of Adults. *Dis Control Priorities Dev Ctries (2nd Ed)*. 2006:681-694. doi:10.1596/978-0-8213-6179-5/chpt-35
4. Shrestha J, Razavi Bazaz S, Aboulkheyr Es H, et al. Lung-on-a-chip: the future of respiratory disease models and pharmacological studies. *Crit Rev Biotechnol*. 2020;40(2):213-230. doi:10.1080/07388551.2019.1710458
5. Cookson WOCM, Cox MJ, Moffatt MF. New opportunities for managing acute and chronic lung infections. *Nat Rev Microbiol*. 2018;16(2):111-120. doi:10.1038/nrmicro.2017.122
6. Janssens T, Ritz T. Perceived triggers of asthma: Key to symptom perception and management. *Clin Exp Allergy*. 2013;43(9):1000-1008. doi:10.1111/cea.12138
7. Linden D, Guo-Parke H, Coyle P V., et al. Respiratory viral infection: A potential “missing link” in the pathogenesis of COPD. *Eur Respir Rev*. 2019;28(151):1-14. doi:10.1183/16000617.0063-2018
8. McCracken GH. Etiology and treatment of pneumonia. *Pediatr Infect Dis J*. 2000;19(4):373-377. doi:10.1097/00006454-200004000-00032
9. Villar J, Pérez-Méndez L, Kacmarek RM. Current definitions of acute lung injury and the acute respiratory distress syndrome do not reflect their true severity and outcome. *Intensive Care Med*. 1999;25(9):930-935. doi:10.1007/s001340050984
10. Rezoagli E, Fumagalli R, Bellani G. Definition and epidemiology of acute respiratory distress syndrome. *Ann Transl Med*. 2017;5(14):1-12. doi:10.21037/atm.2017.06.62
11. Johnson ER, Matthay M. Acute Lung Injury: Epidemiology, Pathogenesis, and Treatment. *J Aerosol Med Pulm Drug Deliv*. 2010;23(4):243-252. doi:10.1089=jamp.2009.0775
12. Woodhead M, Blasi F, Ewig S, et al. Guidelines for the management of adult lower respiratory tract infections. *Eur Respir J*. 2005;26(6):1138-1180. doi:10.1183/09031936.05.00055705
13. Vestbo J, Hurd SS, Agustí AG, et al. Global strategy for the diagnosis, management, and prevention of chronic obstructive pulmonary disease GOLD executive summary. *Am J Respir Crit Care Med*. 2013;187(4):347-365. doi:10.1164/rccm.201204-0596PP
14. Vestbo J, Hurd SS, Agusti AG, et al. GOLD 2013 supplement. *Am J Respir Crit Care Med*. 2013;187(4):online supplement.
15. Silva PL, Pelosi P, Rocco PRM. Personalized pharmacological therapy for ARDS: a light at the end of the tunnel. *Expert Opin Investig Drugs*. 2020;29(1):49-61. doi:10.1080/13543784.2020.1699531
16. Qu JM, Zhu YG, Zhang J, Jiang HN, Xu JF. Novel interventional approaches for ALI/ARDS: Cell-based gene therapy. *Mediators Inflamm*. 2011;2011. doi:10.1155/2011/560194
17. Horie S, McNicholas B, Rezoagli E, et al. Emerging pharmacological therapies for ARDS: COVID-19 and beyond. *Intensive Care Med*. 2020;46(12):2265-2283. doi:10.1007/s00134-020-06141-z
18. European Medical Agency. Orphan designation EU/3/20/2301. 2020. <https://www.ema.europa.eu/en/medicines/human/orphan-designations/eu3202301>. Accessed January 3, 2021.
19. Bayer Pharmaceuticals. Development Pipeline. 2020. <https://pharma.bayer.com/development-pipeline>.

Accessed January 3, 2021.

20. Bains W. Failure Rates in Drug Discovery and Development-Will We Ever Get Any Better? *Drug Discov World*. 2004;9-18.
21. Yusof I, Shah F, Hashimoto T, Segall MD, Greene N. Finding the rules for successful drug optimisation. *Drug Discov Today*. 2014;19(5):680-687. doi:10.1016/j.drudis.2014.01.005
22. Lee D, Stein E, Gooneratne N. SBIR/STTR Grants: Introduction and Overview, *Academic Entrepreneurship for Medical and Health Scientists*. 2019, 1 (2): 4. <https://repository.upenn.edu/ace/vol1/iss2/4>
23. Food and Drug Administration. New Drug Development and Review Process. 2020. <https://www.fda.gov/drugs/cder-small-business-industry-assistance-sbia/new-drug-development-and-review-process>. Accessed January 3, 2021.
24. Chiodin D, Cox EM, Edmund A V., Kratz E, Lockwood SH. Regulatory Affairs 101: Introduction to Investigational New Drug Applications and Clinical Trial Applications. *Clin Transl Sci*. 2019;12(4):334-342. doi:10.1111/cts.12635
25. Van Norman GA. Drugs and Devices: Comparison of European and U.S. Approval Processes. *JACC Basic to Transl Sci*. 2016;1(5):399-412. doi:10.1016/j.jacbts.2016.06.003
26. Krammer F. SARS-CoV-2 vaccines in development. *Nature*. 2020;586(7830):516-527. doi:10.1038/s41586-020-2798-3
27. Srivastava G, Winslow A. Orphan Drugs : Understanding the FDA Approval Process. *Acad Entrep Med Heal Sci*. 2019;1(3). <https://repository.upenn.edu/ace/vol1/iss3/13>.
28. Meekings KN, Williams CSM, Arrowsmith JE. Orphan drug development: An economically viable strategy for biopharma R&D. *Drug Discov Today*. 2012;17(13-14):660-664. doi:10.1016/j.drudis.2012.02.005
29. Agarwall V. Complete Guide on IND Enabling Toxicology Studies. 2020. <https://www.nebiolab.com/complete-guide-on-ind-enabling-toxicology-studies/>. Accessed January 5, 2021.
30. Food and Drug Administration. IND Forms and Instructions. 2017. <https://www.fda.gov/drugs/investigational-new-drug-ind-application/ind-forms-and-instructions>. Accessed January 5, 2021.
31. Holbein ME. Understanding FDA Regulatory Requirements for Investigational New Drug Applications for Sponsor-Investigators. *J Investig Med*. 2009;57(6):688-694. doi:10.231/JIM.0b013e3181afdb26
32. FDA. CFR - Code of Federal Regulations Title 21. <http://www.accessdata.fda.gov/scripts/cdrh/cfdocs/cfcr/CFRSearch.cfm?CFRPart=50&showFR=1&subpartNode=21:1.0.1.1.20.2>. Published 2015. Accessed January 5, 2021.
33. Andrade EL, Bento AF, Cavalli J, et al. Non-clinical studies in the process of new drug development - Part II: Good laboratory practice, metabolism, pharmacokinetics, safety and dose translation to clinical studies. *Brazilian J Med Biol Res*. 2016;49(12):e5646. doi:10.1590/1414-431X20165646
34. Administration F and drug. Guidance for Industry Process Validation: General Principles and Practices. 2011. doi:10.1201/9781420035520.ch3
35. International Council for Harmonisation of Technical Requirements for Pharmaceuticals for Human Use. Q7: Good manufacturing practice guide for active pharmaceutical ingredients. *ICH Guidel*. 2000.
36. International Council for Harmonisation of Technical Requirements for Pharmaceuticals for Human Use. ICH Guidelines. 2021. <https://www.ich.org/page/ich-guidelines>. Accessed January 6, 2021.
37. EMEA. Non-clinical Safety Studies for the Conduct of Human Clinical Trials for Pharmaceuticals: ICH M3 and M3(R2). 2013;3(July):299-309. doi:10.1007/978-1-4614-5950-7_14

38. ICH (International Council for Harmonisation of Technical Requirements for Pharmaceuticals for Human Use). ICH Harmonised Tripartite Guideline Pharmaceutical Development Q8(R2). *Int Conf Harmon.* 2009;3(June):1-24.
https://www.ich.org/fileadmin/Public_Web_Site/ICH_Products/Guidelines/Multidisciplinary/M3_R2/Step4/M3_R2__Guideline.pdfhttp://www.ich.org/fileadmin/Public_Web_Site/ICH_Products/CTD/M4E_R2_Efficacy/M4E_R2__Step_4.pdf<http://www.ich.org/fileadmin/Publ>.
39. van Dijk J, Gustavsson M, Dekker SC, van Wezel AP. Towards ‘one substance – one assessment’: An analysis of EU chemical registration and aquatic risk assessment frameworks. *J Environ Manage.* 2020;280(October 2020):111692. doi:10.1016/j.jenvman.2020.111692
40. Umweltbundesamt. REACH Was ist das? 2021.
<https://www.umweltbundesamt.de/themen/chemikalien/reach-chemikalien-reach>. Accessed January 9, 2021.
41. OECD (Organisation for Economic Cooperation and Development). OECD About. 2021.
<https://www.oecd.org/about/>. Accessed January 11, 2021.
42. OECD (Organisation for Economic Cooperation and Development). Test guidelines for chemicals.
<https://www.oecd.org/env/ehs/testing/oecdguidelinesforthetestingofchemicals.htm>. Accessed January 5, 2021.
43. OECD (Organisation for Economic Cooperation and Development). OECD Guidelines for the Testing of Chemicals, Section 4. https://www.oecd-ilibrary.org/environment/oecd-guidelines-for-the-testing-of-chemicals-section-4-health-effects_20745788. Accessed January 9, 2021.
44. OECD (Organisation for Economic Cooperation and Development). Test guidelines 403 acute inhalation toxicity. 2009. doi: 10.1787/9789264070608-en.
45. OECD (Organisation for Economic Cooperation and Development). Test guideline 433 acute inhalation toxicity: fixed concentration procedure. 2018. doi: 10.1787/9789264284166-en
46. OECD (Organisation for Economic Cooperation and Development). Test guideline 436 acute inhalation toxicity - acute toxic class method. 2009. doi: 10.1787/9789264076037-en
47. OECD (Organisation for Economic Cooperation and Development). Test guideline 412 28-day (subacute) inhalation toxicity study. 2018. doi: 10.1787/9789264070783-en
48. OECD (Organisation for Economic Cooperation and Development). Test guideline 413 90-Day subchronic inhalation toxicity study. 2018. doi: 10.1787/9789264070806-en.
49. ECHA. The Use of Alternatives to Testing on Animals for the REACH Regulation. Third Report under Article 117(3) of the REACH Regulation. Vol 117.; 2017.
50. Taylor K, Stengel W, Casalegno C, Andrew D. Experiences of the REACH testing proposals system to reduce animal testing. *ALTEX.* 2014;31(2):107-128. doi:10.14573/altex.1311151
51. Van Norman GA. Limitations of Animal Studies for Predicting Toxicity in Clinical Trials: Is it Time to Rethink Our Current Approach? *JACC Basic to Transl Sci.* 2019;4(7):845-854.
doi:10.1016/j.jacbts.2019.10.008
52. Taylor, Kate. Animal Experimentation: Working Towards a Paradigm Change. *Brill,* 2019; 585-609.
doi:10.1163/9789004391192
53. Meigs L, Smirnova L, Rovida C, Leist M, Hartung T. Animal testing and its alternatives - the most important omics is economics. *ALTEX.* 2018;35(3):275-305. doi:10.14573/altex.1807041
54. Uhl EW, Warner NJ. Mouse Models as Predictors of Human Responses: Evolutionary Medicine. *Curr Pathobiol Rep.* 2015;3(3):219-223. doi:10.1007/s40139-015-0086-y
55. Russell WMS, Burch RL. *The Principles of Humane Experimental Technique.* London: Methuen; 1959.
56. Kirk RGW. Recovering The Principles of Humane Experimental Technique: The 3Rs and the Human

- Essence of Animal Research. *Sci Technol Hum Values*. 2018;43(4):622-648. doi:10.1177/0162243917726579
57. Goh JY, Weaver RJ, Dixon L, Platt NJ, Roberts RA. Development and use of in vitro alternatives to animal testing by the pharmaceutical industry 1980-2013. *Toxicol Res (Camb)*. 2015;4(5):1297-1307. doi:10.1039/c5tx00123d
 58. Taylor K. *Animal Experimentation: Working Towards a Paradigm Change*. Brill; 2019. doi:10.1163/9789004391192
 59. European Commission. Ban on animal testing. https://ec.europa.eu/growth/sectors/cosmetics/animal-testing_en. Published 2021. Accessed January 17, 2021.
 60. European Union. Regulation (EC) No 1223/2009 of the European Parliament and of the Council of 30 November 2009 on cosmetic products. <https://eur-lex.europa.eu/eli/reg/2009/1223/oj>. Published 2009. Accessed January 9, 2021.
 61. Corsini E, Papale A, Galbiati V, Roggen EL. Safety evaluation of cosmetic ingredients: In vitro opportunities for the identification of contact allergens. *Cosmetics*. 2014;1(1):61-74. doi:10.3390/cosmetics1010061
 62. Urbisch D, Mehling A, Guth K, et al. Assessing skin sensitization hazard in mice and men using non-animal test methods. *Regul Toxicol Pharmacol*. 2015;71(2):337-351. doi:10.1016/j.yrtph.2014.12.008
 63. Urbisch D, Honarvar N, Kolle SN, et al. Peptide reactivity associated with skin sensitization: The QSAR Toolbox and TIMES compared to the DPRA. *Toxicol Vitro*. 2016;34:194-203. doi:10.1016/j.tiv.2016.04.005
 64. European Chemicals Agency. How to use new or revised in vitro test methods to address skin sensitisation. 2018;(February):1-11.
 65. OECD (Organisation for Economic Cooperation and Development). Guidance Document on Good In Vitro Method Practices (GIVIMP). 2018;(286). doi:10.1787/9789264304796-en
 66. Lacroix G, Koch W, Ritter D, et al. Air-Liquid Interface in Vitro Models for Respiratory Toxicology Research: Consensus Workshop and Recommendations. *Appl Vitro Toxicol*. 2018;4(2):91-106. doi:10.1089/aivt.2017.0034
 67. Bakand S, Winder C, Khalil C, Hayes A. Toxicity assessment of industrial chemicals and airborne contaminants: Transition from in vivo to in vitro test methods: A review. *Inhal Toxicol*. 2005;17(13):775-787. doi:10.1080/08958370500225240
 68. US Department of human health. About ICCVAM. 2021. <https://ntp.niehs.nih.gov/whatwestudy/niceatm/iccvam/index.html>. Accessed January 17, 2021.
 69. European Commission. EU Reference Laboratory for alternatives to animal testing. <https://ec.europa.eu/jrc/en/eurl/ecvam>. Accessed January 17, 2021.
 70. ECVAM E. - EURL ECVAM Status Report on the Development, Validation and Regulatory Acceptance of Alternative Methods and Approaches.; *Jrc Science for Policy Report* 2019. doi:10.2760/25602
 71. Clippinger AJ, Allen D, Jarabek AM, et al. Alternative approaches for acute inhalation toxicity testing to address global regulatory and non-regulatory data requirements: An international workshop report. *Toxicol Vitro*. 2018;48(October 2017):53-70. doi:10.1016/j.tiv.2017.12.011
 72. U.S. Environmental Protection Agency. Methods for derivation of inhalation reference concentrations and application of inhalation dosimetry. *EPA/600/8-90/066F*, October 1994.
 73. Bogdanffy MS, Sarangapani R, Plowchalk DR, Jarabek A, Andersen ME. A biologically based risk assessment for vinyl acetate-induced cancer and noncancer inhalation toxicity. *Toxicol Sci*. 1999;51(1):19-35. doi:10.1093/toxsci/51.1.19
 74. Wang Y, Tang Z, Huang H, et al. Pulmonary alveolar type I cell population consists of two distinct

- subtypes that differ in cell fate. *Proc Natl Acad Sci U S A*. 2018;115(10):2407-2412. doi:10.1073/pnas.1719474115
75. Rokicki W, Rokicki M, Wojtacha J, Dzeljijli A. The role and importance of club cells (Clara cells) in the pathogenesis of some respiratory diseases. *Kardiochirurgia i Torakochirurgia Pol*. 2016;13(1):26-30. doi:10.5114/kitp.2016.58961
 76. Evans K V., Lee JH. Alveolar wars: The rise of in vitro models to understand human lung alveolar maintenance, regeneration, and disease. *Stem Cells Transl Med*. 2020;9(8):867-881. doi:10.1002/sctm.19-0433
 77. Knudsen L, Ochs M. The micromechanics of lung alveoli: structure and function of surfactant and tissue components. *Histochem Cell Biol*. 2018;150(6):661-676. doi:10.1007/s00418-018-1747-9
 78. Cheek JM, Evans MJ, Crandall ED. Type I cell-like morphology in tight alveolar epithelial monolayers. *Exp Cell Res*. 1989;184(2):375-387. doi:10.1016/0014-4827(89)90337-6
 79. Foster KA, Oster CG, Mayer MM, Avery ML, Audus KL. Characterization of the A549 cell line as a type II pulmonary epithelial cell model for drug metabolism. *Exp Cell Res*. 1998;243(2):359-366. doi:10.1006/excr.1998.4172
 80. Kobayashi S, Shuji K, Juni K. Permeability of Peptides and Proteins in human cultured alveolar A549 cell monolayer. *Pharm Res*. 1995;12(8):1115-1119. <https://doi.org/10.1023/A:1016295406473>
 81. Elbert, Katharina J, Schäfer Ulrich F., Schäfers, Hans-Joachim, Kim, Kwang-Jin, Lehr C-M. Monolayers of human alveolar epithelial cells in primary culture for pulmonary absorption and transport studies. *Pharm Reserach*. 1999;16(5). <https://doi.org/10.1023/A:1018887501927>
 82. Daum N., Kuehn A., Hein S., Schaefer U.F., Huwer H. LC. Isolation, Cultivation, and Application of Human Alveolar Epithelial Cells. *Hum Cell Cult Protoc*. 2012;806. doi:https://doi.org/10.1007/978-1-61779-367-7_3
 83. Kuehn A, Kletting S, De Souza Carvalho-Wodarz C, et al. Human alveolar epithelial cells expressing tight junctions to model the air-blood barrier. *ALTEX*. 2016;33(3):251-260. doi:10.14573/altex.1511131
 84. Inscreenex. Alveolar Epithelial Cells. <https://www.inscreenex.de/products/human-immortalized-cell-lines/alveolar-epithelial-cells-hu.html>. Published 2021. Accessed January 22, 2021.
 85. van Riet S, Ninaber DK, Mikkers HMM, et al. In vitro modelling of alveolar repair at the air-liquid interface using alveolar epithelial cells derived from human induced pluripotent stem cells. *Sci Rep*. 2020;10(1):1-12. doi:10.1038/s41598-020-62226-1
 86. Sakagami M. In vivo, in vitro and ex vivo models to assess pulmonary absorption and disposition of inhaled therapeutics for systemic delivery. *Adv Drug Deliv Rev*. 2006;58(9-10):1030-1060. doi:10.1016/j.addr.2006.07.012
 87. Mangum JB, Everitt JI, Bonner JC, Moore LR, Brody AR. Co-culture of primary pulmonary cells to model alveolar injury and translocation of proteins. *Vitr Cell Dev Biol*. 1990;26(12):1135-1143. doi:10.1007/BF02623690
 88. Hittinger M, Janke J, Huwer H, Scherließ R, Schneider-Daum N, Lehr CM. Autologous co-culture of primary human alveolar macrophages and epithelial cells for investigating aerosol medicines. Part I: Model Characterisation. *ATLA Altern to Lab Anim*. 2016;44(4):337-347. doi:10.1177/026119291604400404
 89. Hittinger M, Mell NA, Huwer H, Loretz B, Schneider-Daum N, Lehr CM. Autologous co-culture of primary human alveolar macrophages and epithelial cells for investigating aerosol medicines. Part II: Evaluation of IL-10-loaded microparticles for the treatment of lung inflammation. *ATLA Altern to Lab Anim*. 2016;44(4):349-360. doi:10.1177/026119291604400405
 90. Kletting S, Barthold S, Repnik U, et al. Co-culture of human alveolar epithelial. 2017:1-11. doi:10.14573/altex.

91. Lehmann AD, Daum N, Bur M, Lehr CM, Gehr P, Rothen-Rutishauser BM. An in vitro triple cell co-culture model with primary cells mimicking the human alveolar epithelial barrier. *Eur J Pharm Biopharm.* 2011;77(3):398-406. doi:10.1016/j.ejpb.2010.10.014
92. Costa A, de Souza Carvalho-Wodarz C, Seabra V, Sarmento B, Lehr CM. Triple co-culture of human alveolar epithelium, endothelium and macrophages for studying the interaction of nanocarriers with the air-blood barrier. *Acta Biomater.* 2019;91(April):235-247. doi:10.1016/j.actbio.2019.04.037
93. De Souza N. Organoids. *Nat Methods.* 2018;15(1):23. doi:10.1038/nmeth.4576
94. Barkauskas CE, Chung MI, Fioret B, Gao X, Katsura H, Hogan BLM. Lung organoids: Current uses and future promise. *Dev.* 2017;144(6):986-997. doi:10.1242/dev.140103
95. Miller AJ, Dye BR, Ferrer-torres D, et al. Generation of lung organoids from human pluripotent stem cells in vitro. *Nat Protoc.* 2019;14(2):518-540. doi:10.1038/s41596-018-0104-8.Generation
96. Barkauskas CE, Cronce MJ, Rackley CR, et al. Type 2 alveolar cells are stem cells in adult lung. *J Clin Invest.* 2013;123(7):3025-3036. doi:10.1172/JCI68782
97. Youk J, Kim T, Evans K V., et al. Three-Dimensional Human Alveolar Stem Cell Culture Models Reveal Infection Response to SARS-CoV-2. *Cell Stem Cell.* 2020;27(6):905-919.e10. doi:10.1016/j.stem.2020.10.004
98. Baptista D, Teixeira LM, Birgani ZT, et al. 3D alveolar in vitro model based on epithelialized biomimetically curved culture membranes. *Biomaterials.* 2021;266 (October 2020). doi:10.1016/j.biomaterials.2020.120436
99. Kim J, Koo BK, Knoblich JA. Human organoids: model systems for human biology and medicine. *Nat Rev Mol Cell Biol.* 2020;21(10):571-584. doi:10.1038/s41580-020-0259-3
100. Shrestha J, Ghadiri M, Shanmugavel M, et al. A rapidly prototyped lung-on-a-chip model using 3D-printed molds. *Organs-on-a-Chip.* 2019;1(January):100001. doi:10.1016/j.ooc.2020.100001
101. Stucki AO, Stucki JD, Hall SRR, et al. A lung-on-a-chip array with an integrated bio-inspired respiration mechanism. *Lab Chip.* 2015;15(5):1302-1310. doi:10.1039/c4lc01252f
102. Benam KH, Villenave R, Lucchesi C, et al. Small airway-on-a-chip enables analysis of human lung inflammation and drug responses in vitro. *Nat Methods.* 2016;13(2):151-157. doi:10.1038/nmeth.3697
103. Cervena T, Vrbova K, Rossnerova A, Topinka J, Rossner P. Short-term and Long-term Exposure of the MucilAir™ Model to Polycyclic Aromatic Hydrocarbons. *Altern Lab Anim.* 2019;47(1):9-18. doi:10.1177/0261192919841484
104. Huang S, Boda B, Vernaz J, Ferreira E, Wiszniewski L, Constant S. Establishment and characterization of an in vitro human small airway model (SmallAir™). *Eur J Pharm Biopharm.* 2017;118:68-72. doi:10.1016/j.ejpb.2016.12.006
105. Mistry A, Bowen LE, Dzierlenga MW, Hartman JK, Slattery SD. Development of an in vitro approach to point-of-contact inhalation toxicity testing of volatile compounds, using organotypic culture and air-liquid interface exposure. *Toxicol Vitro.* 2020;69(July):104968. doi:10.1016/j.tiv.2020.104968
106. Barosova H, Maione AG, Septiadi D, et al. Use of EpiAlveolar Lung Model to Predict Fibrotic Potential of Multiwalled Carbon Nanotubes. *ACS Nano.* 2020;14(4):3941-3956. doi:10.1021/acsnano.9b06860
107. Cao X, Coyle JP, Xiong R, et al. Invited review: human air-liquid-interface organotypic airway tissue models derived from primary tracheobronchial epithelial cells—overview and perspectives. *Vitro Cell Dev Biol - Anim.* 2020. doi:10.1007/s11626-020-00517-7
108. Vitrocell. Exposure systems for inhalation toxicology. <https://www.vitrocell.com/inhalation-toxicology/exposure-systems>. Accessed January 23, 2021.
109. Kooter I, Ilves M, Gröllers-Mulderij M, et al. Molecular Signature of Asthma-Enhanced Sensitivity to CuO Nanoparticle Aerosols from 3D Cell Model. *ACS Nano.* 2019. doi:10.1021/acsnano.9b01823

110. Müller L, Gasser M, Raemy DO, et al. Realistic Exposure Methods for Investigating the Interaction of Nanoparticles with the Lung at the Air-Liquid Interface In Vitro. *Insciences J.* 2011;(May 2014):30-64. doi:10.5640/insc.010130
111. Upadhyay S, Palmberg L. Air-liquid interface: Relevant in vitro models for investigating air pollutant-induced pulmonary toxicity. *Toxicol Sci.* 2018;164(1):21-30. doi:10.1093/toxsci/kfy053
112. Schmid O, Cassee FR. On the pivotal role of dose for particle toxicology and risk assessment: exposure is a poor surrogate for delivered dose. *Part Fibre Toxicol.* 2017;14(1):52. doi:10.1186/s12989-017-0233-1

2 Aims of the thesis

The main goal of this thesis is to establish an *in vitro* test strategy respecting the Three Rs principle to reduce animal experiments in drug development processes in research and industry. Therefore, this dissertation aims at developing an *in vitro* model for safety and efficacy testing of orally inhalable drug products for which no official test guideline is yet available. In addition, this thesis wants to provide an understanding of the advantages and disadvantages of *in vitro* methods with a discussion focused on the acceptance of such models in officially approved guidelines for perspective inhalative therapies. Therefore, a three-step approach is proposed, pursuing three major aims are:

1. The first study combined complex *in vitro* methods which should provide information about the advantages and disadvantages of a more physiological experimental setup. By recognizing possible deficiencies in this initial work, the following studies could be set up more target oriented.
2. In a second study, a more simplified method was able to provide an improved correlation with a human data set focussing on acute toxicity. By obtaining valuable results, an *in vitro* classification system for approved excipients was established.
3. As a final study, the inflammatory reactions of the alveolar epithelium could be simulated by a simplified experimental set-up. This inflammation model can be used for the *in vitro* testing of not currently approved anti-inflammatory/inflammatory substances and drug products in future.

3 Major outcomes of the thesis – Extended summary

This thesis aims at establishing a suitable *in vitro* test strategy based on various approaches, which can be standardized and be valid enough to support prospective guidelines.

Therefore, the first approach attempts to simulate a physiological scenario *in vitro* using a more complex experimental design. In addition, an ointment formulation was applied to investigate if the test system can be used to evaluate an anti-inflammatory effect. The ointment is intended for reducing pollen exposure by applying it to the human nasal mucosa.

To simulate the physiological exposure *in vitro*, the cell culture system MucilAir™ was used under air-liquid conditions and was placed as an insert in the Vitrocell® Powder Chamber (VPC). The VPC enables the targeted exposure of pollen (*Iva xanthiifolia*) on MucilAir™ which was treated beforehand with the ointment formulation. After exposure, the pollen penetration was determined with the aid of confocal scanning microscopy (CLSM) and the cytokine release of TNF- α , IL-6 and IL-8 was measured.

It turned out that the ointment formulations should be regarded as a protective layer on the MucilAir™ system. Therefore, no increased cytokine release could be measured in comparison to the LPS control.

However, the results of this study could not be compared with *in vivo* data since the cytokine release was not sufficient and no adequate human data sets were available. In addition, the experimental design had disadvantages, such as the undefined amount of exposed pollen, lack of cell viability measurements, the indefinite thickness of the ointment layer on MucilAir™ and the poor quantity of data.

Due to this lack of standardization and validation, the question was considered whether a reduced method complexity in a first evaluation level would be more target oriented. Therefore, in the subsequent study, the focus was only on the cytotoxicity.

The second study presented in this thesis aimed at correlating *in vitro* data to human *in vivo* data based on the cytotoxicity as standalone parameter. Therefore, the safety assessment of excipients (*SAFE*) classification was developed to link data of human epithelial cells to approved FDA concentrations for orally inhaled drug products.

The *SAFE* system includes the *in vitro* calculated IC50 values obtained by a standardised cell viability measurement (MTT assay) after the exposure of 23 excipients to A549 and Calu-3 monolayer cells. The resulting IC50 values were correlated with the approved FDA concentrations of these excipients. A threshold of 0.1% (1 mg/mL) separates four safety classes, which

allows a categorisation by the resulting IC₅₀ values. The hazard potential of a substance increases with the ascending classification class.

The *SAFE* classification provides an opportunity to classify components of potential drug formulations *in vitro* based on the IC₅₀ values. Two aspects can be clarified by applying the *SAFE* approach. On the one hand, potential high toxicity of a substance can be excluded directly before the costly development process starts, and, on the other hand, if future *in vitro* testing is to be preferred, a suitable concentration range can be evaluated in which cell compatibility is ensured. Nevertheless, one single parameter is not sufficient to provide a safety assessment of a drug component. Therefore, the final study extended the test strategy to the inflammatory consequences after substance exposure.

The ongoing COVID-19 pandemic demonstrates how inflammatory lung diseases can dramatically increase over a short period of time. So, in the third and last part of this thesis, an *in vitro* inflammation model was developed to show fast and reliable anti-inflammatory effects of potential drug products to provide treatment options for inflammatory lung diseases relatively quickly, if needed.

For this purpose, a monolayer cell system was developed using an innovative cell line, the human Alveolar Epithelial Lentivirus immortalised (hAELVi) cells. After a stimulation with the pro-inflammatory cytokines TNF- α and IFN- γ , the hAELVi showed typical inflammatory reactions of the epithelium, such as a decreased barrier property indicated by a low transepithelial electrical resistance (TEER) $< 500 \Omega \times \text{cm}^2$ and an increased permeability of the cells with a calculated apparent permeability coefficient (P_{app}) of $9.30 \times 10^{-6} \text{ cm/s}$ by monitoring the tracer molecule sodium fluorescein. In addition, the supplementation of hydrocortisone (HC) in the cell culture media did not allow any significant inflammatory reaction. Due to the high quantity of the data obtained in this study, a critical TEER value of $245 \Omega \times \text{cm}^2$ could be calculated using a reciprocal linear fit. Reaching this value, e.g., by a possible substance exposure or cytokine stimulation, a significant inflammation of the cells due to a loss of barrier function and an increased sodium fluorescein permeability can be observed. A treatment of the inflamed hAELVi cells with potential anti-inflammatory inhalable therapies can be used for the *in vitro* safety and efficacy assessment in further studies.

In this dissertation no standardized and officially accepted *in vitro* test strategy could be developed. However, it became clear that a promising approach to developing a safety assessment follows a stepwise procedure. This includes first the investigation of cytotoxicity by applying

the *SAFE* classification, which is followed by the inflammatory testing using the hAELVi inflammation protocol resulting in a more complete picture of the consequences of a substance exposure. Further studies should integrate more potential cellular targets, for example, an increased ROS production or a changed protein modification, which could have harmful effects on the entire organism. Another important future development aspect is the optimisation of experimental conditions implementing co-culture systems under air-liquid cultivation to increase the predictability of *in vitro* systems.

4 Results: Original publications

4.1 Combining MucilAir™ and Vitrocell® Powder Chamber for the In Vitro Evaluation of Nasal Ointments in the Context of Aerosolized Pollen

Reference

Combining MucilAir™ and Vitrocell® PowderChamber for the In Vitro Evaluation of Nasal Ointments in the Context of Aerosolized Pollen

Julia Metz, Katharina Knoth, Henrik Groß, Claus-Michael Lehr, Carolin Stäbler, Udo Bock and Marius Hittinger

Pharmaceutics 2018, *10*, 56, doi: 10.3390/pharmaceutics10020056

Original publication is reprinted from the MDPI Journal of Pharmaceutics, 2018: *Combining MucilAir™ and Vitrocell® PowderChamber for the In Vitro Evaluation of Nasal Ointments in the Context of Aerosolized Pollen*; Julia Metz, Katharina Knoth, Henrik Groß, Claus-Michael Lehr, Carolin Stäbler, Udo Bock and Marius Hittinger. *Pharmaceutics* 2018, *10*, 56, doi: 10.3390/pharmaceutics10020056.

For all articles published in MDPI journals, copyright is retained by the authors. Articles are licensed under an open access Creative Commons CC BY 4.0 license.

Co-author statement in connection with submission of PhD thesis of Julia Metz

Related to: *‘Vorläufiger Leitfaden und vorläufige Vorgaben für die Erstellung, Einreichung und Veröffentlichung von kumulativen Dissertationsschriften, Beschluss des Promotionsausschusses vom 06.12.2018’*

Paper title: Combining MucilAir™ and Vitrocell® Powder Chamber for the In Vitro Evaluation of Nasal Ointments in the Context of Aerosolized Pollen

Published

Accepted

Submitted

In preparation

Place of publication: Pharmaceutics 2018, 10, 56, doi: 10.3390/pharmaceutics10020056

Has the article/manuscript been used in other PhD or doctoral dissertations?

No Yes If yes, please specify

List of authors: Julia Metz, Katharina Knoth, Henrik Groß, Claus-Michael Lehr, Carolin Stäbler, Udo Bock and Marius Hittinger

Specification of the contributions:

Julia Metz conceived and planned the experiments. Julia Metz carried out the exposure experiments with the Vitrocell® Powder Chamber, the confocal scanning laser microscopy measurements, the scanning electron microscopy, cell culture treatment with the ointment and the ELISA measurements. Katharina Knoth supported the cell culture treatment with the ointment and contributed to sample preparation. Julia Metz, Henrik Groß, Claus-Michael Lehr, Carolin Stäbler, Udo Bock and Marius Hittinger contributed to the interpretation of the results. Julia Metz took the lead in writing the manuscript. All authors provided critical feedback and helped shape the research, analysis, and manuscript.



Article

Combining MucilAir™ and Vitrocell® Powder Chamber for the In Vitro Evaluation of Nasal Ointments in the Context of Aerosolized Pollen

Julia Metz ^{1,2}, Katharina Knoth ¹, Henrik Groß ¹, Claus-Michael Lehr ^{1,2,3}, Carolin Stäbler ⁴, Udo Bock ^{5,*} and Marius Hittinger ¹

¹ Department of Drug Delivery, PharmBioTec GmbH, 66123 Saarbrücken, Germany; j.metz@pharmbiotec.de (J.M.); k.knoth@pharmbiotec.de (K.K.); h.gross@pharmbiotec.de (H.G.); Claus-Michael.Lehr@helmholtz-hzi.de (C.-M.L.); m.hittinger@pharmbiotec.de (M.H.)

² Department of Biopharmaceutics and Pharmaceutical Technology, Department of Pharmacy, Saarland University, 66123 Saarbrücken, Germany

³ Helmholtz Institute for Pharmaceutical Research Saarland (HIPS), Helmholtz Center for Infection Research (HZI), 66123 Saarbrücken, Germany

⁴ Department of Scientific Affairs Consumer Health, Bayer Vital GmbH, 51368 Leverkusen, Germany; carolin.staebler@bayer.com

⁵ Bock Project Management, 54456 Tawern, Germany

* Correspondence: udo.bock@bock-pm.com; Tel.: +49-6501-602-7854

Received: 30 March 2018; Accepted: 27 April 2018; Published: 10 May 2018



Abstract: Hay fever is notoriously triggered when nasal mucosa is exposed to allergenic pollen. One possibility to overcome this pollen exposure may be the application of an ointment with physical protective effects. In this context, we have investigated Bepanthen® Eye and Nose Ointment and the ointment basis petrolatum as reference while using contemporary in vitro techniques. Pollen from false ragweed (*Iva xanthiifolia*) was used as an allergy-causing model deposited as aerosol using the Vitrocell® Powder Chamber (VPC) on Transwell® inserts, while being coated with either Bepanthen® Eye and Nose Ointment and petrolatum. No pollen penetration into ointments was observed upon confocal scanning laser microscopy during an incubation period of 2 h at 37 °C. The cellular response was further investigated by integrating the MucilAir™ cell system in the VPC and by applying pollen to Bepanthen® Eye and Nose Ointment covered cell cultures. For comparison, MucilAir™ were stimulated by lipopolysaccharides (LPS). No increased cytokine release of IL-6, TNF- α , or IL-8 was found after 4 h of pollen exposure, which demonstrates the safety of such ointments. Since nasal ointments act as a physical barrier against pollen, such preparations might support the prevention and management of hay fever.

Keywords: allergy prevention; pollen; aerosol deposition in vitro system; nasal mucosa; Bepanthen® Eye and Nose Ointment

1. Introduction

Pollen allergy is a major public health problem worldwide and around 400 million people suffer from allergic rhinitis, according to the World Health Organization (WHO) [1]. The epidemiological research program “International Study of Asthma and Allergies in Childhood (ISAAC)” announced that the reasons for the worldwide spread of allergy cases are due to economic development, dietary and climate factors, infections, and pollen [2]. In addition to asthma and atopic eczema, allergic rhinoconjunctivitis (AR) as resulting from pollen as major allergens decreases the life quality of affected persons significantly [3,4]. The primary symptoms of AR that is caused by hay fever

are sneezing, itching, secretion, and obstruction, followed by secondary and tertiary symptoms e.g., dyspnea, nasal hyperactivity up to conjunctivitis, sinusitis, and asthma [4].

Oral H1 antihistamines and intranasal corticosteroids build the two main classes of drugs for AR-treatment. A well-known and frequent property of oral treatment with H1 antihistamines is the negative impact on the nervous system, such as sedative effects [5]. These adverse effects were reduced in the second generation of H1 antihistamines, such as Cetirizine [6]. However, headaches, fatigue, and gastrointestinal distress were still observed [7]. Consequently, the demand for complementary and alternative medicines (CAM) for reducing allergy symptoms with less adverse effects is growing [8]. The research of new therapy strategies that are based on CAM is highly cost-intensive [9]. These CAMs are associated with a delayed response, which is not suitable in the acute case for reducing allergy symptoms. In addition to traditional CAMs against hay fever, such as homeopathic remedies [10] and nasal ointments, which act as a physical barrier to pollen and are able to provide a supportive effect without adverse effects that are similar to that of H1 antihistamines [11,12].

Bepanthen[®] Eye and Nose Ointment has the indication to support wound-healing around the nose and eye area. The aim of this study was to investigate the potential of such ointments as CAM to prevent AR reactions by acting as a sole physical barrier to pollen, and thus preventing interaction with immune cells and subsequent allergy symptoms [13]. For this purpose, two innovative in vitro techniques were combined in this study: The Vitrocell[®] Powder Chamber [14] and the human cell based MucilAir[™] system [15–17]. Their combined use allows for the controlled application of aerosolized pollen on a human mucosal tissue surrogate, aiming to reflect a similar scenario in humans. In the first step, different pollens were selected with focus on their auto-germination and their penetration depth into nasal ointments at the air-liquid interface. Second, the release of pro-inflammatory cytokines (IL-6, IL-8, and TNF- α) was quantified as an initial cellular response to pollen contact and to confirm the protective effect.

2. Materials and Methods

2.1. Microscopy

Size and shape of four selected pollen species, *Iva xanthiifolia*, *Populus nigra italica*, *Populus tremuloides*, and *Populus deltoids* (all from: Sigma-Aldrich, St. Louis, MO, USA) were examined through an electron microscope, the EVO HD 15 (Zeiss, Jena, Germany). Samples were sputtered with a thin gold layer using a Q150R ES sputter coater (Quorum technologies, Houston, TX, USA) before imaging at 5 kV and 7.5 mm working distance. A LSM 710 Axio Observer (Zeiss, Jena, Germany) visualized auto-germination at a wavelength of 488 nm using an EC-Plan-Neofluar 10 \times /0.30M27 objective (Zeiss, Jena, Germany). ZEN 2 blue edition (Zeiss, Jena, Germany) was used as computer software. Additional wavelengths (405 & 561 nm) were applied when examining the ointment samples. For SEM imaging, MucilAir[™] cell inserts were dehydrated with an ethanol (VWR Radnor, PA, USA) series at room temperature (RT) (70-80-90-96 (two times) and 100% for 10 min each), followed by sputter coating.

2.2. Parameters for Pollen Deposition with the Vitrocell[®] Powder Chamber

The Powder Chamber (VITROCELL[®] Systems GmbH, Waldkirch, Germany) consists of four different parts (a particle release, sedimentation tubes, exposure tray, and a controller), as shown in Figure 1a. An aliquot of 20 mg pollen was aerosolized per run. The amount of pollen that was deposited could be controlled by varying the sedimentation tube length and the time in exposition and sedimentation mode, respectively (Figure 1b). The optimal parameters for pollen deposition in the VPC were: 30 L/min flow rate; a tube length of 30 cm, a sedimentation time of 0 sec and an exposition time of 15 min.

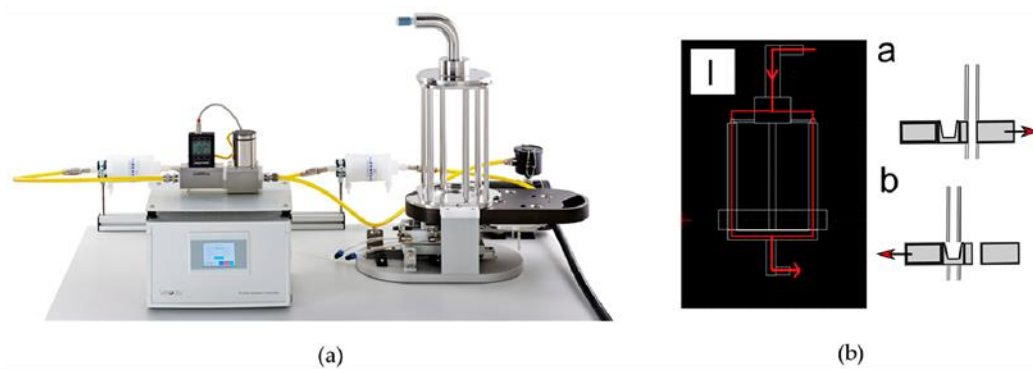


Figure 1. Vitrocell[®] Powder Chamber (VPC) as an aerosol exposure system for pollen deposition. (a) Composition of the VPC consisting of a tube for particle dosing, sedimentation tubes, exposure tray, and a controller [18]; (b) the air/ pollen flow is indicated by the red line through the sedimentation tubes (I); the VPC can be switched from a sedimentation-mode (a) to an exposition mode; (b). The sedimentation mode (a) allows for passing of large particles before the cell system is switched under the particle filled tube (b). As pollen are comparable to large particles, the time in sedimentation mode was set to zero seconds. The system immediately switched to exposition mode and a maximum dose of pollen was deposited on the cells. modified from [14].

2.3. Penetration of Pollen into an Ointment Layer

The penetration depth of pollen into the Bepanthen[®] Eye and Nose Ointment and petrolatum (both Bayer Vital GmbH, Leverkusen, Germany) served as an endpoint for evaluating the physical protective function of the ointments against pollen. Petrolatum is one of the main components in Bepanthen[®] Eye and Nose Ointment. The penetration depth was determined by confocal laser microscopy (CLSM). Thus, the ointments were distributed in modified Transwell[®] inserts (Corning, New York, NY, USA) where the membrane was replaced by a cover glass of similar size. A droplet (approx. 100 μ L) of ointment was placed on the insert and was carefully distributed with a small brush. Transwell[®] inserts used for comparison, were prepared in the same way, but without ointment. Three of the four deposition wells of the VPC were used as follows: (i) petrolatum; (ii) Bepanthen[®] Eye and Nose Ointment; and (iii) control (empty insert). Pollen was aerosolized and deposited on the inserts. This experiment was conducted at room temperature and repeated three times, using fresh inserts for each cycle. Pollen penetration depth was measured by CLSM, as shown in Figure 2, within 30 min after the deposition experiments, keeping the samples on ice for transport. To follow pollen penetration over time, the samples were kept at 37 $^{\circ}$ C on a hot stage and CLSM z-stacks were taken at randomly chosen positions immediately (0 h, 1 h, and 2 h later).

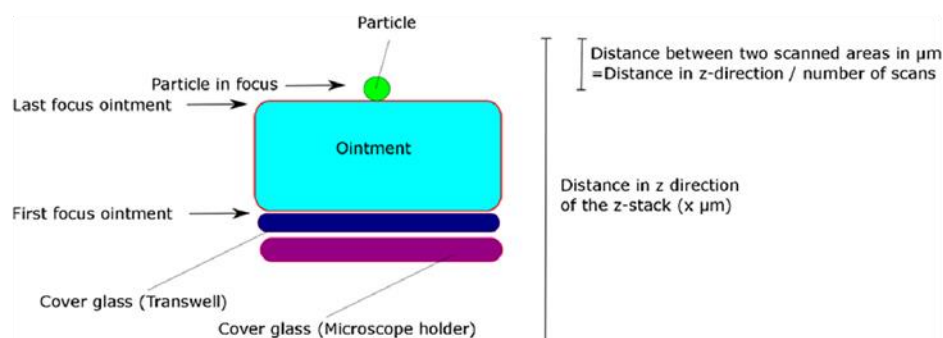


Figure 2. Situation for observing pollen penetration into ointment film preparation by confocal laser microscopy (CLSM) (not to scale).

2.4. Cytokine Release after Deposition on MucilAir™

MucilAir™ cell cultures (Epithelix Sàrl, Genève, Switzerland) were cultivated, according to manufacturer instructions, using the recommended medium under physiological air-liquid interface conditions (ALI). MucilAir™ is a reconstituted cell model based on human primary cells, which is known for its tight barrier, cytokine release, and mucus production [16]. After arrival, cells were cultured at the air-liquid interface for one day before the experiments were performed (at the air-liquid interface). 20 mg pollen with highest fluorescence intensity (*Iva xanthiifolia*) were deposited as aerosol on MucilAir™ with the aforementioned instrument settings. Three sham depositions without pollen ($n = 1$ MucilAir™ insert per cycle) were performed as negative control. Three MucilAir™ inserts were incubated with 10 μ L lipopolysaccharides (LPS) (10 μ g/ mL, Escherichia coli, Sigma-Aldrich, St. Louis, MO, USA) in 990 μ L 1 \times DPBS (Gibco™, Thermo Fisher Scientific, Waltham, MA, USA) in the apical side (positive control). Six cycles were performed with one insert MucilAir™ protected by Bepanthen® Eye and Nose Ointment and one insert without ointment protection in each cycle. In summary, three positive (LPS incubated samples) and three negative (sham deposition) controls, six wells that were protected by ointment and six wells without protection from deposited pollen were investigated (Figure 3). An inverse light microscope Primovert (Zeiss, Jena, Germany) visualized the distribution of pollen after deposition with the VPC on the MucilAir™ system. Transwell® inserts were transferred into the VPC wells. As positive control 10 μ g/ mL LPS in 1 \times DPBS (Waltham, MA, USA) was used to stimulate an inflammatory response in the MucilAir™ system [19,20]. Bepanthen® Eye and Nose Ointment was pre-heated to 37 °C and was carefully added from the tube in a small droplet on top of the cell culture insert. The ointment was distributed carefully by using a sterile brush.

Figure 3 shows an experimental overview. Cytokines were quantified by Enzyme-linked Immunosorbent Assays (ELISA Kits, Thermo Fisher Scientific, Waltham, MA, USA). The release of the cytokines TNF- α , Interleukin-6, and Interleukin-8 was measured after pollen deposition on MucilAir™ and in both control groups 0, 4, and 24 h (sample volume: 200 μ L). The ELISA kits were used according to the manufacturers' guidelines.

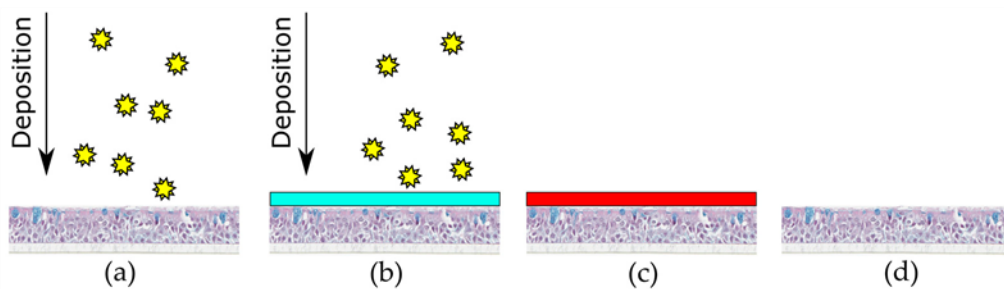


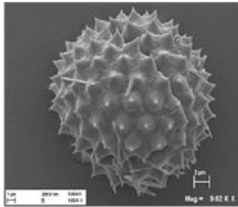
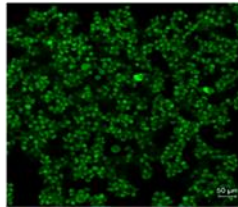
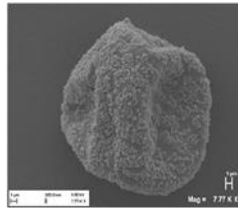
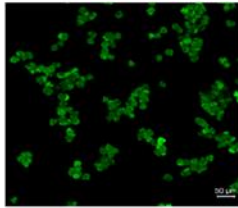
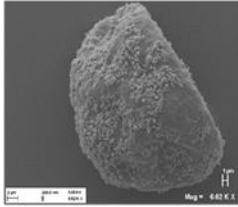
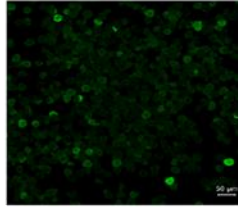
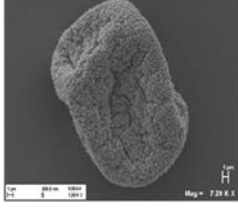
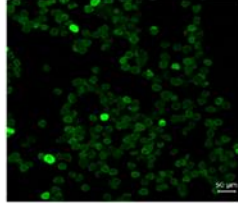
Figure 3. Experimental design for pollen deposition on MucilAir™. (a) pollen (symbolized by stars) deposited via VPC to MucilAir™ ($n = 6$); (b) pollen deposited via VPC and protected by Bepanthen® Eye and Nose Ointment (light blue bar) to MucilAir™ ($n = 6$); (c) positive controls LPS stimulation on MucilAir™ ($n = 3$); and, (d) untreated negative control MucilAir™ in VPC ($n = 3$).

3. Results

3.1. Pollen Selection

Table 1 lists the investigated pollen with focus on their size, shape (SEM) and characteristic autofluorescence (CLSM). All pollen had a size of approximately 30 μ m and a similar behavior within the Powder Chamber was expected, accordingly. *Iva xanthiifolia* was selected for further experiments because of its strong autofluorescence and its known allergic potential and increasing relevance [15].

Table 1. Overview of the characteristics, size, shape, and autofluorescence of used pollen.

Pollen Species	Characteristics	Scanning Electron Microscopy	Confocal Light Scanning Microscopy
<i>Iva xanthiifolia</i>	Size: ~28 μm Shape: serrated, rough surface Allergic potential: allergenic Neophyt [21]		
<i>Populus nigra italica</i>	Size: ~26 μm Shape: uneven, particulate surface Allergic potential: ♂ dioecious [22]		
<i>Populus tremuloides</i>	Size: ~30 μm Shape: ovate, particulate surface Allergic potential: not known		
<i>Populus deltoides</i>	Size: ~28 μm Shape: longish, porous surface Allergic potential: yes [23]		

3.2. Penetration of Pollen into an Ointment Layer

Pollen from the *Iva xanthiifolia* was deposited with the VPC and the deposited amount of pollen was counted on modified, untreated Transwell[®] inserts. 31 ± 19 pollen were detected per CLSM image corresponding to 4231 ± 2592 pollen/ cm^2 . The results indicate that the pollen deposition process using the VPC has certain variability depending on the position and inter-cycle differences. The ointment thickness (petrolatum) was measured by CLSM and had a range of 20–250 μm . The z-focus of the instrument of the CLSM Bepanthen[®] Eye and Nose Ointment was limited to approximately 100 μm penetration depth (signal was scattered by excipients).

The penetration depth of *Iva xanthiifolia* into the Bepanthen[®] Eye and Nose Ointment and petrolatum was examined over two h at 37 °C after pollen deposition. No significant penetration of pollen was observed into either the Bepanthen[®] Eye and Nose Ointment or the petrolatum, demonstrating that both ointments act as a physical barrier to pollen, which is shown in Figure 4: The first focal plane, on which the first autofluorescence signal appeared, was designated as the start of the ointment layer (Figure 4a,b, figures left (1), ointment in blue). The last autofluorescence signal from the ointment was detected on the same level when the autofluorescence signal of pollen was measured (Figure 4a,b, right (2), pollen in green), which emphasizes that no penetration occurred. The calculated distance is similar to the ointment thickness applied.

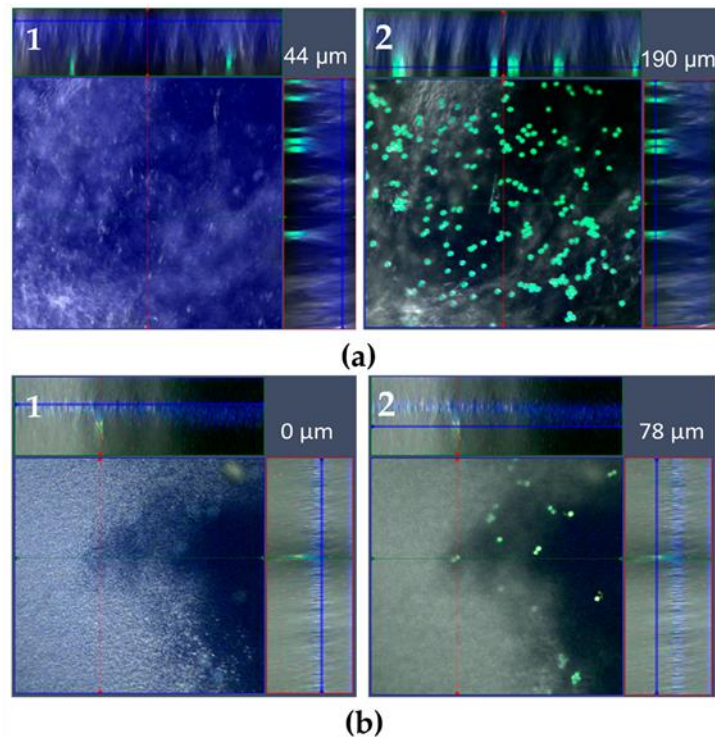


Figure 4. Pollen deposition of the *Iva xanthiifolia* (z-stack by CLSM). (a) *Iva xanthiifolia* deposited via VPC on petrolatum. Image 1 shows the focus area of the ointment beginning with a high of 44 μm by performing the z-stack. Image 2 on the right shows the focus area of the pollen (green), which is the last area in which ointment is localized (190 μm). Consequently, no penetration of pollen was observed. The blue scattered light from the laser further stresses the thickness of the ointment; (b) Bepanthe[®] Eye and Nose Ointment via CLSM. Image 1 indicates the first focus level of the Bepanthe[®] Eye and Nose Ointment on the cover slip, image 2 demonstrates the second focus level on the top of the Bepanthe[®] Eye and the Nose Ointment with deposited pollen. The images were selected from a z-stack, which emphasizes the limited fluorescence signal of pollen in the ointment. The ointment (beginning left, 0 μm) and pollen on top (right, 78 μm) highlight both limiting imaging points.

3.3. Cytokine Release after Deposition on MucilAirTM

The deposition of pollen on the epithelial layer was proven by light microscopy. Some visible cilia beating and a slow movement of pollen was observed. Most of the pollen were located at the edges after 24 h when the last cytokine samples were taken. Figure 5 summarizes the levels of TNF- α , IL-6, and IL-8. The first diagram shows the control group with LPS stimulation against a negative control group and the second diagram shows the results from the treatment with Bepanthe[®] Eye and Nose Ointment against the negative control group. No differences were found for IL-6 and TNF- α for LPS stimulation, as well as for treatment with Bepanthe[®] Eye and Nose Ointment (Figure 5a,b). The IL-8 release was increased after LPS stimulation as compared to the control group without stimulation. Bepanthe[®] Eye and Nose Ointment has no influence on the IL-8 release over 24 h (Figure 5c). The detected concentrations of IL-6 and TNF- α were low and did not allow for further analysis. After 24 h, a significant increase of IL-8 was observed for the LPS group when compared to the control group, which implicates a moderate reaction of the MucilAirTM system. The treatment of Bepanthe[®] Eye and Nose Ointment did not influence the release of cytokines, nor did it trigger an inflammatory response of MucilAirTM.

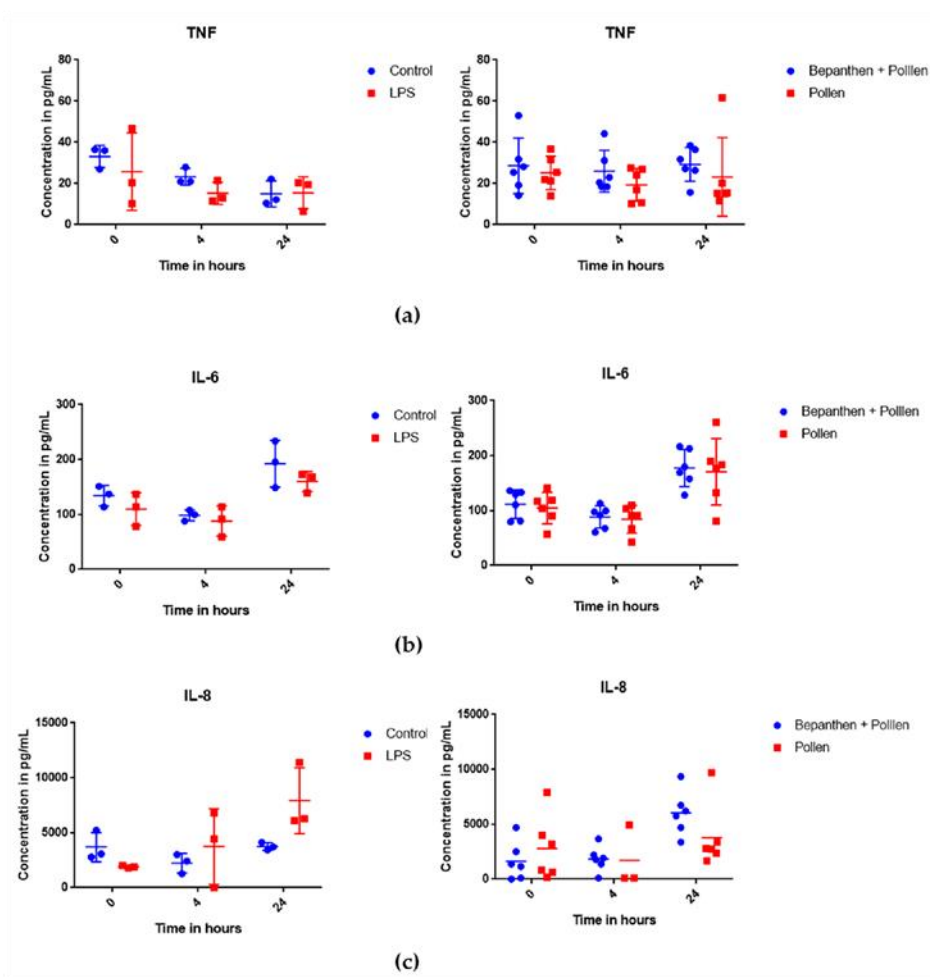


Figure 5. Cytokine release of MucilAir™ with pollen deposition on Bepanthen® Eye and Nose Ointment ($n = 6$ per time point and group) and control with lipopolysaccharides (LPS) stimulation over 24 h ($n = 3$ per time point and group); (a) release of TNF- α ; (b) release of Interleukin-6; and, (c) release of Interleukin-8 (dilution of 1:1000).

SEM was performed to visualize pollen with the resulting cell culture interactions (Figure 6). The images indicated pollen, which sticks to mucus and cellular like structures.

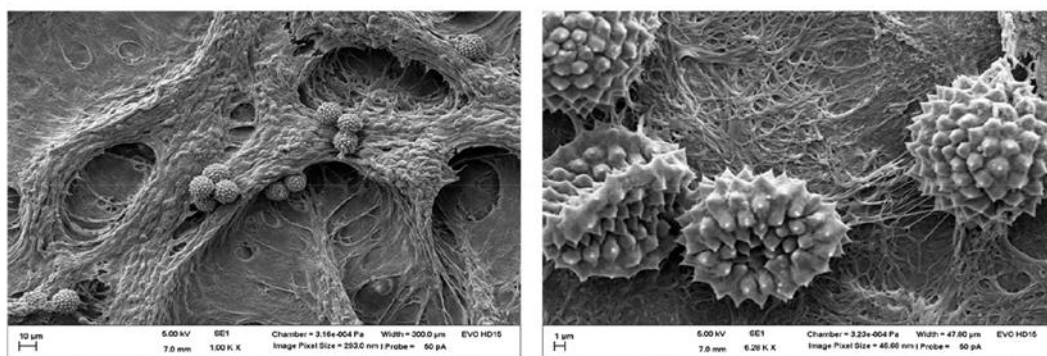


Figure 6. Scanning electron microscopy (SEM) images after deposition with VPC of pollen from *Iva xanthiifolia* on MucilAir™. Left: SEM picture of *Iva xanthiifolia* on MucilAir™ with an image pixel size of 293.0 nm and a magnification of 1.000 \times ; right: SEM picture *Iva xanthiifolia* on MucilAir™ with an image pixel size of 46.68 nm and a higher magnification of 6.280 \times .

4. Discussion

The aim of this study was to investigate the protective effects of nasal ointments acting as a physical barrier against aerosolized pollen. We decided for the combination of an innovative aerosol deposition system (VPC) in combination with the MucilAir™ cell culture model of human nasal mucosa. Due to its prominent autofluorescence and due to its allergic potential and the future importance in EU [21], *Iva xanthiifolia* was selected among other pollen species that are listed in Table 1. A different behavior as aerosol in the Powder Chamber was not expected as all investigated pollen were of similar size. The VPC allowed for an efficient and homogeneous aerosolization, and the deposition of this pollen. However, no penetration of pollen could be observed in either petrolatum or Bepanthen® Eye and Nose Ointment when spread on glass slides. This finding already suggests some kind of protective effect of such nasal ointments. In such settings however, any physiological clearance due to mucociliary beating and mucus are missing [24].

Various *in vitro* models simulating the mechanical and the functional facets of the upper respiratory system *in vivo* are available. These models can be divided into cell culture models, like primary cells or nasal tissue cells, excised nasal tissues, and different experimental set-ups regarding the permeation pathways [24]. The overall goal of these models is to come as close as possible to the *in vivo* conditions failing on the reconstitution of the complex communication and the interaction of the different components of nasal mucosa. Hence, the MucilAir™ cell culture systems were developed to set-up for such experimental designs by consisting of differentiated and functional cells of the human airway epithelium with goblet cells, which produce mucus, basal cells, and ciliated cells [16,19,25]. In our study, the VPC was combined for the first time with MucilAir™ model to address this biological complexity. The observed ciliated movement of pollen to the edges of the Transwell® membrane within 24 h combined with SEM images of mucus-trapped pollen emphasized a functional mucociliary clearance (MCC) within the *in vitro* system. *In vivo*, the MCC, and the mucus layer itself are for nasal drug delivery one of the limiting factors resulting in impeded drug permeability [11,24]. Mucus is of utmost importance, since the ciliated cells transport the mucus to nasopharynx in order to remove foreign particles [26]. Bepanthen® Eye and Nose Ointment influences the physiological function of the mucociliary system of the upper respiratory tract in our study that is caused by building an additional layer on the system. In this *in vitro* setup, the ointment has the same function as the physical barrier to trap the pollen by passing the nose by air. One of the main side actions of Bepanthen® Eye and Nose Ointment is that the cilia's function of transporting pollen might be decreased. Nevertheless, this should be a minor factor that is caused by the early positioning of the layer in the very first contact area of the nose. The effect on the morphological change or possible disruption of the physiological nasal mucosa by the application of the substance should be considered in further studies.

The deposition of allergenic pollen leads to symptoms of allergy and inflammation processes in the immune system [13,27], resulting in an increased pro-inflammatory cytokine release. The MucilAir™ system is suitable for the investigation of potential allergic cytokines, as it has already been used as an examination system for respiratory sensitizers [15]. According to our hypothesis, the application of Bepanthen® Eye and Nose Ointment should decrease the release of typical involved cytokines, such as IL-6, TNF- α , and IL-8. However, the release of IL-6 and TNF- α was not influenced by any of the chosen conditions. This might be due to a comparatively low number of immune cells present in the currently available *in vitro* models of the nasal mucosa. It has been shown, that the MucilAir™ releases IL-8 after stimulation with LPS [15]. Consequently, LPS was applied as a pro-inflammatory mediator to the MucilAir™ [19,28], leading to an increased IL-8 secretion after 24 h. Interestingly, the mean of IL-8 secretion was even higher after the treatment with Bepanthen® Eye and Nose Ointment and deposited pollen when compared to the control group. This might be caused by associated mechanical stress on the cellular layer itself. Pollen did not stimulate any cytokine release (IL-8, TNF- α and IL-6), which is based on a protective mucus layer, as indicated by the SEM images. Furthermore, the concentration of 10 $\mu\text{g}/\text{mL}$ LPS might be further increased to stimulate the MucilAir™ system in order to generate a

more pronounced response [29]. Nonetheless, in an inflammatory state the properties of mucus change and the native barrier might be less efficient, which is hard to mimic in vitro [30–32].

This study combines two innovative in vitro systems for respiratory research, the MucilAir™ and the VPC to address the in vivo situation of pollen deposition. The set-up offered air-liquid experimental conditions, including differentiated and functional cells of the human airway epithelium with goblet cells, basal cells, and ciliated cells [16,19,25]. However, further adjustments, such as the implementation of other cell types e.g., immunological cells are necessary to address interactions with pollen in vitro and to enhance the readout.

5. Conclusions

This study was designed to prove the capacity of nasal ointments in vitro to act as a physical barrier against pollen, and subsequently reduce allergic potential. The combination of the in vitro model MucilAir™ with the air-liquid deposition instrument VPC for the application of dry particles (pollen) was a first step in the direction of a relevant in vitro test method for nasal ointment efficacy studies. We demonstrated that nasal ointments are able to physically prevent the penetration of pollen. Conversely, we were neither able to confirm nor negate any reduction of the allergenic potential of pollen by the application of nasal ointments in terms of cytokine release profiles by using the MucilAir™ system with IL-6, IL-8, and TNF- α as read-out markers making further adjustments necessary. The combination of the VPC with MucilAir™ can nevertheless be seen as a promising step on the way to more complex models addressing the air-liquid interface.

Author Contributions: M.H., H.G., C.S. and U.B. conceived and designed the experiments. J.M., M.H. and K.K. performed and adjusted the experiments. J.M., M.H., K.K., U.B. and C.-M.L. analyzed the data and prepared the manuscript.

Acknowledgments: Bayer Vital GmbH funded the study.

Conflicts of Interest: Carolin Stäbler is an employee of the sponsor (Bayer Vital GmbH).

References

1. WHO. Global Surveillance, Prevention and Control of Chronic Respiratory Diseases; World Health Organization: Geneva, Switzerland, 2007; pp. 1–146.
2. Asher, M.I.; Montefort, S.; Björkstén, B.; Lai, C.K.; Strachan, D.P.; Weiland, S.K. Worldwide time trends in the prevalence of symptoms of asthma, allergic rhinoconjunctivitis, and eczema in childhood: ISAAC Phases One and Three repeat multicountry cross-sectional surveys. *Lancet* **2006**, *368*, 733–743. [CrossRef]
3. Burr, M.L.; Emberlin, J.C.; Treu, R.; Cheng, S.; Pearce, N.E. Pollen counts in relation to the prevalence of allergic rhinoconjunctivitis, asthma and atopic eczema in the International Study of Asthma and Allergies in Childhood (ISAAC). *Clin. Exp. Allergy* **2003**, *33*, 1675–1680. [CrossRef] [PubMed]
4. Bachert, C.; Borchard, U.; Wedi, B.; Klimek, L.; Rasp, G.; Riechelmann, H. Allergische rhinokonjunktivitis: Leitlinie der deutschen gesellschaft für allergologie und klinische Immunologie (DGAI). *Allergo J.* **2003**, *12*, 182–194. [CrossRef]
5. Day, J. Pros and cons of the use of antihistamines in managing allergic rhinitis. *J. Allergy Clin. Immunol.* **1999**, *103*, 395–399. [CrossRef]
6. Estelle, R.F.; Simons, R.; Simons, K.J. The pharmacology and use of H1-Receptor-antagonist drugs. *Drug Ther.* **1994**, *330*, 1663–1670. [CrossRef]
7. Golightly, L.; Greos, L. Second-Generation Antihistamines Allergic Disorders. *Drugs* **2005**, *65*, 341–384. [CrossRef] [PubMed]
8. Frass, M.; Strassl, R.P.; Friehs, H.; Mullner, M.; Kundi, M.; Kaye, A. Use and Acceptance of Complementary and Alternative Medicine Among the General Population and Medical Personnel: A Systematic Review. *Ochsner J.* **2012**, *12*, 45–56. [CrossRef] [PubMed]
9. Engel, L.W.; Straus, S.E. Development of therapeutics: Opportunities within complementary and alternative medicine. *Nat. Rev. Drug Discov.* **2002**, *1*, 229–237. [CrossRef] [PubMed]

10. Ziment, I.; Tashkin, D.P. Alternative medicine for allergy and asthma. *J. Allergy Clin. Immunol.* **2000**, *106*, 603–614. [CrossRef] [PubMed]
11. Arora, P.; Sharma, S.; Garg, S. Permeability issues in nasal drug delivery. *Drug Discov. Today* **2002**, *7*, 967–975. [CrossRef]
12. Kloecker, N.; Rudolph, P.; Verse, T. Evaluation of protective and therapeutic effects of dexpanthenol on nasal decongestants and preservatives: Results of cytotoxic studies In Vitro. *Am. J. Rhinol.* **2004**, *18*, 315–320.
13. Galli, S.J.; Tsai, M.; Piliponsky, A.M. The development of allergic inflammation. *Nature* **2008**, *454*, 445–454. [CrossRef] [PubMed]
14. Hittinger, M.; Barthold, S.; Siebenbürger, L.; Zäh, K.; Gress, A.; Guenther, S.; Wiegand, B.; Boerger, C.; Berger, M.; Krebs, T.; et al. Proof of concept of the Vitrocell® dry powder chamber: A new in vitro test system for the controlled deposition of aerosol formulation. In Proceedings of the Europe Respiratory Drug Delivery 2017 Scientific Conference, Antibes, France, 25–28 April 2017; pp. 283–288.
15. Huang, S.; Wiszniewski, L.; Constant, S.; Roggen, E. Potential of in vitro reconstituted 3D human airway epithelia (MucilAir) to assess respiratory sensitizers. *Toxicol. Vitro* **2013**, *27*, 1151–1156. [CrossRef] [PubMed]
16. Epithelix. MucilAir by Epithelix. Available online: <http://www.epithelix.com/products/mucilair> (accessed on 13 January 2018).
17. Balogh Sivars, K.; Sivars, U.; Hornberg, E.; Zhang, H.; Brändén, L.; Bonfante, R. A 3D Human airway model enables prediction of respiratory toxicity of inhaled drugs in vitro. *Toxicol. Sci.* **2018**, *162*, 301–308. [CrossRef] [PubMed]
18. Vitrocell-Powder-Chamber. Available online: <https://www.vitrocell.com/inhalation-toxicology/exposure-systems/vitrocell-powder-chamber> (accessed on 29 March 2018).
19. Kooter, I.M.; Gröllers-Mulderij, M.; Duistermaat, E.; Kuper, F.; Schoen, E.D. Factors of concern in a human 3D cellular airway model exposed to aerosols of nanoparticles. *Toxicol. In Vitro* **2017**, *44*, 339–348. [CrossRef] [PubMed]
20. Balloy, V.; Deveaux, A.; Lebeaux, D.; Tabary, O.; Le Rouzic, P.; Ghigo, J.M. Azithromycin analogue CSY0073 attenuates lung inflammation induced by LPS challenge. *Br. J. Pharmacol.* **2014**, *171*, 1783–1794. [CrossRef] [PubMed]
21. Follak, S. Notizen zum Vorkommen von *Iva xanthiifolia* in der Südwestslowakei. *Stapfa* **2014**, *101*, 71–77.
22. Cariñanos, P.; Casares, P.M. Urban green zones and related pollen allergy: A review. Some guidelines for designing spaces with low allergy impact. *Landsc. Urban Plan.* **2011**, *101*, 205–214. [CrossRef]
23. Heinzerling, L.; Frew, A.J.; Bindeslev, J.C.; Bonini, S.; Bousquet, J.; Bresciani, M. Standard skin prick testing and sensitization to inhalant allergens across Europe—A survey from the GA₂LEN network. *Allergy Eur. J. Allergy Clin. Immunol.* **2005**, *60*, 1287–1300. [CrossRef] [PubMed]
24. Christiane, S.M.; Peter, H.; Lang, S.R.; Ditzinger, G.; Merkle, H.P. In vitro cell models to study nasal mucosal permeability and metabolism. *Adv. Drug Deliv. Rev.* **1998**, *29*, 51–79. [CrossRef]
25. Huang, S.; Boda, B.; Vernaz, J.; Ferreira, E.; Wiszniewski, L.; Constant, S. Establishment and characterization of an in vitro human small airway model (SmallAir™). *Eur. J. Pharm. Biopharm.* **2017**, *118*, 68–72. [CrossRef] [PubMed]
26. Neugebauer, P.; Mickenhagen, A.; Siefer, O.; Walger, M. A new approach to pharmacological effects on ciliary beat frequency in cell cultures—Exemplary measurements under *Pelargonium sidoides* extract (EPs 7630). *Phytomedicine* **2005**, *12*, 46–51. [CrossRef] [PubMed]
27. Theodorou, G.L.; Marousi, S.; Ellul, J.; Mougiou, A.; Theodori, E.; Mouzaki, A. T helper 1 (Th1)/ Th2 cytokine expression shift of peripheral blood CD4⁺ and CD8⁺ T cells in patients at the post-acute phase of stroke. *Clin. Exp. Immunol.* **2008**, *152*, 456–463. [CrossRef] [PubMed]
28. Huang, S.; Wiszniewski, L.; Constant, S. Chapter 8: The Use of In Vitro 3D Cell Models in Drug Development for Respiratory Diseases. In *The Use of In Vitro 3D Cell Models in Drug Development for Respiratory Diseases, Drug Discovery and Development—Present and Future*; InTech: Rijeka, Croatia, 2011; pp. 169–191, ISBN 978-953-307-615-7.
29. De, S.B.; Ranzini, F.; Piqué, N. Protective barrier properties of Rhinosectan® spray (containing xyloglucan) on an organotypic 3D airway tissue model (MucilAir): Results of an in vitro study. *Allergy Asthma Clin. Immunol. BioMed Central* **2017**, *13*, 37. [CrossRef]
30. Murgi, X.; Lorentz, B.; Hartwig, O.; Hittinger, M.; Lehr, C.M. The role of mucus on drug transport and its potential to affect therapeutic outcomes. *Adv. Drug Deliv. Rev.* **2017**, *124*, 82–97. [CrossRef] [PubMed]

31. Cohn, L.; Homer, R.J.; Niu, N.; Bottomly, K. T helper 1 cells and interferon gamma regulate allergic airway inflammation and mucus production. *J. Exp. Med.* **1999**, *190*, 1309–1318. [[CrossRef](#)] [[PubMed](#)]
32. Scavuzzo, M.C.; Rocchi, V.; Fattori, B.; Ambrogi, F.; Carpi, A.; Ruffoli, R. Cytokine secretion in nasal mucus of normal subjects and patients with allergic rhinitis. *Biomed. Pharmacother.* **2003**, *57*, 366–371. [[CrossRef](#)]



© 2018 by the authors. Licensee MDPI, Basel, Switzerland. This article is an open access article distributed under the terms and conditions of the Creative Commons Attribution (CC BY) license (<http://creativecommons.org/licenses/by/4.0/>).

4.2 Safety Assessment of Excipients (SAFE) for Orally Inhaled Drug Products

Reference

Safety Assessment of Excipients (SAFE) for Orally Inhaled Drug Products

Julia Katharina Metz, Lara Scharnowske, Fabian Hans, Sabrina Schnur, Katharina Knoth, Horst Zimmer, Markus Limberger, Henrik Groß, Claus-Michael Lehr and Marius Hittinger

ALTEX 2020, 37(2), 275-286. doi:10.14573/altex.1910231

Original publication is reprinted from ALTEX, 2018: *Safety Assessment of Excipients (SAFE) for Orally Inhaled Drug Products*; Julia Katharina Metz, Lara Scharnowske, Fabian Hans, Sabrina Schnur, Katharina Knoth, Horst Zimmer, Markus Limberger, Henrik Groß, Claus-Michael Lehr and Marius Hittinger

ALTEX 2020, 37(2), 275-286. doi:10.14573/altex.1910231

For all articles published in ALTEX, copyright is retained by the authors. Articles are licensed under an open access Creative Commons CC BY 4.0 license.

Co-author statement in connection with submission of PhD thesis of Julia Metz

Related to: *‘Vorläufiger Leitfaden und vorläufige Vorgaben für die Erstellung, Einreichung und Veröffentlichung von kumulativen Dissertationsschriften, Beschluss des Promotionsausschusses vom 06.12.2018’*

Paper title: Safety Assessment of Excipients (SAFE) for Orally Inhaled Drug Products

- Published
- Accepted
- Submitted
- In preparation

Place of publication: ALTEX 2020, 37(2), 275-286. doi:10.14573/altex.1910231

Has the article/manuscript been used in other PhD or doctoral dissertations?

- No Yes If yes, please specify

List of authors: Julia Katharina Metz, Lara Scharnowske, Fabian Hans, Sabrina Schnur, Katharina Knoth, Horst Zimmer, Markus Limberger, Henrik Groß, Claus-Michael Lehr and Marius Hittinger

Specification of the contributions:

Julia Katharina Metz conceived and planned the experiments. Julia Katharina Metz carried out the data collection of the human data (FDA), the cell viability assays (MTT) and the calculation of the IC₅₀ and the statistical data interpretation. Lara Scharnowske and Fabian Hans helped in performing MTT assays, Sabrina Schnur and Katharina Knoth supported the routine cell culture and contributed to sample preparation. Julia Katharina Metz, Henrik Groß, Claus-Michael Lehr, Horst Zimmer, Markus Limberger and Marius Hittinger contributed to the interpretation of the results. Julia Metz took the lead in writing the manuscript. All authors provided critical feedback and helped shape the research, analysis, and manuscript.



Research Article

Safety Assessment of Excipients (SAFE) for Orally Inhaled Drug Products

Julia K. Metz^{1,2}, Lara Scharnowske^{1,2}, Fabian Hans¹, Sabrina Schnur^{1,2}, Katharina Knoth¹, Horst Zimmer³, Markus Limberger⁴, Henrik Groß¹, Claus-Michael Lehr^{2,5} and Marius Hittinger¹

¹PharmBioTec GmbH, Saarbrücken, Germany; ²Department of Pharmacy, Saarland University, Saarbrücken, Germany; ³Ursatec Verpackung GmbH, Tholey, Germany; ⁴Quasaar GmbH, Überherrn, Germany; ⁵Helmholtz Institute for Pharmaceutical Research Saarland (HIPS), Saarbrücken, Germany

Abstract

The development of new orally inhaled drug products requires their demonstration of safety, which must be proven in animal experiments. New *in vitro* methods may replace, or at least reduce, these animal experiments, provided they are able to correctly predict safety or possible toxicity in humans. However, the challenge is to link *in vitro* data obtained in human cells to human *in vivo* data. We here present a new approach to the safety assessment of excipients (SAFE) for pulmonary drug delivery. The SAFE model is based on a dose response curve of 23 excipients tested on the human pulmonary epithelial cell lines A549 and Calu-3. The resulting *in vitro* IC₅₀ values were correlated with the FDA-approved concentrations in pharmaceutical products for either pulmonary (if available) or parenteral administration. Setting a threshold of 0.1% (1 mg/mL) for either value yielded four safety classes and allowed to link IC₅₀ data as measured in human cell cultures *in vitro* with the concentrations of the same compounds in FDA-approved drug products. The necessary *in vitro* data for novel excipients can be easily generated, and the SAFE approach allows putting them into context for eventual use in human pulmonary drug products. Excipients that are most likely not safe for use in humans can be excluded early on from further pharmaceutical development. The SAFE approach thus helps to avoid unnecessary animal experiments.

1 Introduction

The enormous expense of and the ethical need to reduce animal experiments during preclinical trials has led to the implementation of *in vitro* tests in European Medicines Agency (EMA) and Organization for Economic Co-operation and Development (OECD) guidelines (EMA, 2016; OECD, 2000), and the Food and Drug Agency (FDA) Guidance for Industries “Drug Metabolism/Drug Interaction Studies in the Drug Development Process: Studies *In Vitro*” recommends *in vitro* studies of the safety and efficacy testing of potential drugs to exclude any toxic or non-effective drugs at an early stage and thus reduce the risk of failing during clinical trials (FDA, 1997). However, although regulatory agencies encourage the use of *in vitro* assays for the screening and evaluation of new drug formulations, animal testing is still the standard procedure to evaluate inhaled drug products (Silva and Sorli, 2018). Mice, rats, dogs and non-human primates are the most widely used animals for this purpose (Pritchard et al., 2003).

The total costs of drug development have increased from \$800m to \$2,000m per drug, whereby drug development for delivery via inhalation has reached average costs of \$1,134m per new drug formulation (Adams and Van Brantner, 2006). In 2004, the FDA founded the Critical Path Initiative, which is a project aimed at optimizing the costly drug development process. In the process, the determination of the safety and efficacy of new drug formulations was found to be a main cost contributor (Woodcock and Woosley, 2008). Indeed, the costs of animal testing during drug development lie between \$430m and \$1,098m per drug (DiMasi et al., 2016).

Next to the financial and ethical aspects, the questionable prediction of the human response by data from animal experiments is an ongoing discussion (Bracken, 2009; Fröhlich, 2017). Safety issues account for 24% of clinical study terminations (Harrison, 2016). According to Li (2004), some reasons for this uncertainty might be that animals have different toxic and detoxifying molecular mechanisms and thus have a different sensitivity to com-

Received October 23, 2019; Accepted January 27, 2020;
Epub January 29, 2020; © The Authors, 2020

ALTEX 37(2), 275-286. doi:10.14573/altex.1910231

Correspondence: Marius Hittinger, PhD
PharmBioTec GmbH
Science Park 1, Campus D 1.1
66123 Saarbrücken, Germany
(m.hittinger@pharmbiotec.de)

This is an Open Access article distributed under the terms of the Creative Commons Attribution 4.0 International license (<http://creativecommons.org/licenses/by/4.0/>), which permits unrestricted use, distribution and reproduction in any medium, provided the original work is appropriately cited.



pounds compared with humans. In addition, studies are limited in the investigation of toxic endpoints, the number of tested individuals is restricted, and studies struggle with dose adaptation.

An example of a successfully established *in vitro* assay is the skin sensitization assay based on the stimulation of different human cell lines (OECD, 2018a). However, while there has been progress in the development of some *in vitro* assays, there is still a lack of adequate cell- and tissue-based *in vitro* models for other organs such as the respiratory tract. An OECD guideline (OECD, 2018b) now defines the certification process and the required quality controls for *in vitro* tests that serve the future evaluation of the assessment of human safety.

To face the challenge of developing an adequate *in vitro* model of the respiratory tract for safety evaluation, especially to assess nanoparticle (NP) deposition in the lung, the development of complex cell culture systems using two or more cell lines is gaining ground (Chary et al., 2018). But, no systematic data sets for the toxicological assessment of nanoparticles are available due to non-standardized parameters, different testing systems (cells, animals), and the different types and characteristics of the particles themselves (Mahmoudi et al., 2012). The many different endpoints of *in vitro* data obtained during safety studies – cell toxicity, proinflammatory reactions, translocation of nanoparticles in the tissue, and the resulting uptake mechanism, to name a few – should be evaluated in a comprehensive way to enable their inclusion into a guideline process (Drasler et al., 2017).

The correlation of the *in vitro* and *in vivo* activity of nanoparticles (NP), such as TiO₂, gold and polystyrene particles, was investigated by Rushton et al. (2010). Their *in vitro* assay, which was based on the secretion of reactive oxygen species (ROS), correlated significantly with *in vivo* observations (PMN recruitment) with an R² of 0.81. They proposed an NP hazard scale based on the *in vivo* activity of the NP surface area (Rushton et al., 2010). However, such a hazard classification related to risk (or safety) assessment of NP is still not fully established due to a lack of data on exposure processes, biokinetics, and organ-specific lung toxicity (Oberdörster, 2010; Upadhyay and Palmberg, 2018).

While the elucidation of adverse outcome pathways (AOPs) with their related cellular, tissue/organ and organism/population level key events might help to predict the toxicity of inhaled substances (Clippinger et al., 2018a; Halappanavar et al., 2019), there is still no safety classification system of substances used for oral inhalation products, including excipients, i.e. bulking agents, that are already approved by FDA for some marketed drug products. However, even larger datasets, such as those obtained by some “omics”-technologies, so far cannot overcome all limitations of *in vitro* and *in vivo* generated data. Therefore, especially the prediction of adverse effects remains a challenge (Ghallab and Bolt, 2014).

An important first step towards such an *in vitro* based safety classification might be the comparison of *in vitro* data with LD50 values, which are used as a basis for hazard classification (Strickland et al., 2018). In particular, the *in vitro* MTT assay has shown high sensitivity with regard to the cytotoxic effects of substances,

generating a simple and reproducible determination of an IC50 value (Scherließ, 2011). Sauer et al. (2013) correlated *in vivo* LD50 and *in vitro* IC50 toxicity data from standardized MTT assays for 19 chemicals in order to categorize them into four hazard classes that predict their acute inhalative toxicity *in vivo* on the basis of the *in vitro* data. The resulting comparison allowed the identification of harmful substances. However, this classification system relates *in vitro* data to animal *in vivo* data and not to human clinical data.

In order to bridge the gap between human *in vitro* and human clinical data, we attempted to correlate these directly. The *in vitro* cytotoxicity of 23 excipients, which may be employed in an FDA-approved concentration range (i.e. considered as safe), was assessed and used to set up a four-quadrant analysis to classify the safety of other excipients to be potentially used in orally inhaled drug products.

2 Material and methods

2.1 Cell lines

The human cell line A549 (ACC107; Lieber et al., 1976) was obtained from DSMZ and was cultivated in RPMI 1640 (Roswell Park Memorial Institute 1640, gibco™, Fisher Scientific, USA) supplemented with 10% FBS (fetal bovine serum, South American origin, PAN-Biotech, Germany) and 1% antibiotics (penicillin (10,000 U/mL) / streptomycin (10,000 µg/mL), gibco™, Fisher Scientific, USA). The human cell line Calu-3 (ATCC® HTB 55™; Fogh et al., 1977) was cultured in MEM (minimal essential medium, gibco™, Fisher Scientific, USA) supplemented with 10% FBS, 1% 100x MEM NEAA (non-essential amino acids solution, gibco™, Fisher Scientific, USA), 1% 100 mM sodium pyruvate solution (gibco™, Fisher Scientific, USA) and 1% antibiotics. The A549 and Calu-3 cells were maintained in a humidified atmosphere with 5% CO₂ at 37°C to passage number 50.

2.2 Selection of the test substances

The 23 substances listed in Table 1 together with the corresponding supplier and their solubility in water were used in the study. All substances are approved for a specified concentration range in parenteral or pulmonary drug application according to the Inactive Ingredient Search for Approved Drug Products¹. A compilation of the approved concentrations from this database is given in Table 2. A pulmonary-approved concentration was available for citric acid monohydrate, citric acid anhydrous, glycerol, L-ascorbic acid, polysorbate 80, and sodium chloride. Where no data for inhalation were given, the parenteral concentration was used.

2.3 Determination of the *in vitro* IC50 value

Preparation of test concentrations

Standardized MTT assays were performed to determine the *in vitro* IC50 using several dilutions of the test compounds. In the first round of assays, the concentration range was narrowed to

¹ <https://www.accessdata.fda.gov/scripts/cder/iig/index.cfm>



Tab 1: List of test substances with the related CAS number, supplier and solubility in water

Substance	CAS number	Supplier	Water solubility
Albumin from human serum	70024-90-7	Baxalta, Shire, Germany	200 g/L (20°C)
Benzoic acid	65-85-0	Roth, Germany	2.9 g/L (20°C)
Benzyl alcohol	100-51-6	Fisher Scientific, United Kingdom	40 g/L (20°C)
Citric acid monohydrate	5949-29-1	Roth, Germany	50 g/L (20°C)
Citric acid anhydrous	77-92-9	PanReac AppliChem ITW Reagents, Germany	100 g/L (20°C)
Docusate sodium	577-11-7	Sigma Aldrich, USA	15 g/L (25°C)
Glycerol	56-81-5	PanReac AppliChem ITW Reagents, Germany	Fully miscible
L(+)-Ascorbic acid	50-81-7	VWR Chemicals Belgium	50 g/L (20°C)
L-Alanine	56-41-7	PanReac AppliChem ITW Reagents, Germany	100 g/L (20°C)
L-Arginine	74-79-3	Sigma Aldrich, USA	150 g/L (20°C)
L-Cysteine	52-90-4	Roth, Germany	25 g/L (20°C)
L-Methionine	63-68-3	Sigma, Germany	25 g/L (20°C)
L-Proline	147-85-3	Roth, Germany	1500 g/L (20°C)
Palmitic acid	57-10-3	Merck, Germany	insoluble
Poloxamer 188 (Kolliphor® 188)	/	Sigma Aldrich, USA	No data available
Polyethylene glycol 200 (PEG 200)	25322-68-3	Merck, Germany	70 g/L (20°C)
Polyethylene glycol 300 (PEG 300)		Super refined™, CRODA, United Kingdom	soluble
Polyethylene glycol 400 (PEG 400)		Rotipuran®, Roth, Germany	No data available
Polyethylene glycol 600 (PEG 600)		Super refined™, CRODA, United Kingdom	soluble
Polysorbate 80 (Tween-80)	9005-65-6	Sigma Aldrich, Switzerland	Fully miscible
Polysorbate 80 (HX2)		NOF CORPORATE, Japan	No data available
Polysorbate 20 (Tween 20)	9005-64-5	Super refined™, CRODA, United Kingdom	Fully miscible
Sodium chloride	7647-14-5	Roth, Germany	> 300 g/L (20°C)

approximate the IC₅₀. The initial concentrations were chosen based on the *in vitro* classification scheme (Sauer et al., 2013) of different cell culture systems, starting from 0.1 and continuing up to 10 mg/mL. Dilutions were prepared in HBSS (Hank's Balanced Salt Solution, gibco™, Fisher Scientific, USA) the day before the MTT assay and stored at 4°C. In order to specify the IC₅₀ value in further experiments, a total of three cycles of MTT assays were performed for both cell lines. Where the IC₅₀ of an excipient exceeded 10 mg/mL, the substance was employed up to its maximal solubility in water (Tab. 1). For the relative representation of the *in vitro* IC₅₀, 1 g (undiluted substance) was set as the 100% mark to enable unit equivalence to the FDA concentration.

Cell viability measurements

2x10⁵ cells/mL A549 or Calu-3 were seeded in a 96-well plate (Greiner Bio-one, Germany) in 200 µL medium. 24 h later, the cells were visualized by light microscopy (PrimoVert, Zeiss, Ger-

many) to verify epithelial confluence of nearly 100%. The cells were washed twice with HBSS and 200 µL of the test substances were applied. After incubation for 4 h on a shaker at 35 rpm and 37°C, the cells were washed once with HBSS. 0.5 mg/mL MTT reagent (methylthiazolyl-diphenyl-tetrazolium bromide, Acros Organics, USA) was added for 4 h at 37°C and 35 rpm and protected from light. Absorbance was measured at 550 nm with a plate reader (Synergy 2, BioTek Instruments GmbH). To calculate the cell viability after substance exposure, a positive control of 1% Triton X-100 (PanReac AppliChem ITW Reagents, Germany) and a negative control of HBSS were used as described in Formula 1.

Formula 1: Calculation of the cell viability based on the absorbance measurements obtained from the MTT assay

$$\text{Viability [\%]} = \frac{(\text{absorbance}_{\text{test substance}} - \text{absorbance}_{1\% \text{ Triton X-100}})}{(\text{absorbance}_{\text{HBSS}} - \text{absorbance}_{1\% \text{ Triton X-100}})} \times 100$$



Tab. 2: List of excipients with their associated parenteral and pulmonary FDA-approved concentration from the Inactive Ingredient Search for Approved Drug Products

"No approved concentration" means that no FDA-approved product was identified.

Substance	CAS number	FDA-approved concentration range – parenteral	FDA-approved concentration range – pulmonary
Albumin from human serum	70024-90-7 FDA:9048468	0.1-2% 80% (powder for injection solution, lyophilised)	no approved concentration
Benzoic acid	65-85-0	0.0031-5%	no approved concentration
Benzyl alcohol	100-51-6	0.4-18% 9.45 mg/mL Powder for injection: 10.4 mg/mL	no approved concentration
Citric acid monohydrate	5949-29-1	0.05-38.46% 2.2-5.2 mg/mL Powder for injection: 384.46 mg	0.028% 4.04 mg/Inh 4.2 mg/mL 0.002-4.04 mg/Inh
Citric acid anhydrous	77-92-9	1-7% Powder for injection: 42.19% 2-10 mg/mL	0.56 mg/2 mL 0.0003-0.027%
Docusate sodium	577-11-7	intramuscular: 0.015%W/V	no approved concentration
Glycerol	56-81-5	2.5-15.36% 18.82 mg/mL	7.3%
L(+)-Ascorbic acid	50-81-7	50.4-62.5% Powder for injection: 0.088-48%	959.5 mg/Inh 0.11-1.02%
L-Alanine	56-41-7	no approved concentration	no approved concentration
L-Arginine	74-79-3	5-39% Powder for injection: 14-78%, 70.7 g	no approved concentration
L-Cysteine	52-90-4	0.01-0.1% Powder for injection: 2.6%	no approved concentration
L-Methionine	63-68-3	0.004-49.2%	no approved concentration
L-Proline	147-85-3	0.34-35.6%	no approved concentration
Palmitic acid	57-10-3	0.001%	no approved concentration
Poloxamer 188 (Kolliphor® 188)	/	0.2-0.6%	no approved concentration
Polyethylene glycol 200 (PEG 200)	25322-68-3	intramuscular: 30%	no approved concentration
Polyethylene glycol 300 (PEG 300)		4.42-65% 320 mg/5 mL 650 mg/1 mL	no approved concentration
Polyethylene glycol 400 (PEG 400)		0.49-75.58% 0.67 mL/1 mL	no approved concentration
Polyethylene glycol 600 (PEG 600)		5%	no approved concentration
Polysorbate 80 (Tween-80)	9005-65-6	0.5-63% 260 mg/1 mL 400 mg/ 5mL	0.02 µg 0.22 mg 0.37 mg/2 mL 0.02-0.04%
Polysorbate 80 (HX2)			
Polysorbate 20 (Tween 20)	9005-64-5	0.003-4.8% Powder for injection: 0.044% 10 mg/mL	no approved concentration
Sodium chloride	7647-14-5	0.9-90% 9-18 mg/1 mL 801.1 µl/1 mL	11.25 mg/5 mL 8 mg/1 mL 8.5-27 mg/3 mL 0.9-1.13%

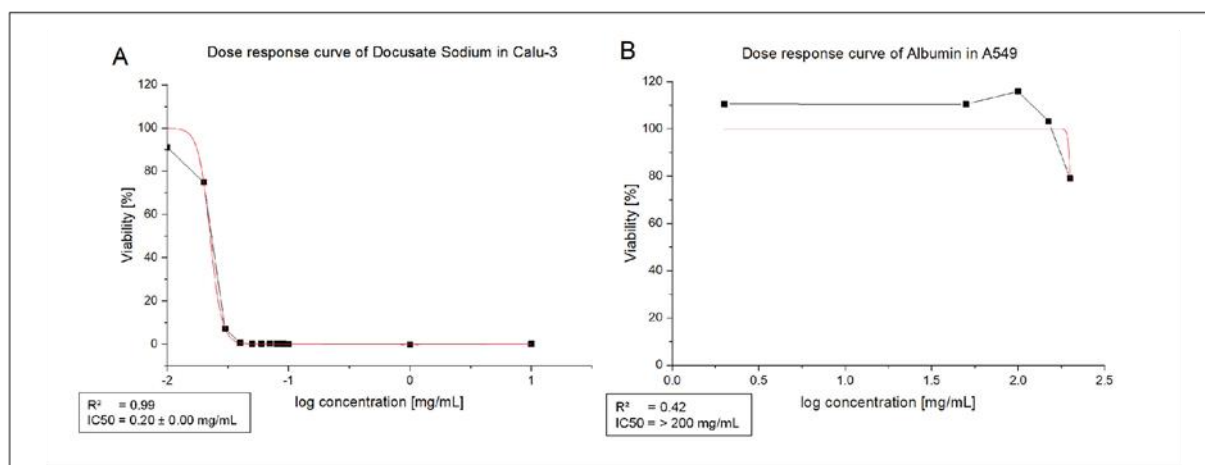


Fig. 1: Exemplary presentation of the dose response curve of docusate sodium in Calu-3 and albumin from human serum in A549 for determination of the IC₅₀ *in vitro*

The applied concentration is given in mg/mL, whereby the maximal concentration is set to 1 g (undiluted substance). The red line indicates the sigmoidal fit used for calculation of the IC₅₀ by OriginPro® 2019. (A) Dose response curve of docusate sodium tested on Calu-3 cells; the IC₅₀ is 0.02%. The coefficient of determination (R^2) is 0.99, indicating a good fit. (B) Dose response curve of albumin tested on A549 cells; the IC₅₀ cannot be determined even up to the maximal solubility of 200 mg/mL.

Generation of dose response curves and calculation of the *in vitro* IC₅₀

The software OriginPro® 2019 (additive, Germany) was used for IC₅₀ calculations based on a dose response curve. The concentrations were applied in a logarithmic scale. A sigmoidal fit was performed with a top asymptote set to 100% viability and the bottom asymptote to 0% viability.

2.4 Statistics

For the IC₅₀ determination performed on Calu-3 cells, 3 technical replicates (wells) in 3 independent experiments for each investigated concentration were performed. The IC₅₀ values calculated from A549 data were based on $n = 3$ wells per concentration in several experiments performed to determine the IC₅₀ and narrow the concentrations tested next to it. Details are listed in the supplementary information in each graph. Data are summarized as the mean \pm SD. Dose response curves and the correlation analysis were performed with the software OriginPro® 2019. A linear fit without weighting parameters was performed to calculate the Pearson r correlation coefficient.

3 Results

3.1 IC₅₀ of excipients

The effects of the excipients on the viability of Calu-3 and A549 were determined for 23 excipients with a standardized MTT assay. The IC₅₀ is given in % and scaled logarithmically. Two examples of dose response curves and the calculation of the test-

ed excipient are shown for docusate sodium (CAS: 577-11-7) on Calu-3 cells (Fig. 1A) and albumin from human serum for A549 (Fig. 1B). Docusate sodium has an IC₅₀ of 0.02% tested on Calu-3 cells. For albumin, no determination of the IC₅₀ value on A549 was possible (IC₅₀ > 200 mg/mL). The dose response curves with the IC₅₀ calculation for all tested excipients are shown in Figures S1 and S2².

The *in vitro* IC₅₀ values are listed in Table 3. For the substances albumin from human serum, L-alanine, L-cysteine, L-methionine, palmitic acid, poloxamer 188, and the polyethylene glycols (PEG) 200-600, no calculation of the IC₅₀ was possible in their aqueous solubility range.

No converging fit was obtained in the testing of glycerol (Calu-3), L-proline (A549), and sodium chloride (A549 and Calu-3), but an approximation of the IC₅₀ by the software was possible. *In vitro* calculation of the IC₅₀ was successful for the remaining 11 excipients. The results were compared to the classification by Sauer et al. (2013) (Tab. 3). A comparison of A549 and Calu-3 showed that the observed IC₅₀ values were in a similar range but did not correlate in a regression analysis (Fig. S3¹; Tab. S2¹).

3.2 Linear correlation of FDA-approved concentration range and *in vitro* IC₅₀

For evaluation of the linear correlation between the *in vitro* IC₅₀ value and the approved FDA concentration, regression analysis was performed.

Calu-3 IC₅₀ values (Tab. 3) of the substances benzyl alcohol, citric acid monohydrate, citric acid anhydrous, docusate sodium, glycerol, L-ascorbic acid, L-arginine, L-cysteine, L-proline,

² doi:10.14573/alltex.1910231s



Tab. 3: List of excipients with the IC50 [%] in A549 and Calu-3 cells in comparison to the classification by Sauer et al. (2013)

Substance	CAS number	A549 IC50 <i>in vitro</i> [%]	Calu-3 IC50 <i>in vitro</i> [%]	Classification according to Sauer et al. (2013)
Albumin from human serum	/	> 20 (solubility reached)	> 20 (solubility reached)	Class 4
Benzoic acid	65-85-0	0.048 ±0.100	not measured	Class 2
Benzyl alcohol	100-51-6	0.344 ±0.013	0.305 ±0.032	Class 3
Citric acid monohydrate	5949-29-1	0.095 ±0.003	0.038 ±0.001	Class 2
Citric acid anhydrous	77-92-9	0.018 ±0.003	0.032 ±0.001	Class 2
Docusate sodium	577-11-7	0.020 ±0.001	0.002 ±0.000	Class 1-2
Glycerol	56-81-5	38.875 ±0.054	Fit does not converge (range 1-25)	Class 4
L(+)-Ascorbic acid	50-81-7	0.092 ±0.002	0.017 ±0.003	Class 2
L-Alanine	56-41-7	> 10	> 10	Class 4
L-Arginine	74-79-3	2.162 ±0.220	0.946 ±0.070	Class 4
L-Cysteine	52-90-4	> 2.5	1.214 ±0.087	Class 4
L-Methionine	63-68-3	> 2.5	> 2.5	Class 4
L-Proline	147-85-3	Fit does not converge (range 19-25)	11.651 ±0.629	Class 4
Poloxamer 188 (Kolliphor® 188)	/	solubility reached	solubility reached	Class 4
Polyethylene glycol 200 (PEG 200)	25322-68-3	> 10	> 10	Class 4
Polyethylene glycol 300 (PEG 300)				Class 4
Polyethylene glycol 400 (PEG 400)				Class 4
Polyethylene glycol 600 (PEG 600)				Class 4
Polysorbate 80 (Tween-80)	9005-65-6	0.147 ±0.017	1.117±0.071	Class 3
Polysorbate 80 (HX2)		0.118 ±0.007	0.224 ±0.030	Class 3-4
Polysorbate 20 (Tween 20)	9005-64-5	0.024 ±0.009	0.120 ±0.011	Class 2-3
Sodium chloride	7647-14-5	Fit does not converge (range 1-10)	Fit does not converge (range 1-10)	Class 4

polysorbate 80, polysorbate 80 HX2, polysorbate 20, and sodium chloride were plotted against the approved FDA concentration (Tab. 2). The percentage ranges of the FDA concentrations given for the pulmonary and parenteral application were included. Figure 2 shows a positive slope of the regression line of 0.42 ± 0.12 and a coefficient of determination (COD, R^2) of 0.31, indicating a poor correlation.

Next, a regression analysis was performed for the A549 cell line (Fig. 3). The IC50 values (Tab. 3) and the FDA-approved concentrations (Tab. 2) for benzoic acid, benzyl alcohol, citric acid monohydrate, citric acid anhydrous, docusate sodium, glycerol, L-ascorbic acid, L-arginine, L-proline, polysorbate 80, polysorbate 80 HX2, polysorbate 20, and sodium chloride were plotted. A positive slope of the regression line of 0.60 ± 0.12 was obtained by performing a correlation analysis with an R^2 of 0.49. In comparison to the correlation using the Calu-3 cell line, the R^2 indicates in the A549 plot a slightly better correlation.

3.3 The safety assessment for excipients (SAFE)

3.3.1 Safety assessment based on the IC50 *in vitro* and the FDA-approved concentration

The drawback of the linear regression analysis using the FDA data is that there might be some buffer for a higher approved concentration as the approved value cannot be compared with an LD50 derived from animals. However, knowledge from the Sauer et al. (2013) publication can be utilized to consider known hazard effects. Using the classification suggested in that paper on the IC50 values of the tested excipients against the FDA-approved concentration range, a four-class division was obtained.

The concentration of 0.1% (1 mg/mL) was determined as a critical concentration for the IC50 due to the first occurrence of toxicological effects in the cellular test system according to the acute toxicity classification of the UN (class #1-2: fatal if inhaled, class #3: toxic if inhaled, class #4-5: harmful and maybe

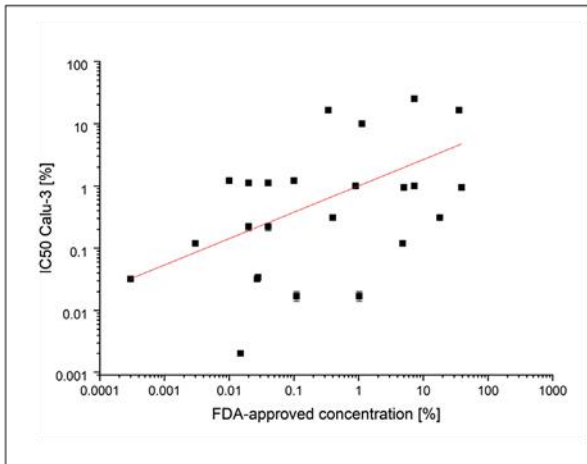


Fig. 2: Regression analysis of IC50 [%] *in vitro* in Calu-3 cells vs FDA approved concentration range [%]

The concentration of the calculated *in vitro* IC50 values was based on a maximal concentration of 1 g. The approved concentrations were obtained from the FDA's database on inactive ingredients. The values for the linear regression analysis are: slope: 0.42 ± 0.13 , sum square of errors: 20.90; Pearson R: 0.55; coefficient of determination (COD, R^2): 0.31; Correlation R^2 : 0.28.

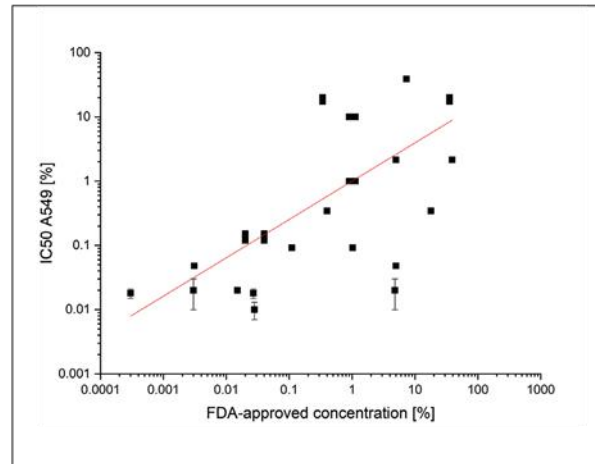


Fig. 3: Regression analysis of IC50 [%] *in vitro* in A549 cells vs approved FDA concentration range [%]

The concentration of the calculated *in vitro* IC50 values was based on a maximal concentration of 1 g. The approved concentrations were obtained from the FDA's database on inactive ingredients. The values for the linear regression analysis are: slope: 0.60 ± 0.12 , sum square of errors: 18.24; Pearson R: 0.70; coefficient of determination (COD, R^2): 0.49; Correlation R^2 : 0.47.

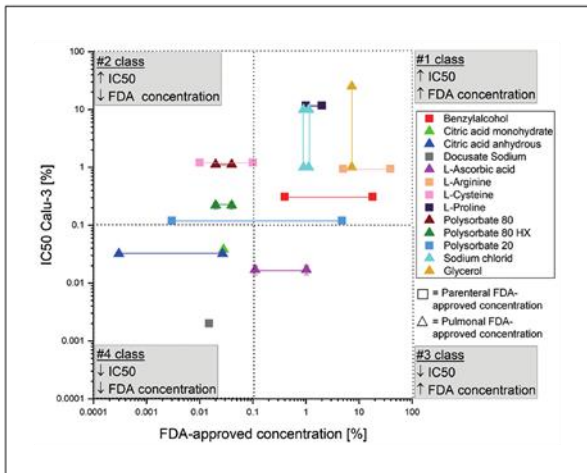


Fig. 4: The IC50 values of the excipients tested in the Calu-3 cell line and the FDA-approved concentration ranges can be set up in a four-class system

The diagram consists of the calculated IC50 values plotted against the approved FDA concentrations (squares: parenteral approved concentration, triangles: pulmonary approved concentration) for the tested excipients. Dividing this diagram into four regular squares from 0.1% IC50 to 0.1% FDA and up to 100% IC50/FDA, results in a four-class system. #1 class: high IC50, high FDA-approved concentration, #2 high IC50, low FDA-approved concentration, #3 class: low IC50, high FDA-approved concentration, #4 class: low IC50, low FDA-approved concentration.

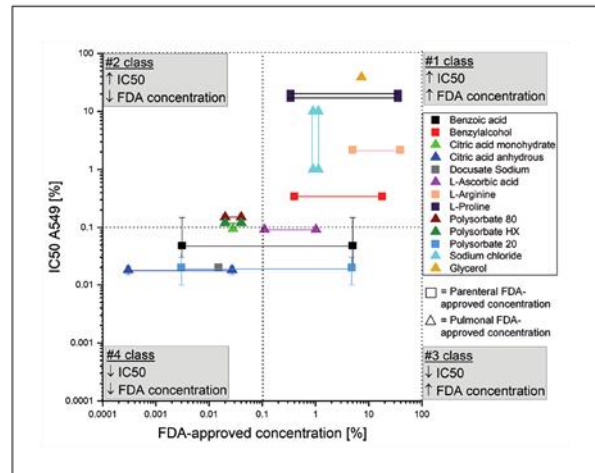


Fig. 5: The IC50 values of the excipients tested in the A549 cell line and the FDA-approved concentration ranges can be set up in a four-class system

The diagram consists of the calculated IC50 values plotted against the approved FDA concentrations (squares: parenteral approved concentration, triangles: pulmonary approved concentration) for the tested excipients. Dividing this diagram into four regular squares from 0.1% IC50 to 0.1% FDA and up to 100% IC50/FDA, results in a four-class system. #1 class: high IC50, high FDA-approved concentration, #2 high IC50, low FDA-approved concentration, #3 class: low IC50, high FDA-approved concentration, #4 class: low IC50, low FDA-approved concentration.



Tab. 4: Line-up of the four class-based classification by Sauer et al. (2013) and the tested concentrations ranges for the SAFE-approach in %

<i>In vitro</i> hazard class	Concentration range for cell monolayer [mg/mL] (Sauer et al., 2013)	Concentration range for SAFE-classification [%]
# 1	< 0.1	< 0.01
# 2	0.1-1	0.01-0.1
# 3	1-10	0.1-1
# 4	> 10	1

harmful if inhaled (United Nations, 2017)). The excipients with an IC50 below 0.1% were categorized in classes 1 and 2 according to Sauer et al. (2013) (Tab. 4). Above an IC50 of 0.1%, no safety concerns are obvious, so that a resulting classification into class 4 is likely. The corresponding classification of all tested excipients according to the system proposed by Sauer et al. (2013) is shown in Table 3.

A four-class system is obtained by setting 0.1% as the limit line of cellular toxicity effects and outlining evenly distributed squares in the plot of IC50 and the approved FDA concentration. In class 1, the *in vitro* IC50 and the FDA-approved concentration are consistently high. For the Calu-3 cell line, benzyl alcohol, glycerol, L-proline, sodium chloride, L-arginine and, in the border region, polysorbate-20, were categorized as class 1. These excipients are non-toxic according to the system of Sauer et al. (2013). In the A549 cell line, class 1 substances have similar values, except polysorbate 20, which is categorized as class 3-4. Class 2 is the quadrant to the left, which is characterized by a high IC50 value and a lower FDA-approved concentration. Polysorbate 80, polysorbate 80 HX2, polysorbate 20, and L-cysteine tested on Calu-3 cells, and polysorbate 80 and polysorbate 80 HX2 tested on A549 cells fall into class 2. Class 3 is characterized by a high FDA-approved concentration and a low IC50 value. L-ascorbic acid tested on Calu-3 belongs to this class, whereas in A549 L-ascorbic acid, benzoic acid and polysorbate 20 are classified here. Class 4 contains the squares at the intersection with a low IC50 value and a corresponding low FDA concentration. Citric acid, docusate sodium, and benzoic acid fall into this category for Calu-3, with an additional test of benzoic acid and citric acid on the limit zone to class 3 on A549. This classification system is visualized for Calu-3 in Figure 4 and for A549 in Figure 5.

3.3.2 Consequences of the four classes for safety assessment of excipients (SAFE)

The SAFE classification can help to estimate, based on *in vitro* IC50 data, whether pulmonary administration to humans will be safe or not. This estimation is based on the results presented in Figures 4 and 5. The concentration of 0.1% (which indicates problems with the animal toxicity study in the preclinical phase) forms the center of the coordinate system and is the dividing line for the resulting classification (Fig. 6).

A higher IC50, which is above 0.1% (classes 1 and 2), is worth considering for further development. A lower IC50 below 0.1%,

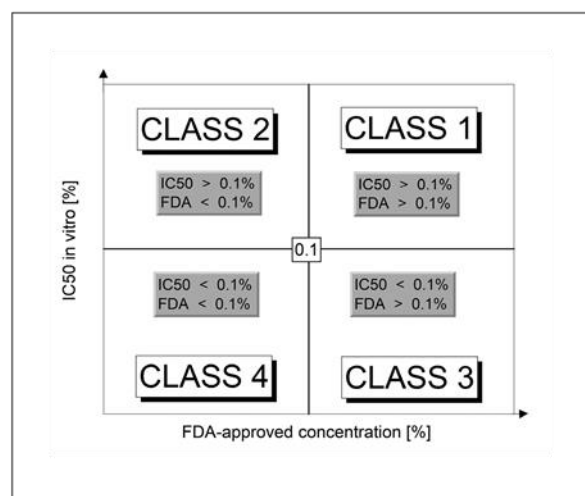


Fig. 6: The SAFE classification

Divided into 4 classes, SAFE gives an indication of the categorization of the *in vitro* IC50 value to the FDA-approved concentration. Arrangement of the 4 classes: Class 1: IC50 is higher than 0.1%, the correlated FDA concentration is higher than 0.1%; Class 2: IC50 is higher than 0.1%, the correlated FDA concentration is lower than 0.1%; Class 3: IC50 is lower than 0.1%, the correlated FDA concentration is higher than 0.1%; Class 4: IC50 is lower than 0.1%, the correlated FDA concentration is lower than 0.1%.

which is here referred to as classes 3 and 4, is not recommended for further development. The target class 1 implements a high IC50 and a high FDA-approved concentration, making it the most appropriate class to continue with further testing and potential use in humans. Most tested excipients are classified in this non-toxic category and no safety issues are expected during subsequent pre-clinical and clinical development. In class 2, the tested *in vitro* concentration could be increased in view of a higher FDA-approved concentration. In classes 3 and 4, in correspondence with the classification by Sauer et al. (2013), cytotoxicity is obvious, and therefore considering such compounds for further development steps may be risky. For a class 4 substance, the approval requirements are likely to be complicated.



The *SAFE* system helps to estimate the risk of excipients and the chance of obtaining FDA approval by using them in new drug formulations.

4 Discussion

The concept of an *in vitro-in vivo*-correlation (IVIVC) aims to predict the bioavailability and the efficacy of the tested drug product based on its release kinetics (Barakat et al., 2015; Shen and Burgess, 2016) in relation to the Biopharmaceutical Classification System (BCS) adapted by the FDA (CDER/FDA, 2017). In line with this classic BCS, a pulmonary biopharmaceutical classification (pBCS) was described, implementing the impacts of lung biology in terms of lung metabolism, drug-drug interactions, presence of transporters and mucus, protein binding, clearance, surfactant, and formulation properties like size, solubility, and used excipients (Hastedt et al., 2016; Gonda, 2006). Despite the consideration of all these physiological aspects, no linear IVIVC can predict the *in vivo* response in the lung on the basis of an *in vitro* dose dependency (Eixarch et al., 2010). Therefore, an *in vitro* testing strategy for predicting the respiratory toxicity of chemicals and drug products is still needed. One initial step toward this goal is the development of a classification system to predict the safety of chemicals and drug products.

The present work is an attempt to break down the complexity of the physiological aspects of the lung to gradually approach an *in vitro* test strategy for orally inhaled drug products that can support formulation development by addressing cytotoxicity towards pulmonary epithelial cells. Sauer et al. (2013) already established an *in vitro* hazard classification system by correlating IC50 values of 19 substances tested in 3 cellular systems for different incubation periods (A549 – 24 hours; EpiAirway™ – 3 hours; MucilAir™ system – 24 hours) with the GHS classification. We slightly modified the experimental setup of Sauer et al. (2013) by shortening the incubation period to 4 h, in order to consider the exposure period mentioned in the OECD acute inhalation toxicity guideline 436 (OECD, 2009), and by using A549 and Calu-3 cells. Challenge of the cells with the test compounds in a salt buffer for 4 instead of 24 h was intended to reduce the influence of both cell proliferation and the incubation medium on the results.

The resulting *in vitro* hazard classification includes different concentration ranges for the cellular systems to predict GHS respiratory category. Independent of the chosen cell system and incubation period, a concentration of 0.1% was in all cases associated with GHS category ≤ 3 . The classification according to Sauer et al. (2013) formed the basis for the *in vitro* IC50 limiting value of 0.1% of the *SAFE* classification. In summary, there is no guarantee to have a safe compound when the IC50 is above the threshold of 0.1%, but it is a clear indication. We recommend when developing a new drug product also to test prolonged incubation periods and other cell types as applicable.

To obtain an IVIVC based on the *in vitro* IC50 evaluation, we attempted to correlate the *in vitro* data on the excipients with the *in vivo* LD50 based GHS classification. A direct comparison with

the GHS classification based on oral LD50 data is not possible for pharmaceutical excipients as most of them are classified as safe (GHS class 4/5, see Tab. S1¹). However, upon compilation of the GHS classification for acute pulmonary toxicity of the tested excipients (Tab. S1¹), we found a large data gap for pulmonary LD50 values, so that no effective, direct correlation of the IC50 values with the *in vivo* data on pulmonary toxicity was possible (ECHA, search for chemicals, guidance on the safe use of the substance; Rowe et al., 2009; GESTIS *Stoffdatenbank*; search in NICEATM Integrated Chemical Environment data base (ICE)).

For pulmonary classification, the exposure route is divided into gases, vapors, dusts and mists (United Nations, 2017). No increased GHS classes were obtained for these application forms. Gases of benzyl alcohol were assigned GHS Class 1, while docusate sodium, sodium chloride, and polysorbate 20 were assigned to GHS Class 2. This use of different routes of administration *in vivo* makes it difficult to achieve a standardized *in vitro* comparison.

More complex cell culture systems have been developed with the aim of achieving a better IVIVC (Fizeşan et al., 2018). By testing the cytotoxicity of inhaled drug products in a commercially available human 3D cellular model of the lung (MucilAir), Sivars et al. (2018) found a good correlation of *in vitro* respiratory toxicity data based on measurement of cell barrier integrity, cell viability, ciliary beating frequency (CBF), mucociliary clearance, and the resulting cytokine release, with *in vivo* toxicity data.

In the mentioned study, MucilAir was cultivated under serum-free conditions to avoid the use of FCS, which is associated with pain and suffering of the animals from which it is obtained. The amount and type of serum proteins is of particular importance as they can influence the binding and activity of compounds and nanomaterials (Drasler et al., 2017; Moore et al., 2015). Therefore, we challenged the cells in salt buffer without FCS, but also intend to replace FCS in the culture medium by defined supplements in future studies.

In addition to the more complex 3D cell culture systems like MucilAir, attempts have been made in recent years to recreate the physiology of the lung using microfluidic systems. Huh et al. (2011) were able to reconstitute the toxic and inflammatory responses of the lung in comparison to exposure data of silica particles from mice by using a “lung-on-a-chip” device. However, more complex systems such as co-cultures or chip-based systems are challenging to validate (Huh et al., 2011; Dipasri et al., 2016).

The *in vitro* test strategy we followed in this study might be extended and combined with further specific methods (e.g., surfactometry) and summarized into a safety assessment of the test compound. Such integrated test strategies for the *in vitro* prediction of acute inhalation toxicity were discussed in 2018 at the workshop “Alternative approaches for acute inhalation toxicity testing to address global regulatory and non-regulatory data requirements” (Clippinger et al., 2018b). The paper summarizes the current state of inhalative *in vitro* technologies as well as the criteria that must still be met to overcome the obstacles for guideline acceptance, such as an information transfer from animal experiments, the correct application of dosimetry and realization to industrial applications with their resulting technical needs.



The toxic effects of substances in the lung depend on different parameters, such as airborne concentration, particle size, solubility in surfactant, reactivity, air exchange, rate of exposure, interactions with other inhaled substances, and the specific immunological response (Bakand et al., 2005). In particular, the consideration of the immunological reaction of the test system is a major part of the safety assessment of a compound. By setting up a tetraculture of A549, HMC-1, THP-1, and EA.hy 926 and using the Vitrocell® CLOUD system, Klein et al. (2013) could show that inflammatory responses are overpredicted under submerged conditions. This could be an explanation for cases where the FDA-approved concentration was high but the IC50 value was low (*SAFE* class 3). To avoid this overestimation, air-liquid interface (ALI) exposure systems – potentially covered with mucus or surfactant – and the dosimetry should be taken into account (Paur et al., 2011).

In order to investigate nanomaterials, existing *in vitro* assays such as the NR8383 alveolar macrophage assay described by Wiemann et al. (2018) can be combined with *SAFE*, taking ongoing discussions on dosimetry (Wiemann et al., 2018; Schmid and Cassee, 2017) and experimental setups (Kong et al., 2011) into account. Dosimetry is an important aspect of focusing the deposition of particles or substances in the alveolar region. Donaldson et al. (2008) obtained a high IVIVC by expressing the dose in terms of A549 cell culture surface area. Schmid and Stoeger (2016) set up a dose-response curve by plotting the particle surface area against the acute inflammatory reaction (PMN influx), attaining a high R^2 of 0.77.

Next to the inflammatory reaction, the influence of compounds on lung surfactant is important as some substances can cause alveolar collapse after inhalation (King, 1982; Schleh et al., 2013). To investigate the influence of airborne substances on lung surfactant, Sørli et al. (2016) established the constrained drop surfactometer (CDS). Their results indicate that the size and the effect of the applied substance on the surface tension of the lung surfactant has an impact on the toxic effect, and can be employed to predict alveolar collapse.

These results from surfactometry as well as the investigation of the inflammatory response induced by substances in the lung indicate that safety investigations of orally inhaled drug products should not be limited to concentration-dependent cytotoxicity tested in a monolayer as in the present work. Nonetheless, the *SAFE* system may assist at early stages of formulation development by relating concentrations in formulations of FDA-approved drug products to concentrations used in human epithelial cell culture experiments. To further expand this approach, inflammatory effects such as the cytokine secretion of macrophages, transport studies to estimate bioavailability, the role of active transporters, and possible interactions with non-cellular barriers (e.g., mucus or surfactant) may be considered as additional endpoints for the safety assessments of orally inhaled drug products.

References

Adams, C. P. and Van Brantner, V. (2006). Market watch: Estimating the cost of new drug development: Is it really \$802 mil-

- lion? *Health Aff* 25, 420-428. doi:10.1377/hlthaff.25.2.420
- Bakand, S., Winder, C., Khalil, C. et al. (2005). Toxicity assessment of industrial chemicals and airborne contaminants: Transition from *in vivo* to *in vitro* test methods: A review. *Inhal Toxicol* 17, 775-787. doi:10.1080/08958370500225240
- Barakat, A., Krämer, J., de Souza Carvalho, C. et al. (2015). *In vitro-in vivo* correlation: Shades on some non-conventional dosage forms. *Dissolut Technol* 22, 19-22. doi:10.14227/DT220215P19
- Bracken, M. B. (2009). Why animal studies are often poor predictors of human reactions to exposure. *JR Soc Med* 102, 120-122. doi:10.1258/jrsm.2008.08k033
- CDER, FDA (2017). Guidances for Industry: Waiver of *In Vivo* Bioavailability and Bioequivalence Studies for Immediate-Release Solid Oral Dosage Forms Based on a Biopharmaceutics Classification System. <https://www.fda.gov/downloads/Drugs/Guidances/ucm070246.pdf>
- Chary, A., Hennen, J., Klein, S. G. et al. (2018). Respiratory sensitization: Toxicological point of view on the available assays. *Arch Toxicol* 92, 803-822. doi:10.1007/s00204-017-2088-5
- Clippinger, A. J., Allen, D., Behrsing, H. et al. (2018a). Pathway-based predictive approaches for non-animal assessment of acute inhalation toxicity. *Toxicol In Vitro* 52, 131-145. doi:10.1016/j.tiv.2018.06.009
- Clippinger, A. J., Allen, D., Jarabek, A. M. et al. (2018b). Alternative approaches for acute inhalation toxicity testing to address global regulatory and non-regulatory data requirements: An international workshop report. *Toxicol In Vitro* 48, 53-70. doi:10.1016/j.tiv.2017.12.011
- DiMasi, J. A., Grabowski, H. G. and Hansen, R. W. (2016). Innovation in the pharmaceutical industry: New estimates of R&D costs. *J Health Econ* 47, 20-33. doi:10.1016/j.jhealeco.2016.01.012
- Dipasri, K., Devarasetty, M., Yildiz, D. V. et al. (2016). Lung-on-a-chip technologies for disease modeling and drug development. *Biomed Eng Comput Biol* 7, Suppl 1, 17-27. doi:10.4137/BECS.S34252
- Donaldson, K., Borm P. J. A., Oberdorster, G. et al. (2008). Concordance between *in vitro* and *in vivo* dosimetry in the proinflammatory effects of low-toxicity, low-solubility particles: The key role of the proximal alveolar region. *Inhal Toxicol* 20, 53-62. doi:10.1080/08958370701758742
- Drasler, B., Sayreb, P., Steinhäuser, K. G. et al. (2017). *In vitro* approaches to assess the hazard of nanomaterials. *NanoImpact* 8, 99-116. doi:10.1016/j.impact.2017.08.002
- Eixarch, H., Haltner-Ukomadu, E., Beisswenger, C. et al. (2010). Drug delivery to the lung: Permeability and physicochemical characteristics of drugs as the basis for a pulmonary biopharmaceutical classification system (pBCS). *J Epithel Biol Pharmacol* 3, 1-14.
- EMA (2016). Guideline on the Principles of Regulatory Acceptance of 3Rs (Replacement, Reduction, Refinement) Testing Approaches. EMA/CHMP/CVMP/JEG-3Rs/450091/2012. https://www.ema.europa.eu/en/documents/scientific-guideline/guideline-principles-regulatory-acceptance-3rs-replacement-reduction-refinement-testing-approaches_en.pdf



- FDA (1997). Guidance for Industry: Drug Metabolism / Drug Interaction Studies in the Drug Development. http://www.washingtonlifescience.com/patient/drug_develop/pdfs/clin3.pdf
- Fizeşan, I., Cambier, S., Moschini, E. et al. (2018). In vitro cellular models, a resourceful tool in respiratory toxicology. *Farmacia* 66, 573-580. doi:10.31925/farmacia.2018.4.2
- Fogh, J., Fogh, J. M. and Orfeo, T. (1977). One hundred and twenty-seven cultured human tumor cell lines producing tumors in nude mice. *J Natl Cancer Inst* 59, 221-226. doi:10.1093/jnci/59.1.221
- Fröhlich, E. (2017). Toxicity of orally inhaled drug formulations at the alveolar barrier: Parameters for initial biological screening. *Drug Deliv* 24, 891-905. doi:10.1080/10717544.2017.133172
- Ghallab, A. and Bolt, H. M. (2014). In vitro systems: Current limitations and future perspectives. *Arch Toxicol* 88, 2085-2087. doi:10.1007/s00204-014-1404-6
- Gonda, I. (2006). Systemic delivery of drugs to humans via inhalation. *J Aerosol Med* 19, 47-53. doi:10.1089/jam.2006.19.47
- Halappanavar, S., Ede, J. D., Shatkin, J. A. et al. (2019). A systematic process for identifying key events for advancing the development of nanomaterial relevant adverse outcome pathways. *NanoImpact* 15, 100178. doi:10.1016/j.impact.2019.100178
- Harrison, R. K. (2016). Phase II and phase III failures: 2013-2015. *Nat Rev Drug Discov* 15, 817-818. doi:10.1038/nrd.2016.184
- Hastedt, J. E., Bäckman, P., Clark, A. R. et al. (2016). Erratum to: Scope and relevance of a pulmonary biopharmaceutical classification system AAPS/FDA/USP Workshop March 16-17th, 2015 in Baltimore, MD. *AAPS Open* 2, 4. doi:10.1186/s41120-016-0005-2
- Huh, D., Hamilton, G. A. and Ingber, D. E. (2011). From 3D cell culture to organs-on-chips. *Trends Cell Biol* 21, 745-754. doi:10.1016/j.tcb.2011.09.005
- King, R. J. (1982). Pulmonary surfactant. *J Appl Physiol Respir Environ Exerc Physiol* 53, 1-8. doi:10.1152/jappl.1982.53.1.1
- Klein, S. G., Serchi, T., Hoffmann, L. et al. (2013). An improved 3D tetra-culture system mimicking the cellular organisation at the alveolar barrier to study the potential toxic effects of particles on the lung. *Part Fibre Toxicol* 10, 31. doi:10.1186/1743-8977-10-31
- Kong, B., Seog, J. H., Graham, L. M. et al. (2011). Experimental considerations on the cytotoxicity of nanoparticles. *Nanomedicine* 6, 929-941. doi:10.2217/nmm.11.77
- Li, A. P. (2004). Accurate prediction of human drug toxicity: A major challenge in drug development. *Chem Biol Interact* 150, 3-7. doi:10.1016/j.cbi.2004.09.008
- Lieber, M., Smith, B., Szakal, A. et al. (1976). A continuous tumor-cell line from a human lung carcinoma with properties of type II alveolar epithelial cells. *Int J Cancer* 17, 62-70. doi:10.1002/ijc.2910170110
- Mahmoudi, M., Hofmann, H., Rothen-Rutishauser, B. et al. (2012). Assessing the in vitro and in vivo toxicity of superparamagnetic iron oxide nanoparticles. *Chem Rev* 112, 2323-2338. doi:10.1021/cr2002596
- Moore, T., Rodriguez-Lorenzo, L., Hirsch, V. et al. (2015). Nanoparticle colloidal stability in cell culture media and impact on cellular interactions. *Chem Soc Rev* 44, 6287-6305. doi:10.1039/C4CS00487F
- Oberdörster, G. (2010). Safety assessment for nanotechnology and nanomedicine: Concepts of nanotoxicology. *J Intern Med* 267, 89-105. doi:10.1111/j.1365-2796.2009.02187.x
- OECD (2000). Guidance Document on the Recognition, Assessment and Use of Clinical Signs as Humane Endpoints for Experimental Animals Used in Safety Evaluation. *OECD Series on Testing and Assessment No. 19*. OECD Publishing, Paris. doi:10.1787/9789264078376-en.
- OECD (2009). Test No. 436: Acute Inhalation Toxicity – Acute Toxic Class Method. *OECD Guidelines for the Testing of Chemicals, Section 4*. OECD Publishing, Paris. doi:10.1787/9789264076037-en
- OECD (2018a). Test No. 442E: In Vitro Skin Sensitisation Assays Addressing the Key Event on Activation of Dendritic Cells on the Adverse Outcome Pathway for Skin Sensitisation. *OECD Guidelines for the Testing of Chemicals, Section 4*. OECD Publishing, Paris. doi:10.1787/9789264264359-en
- OECD (2018b). Guidance Document on Good In Vitro Method Practices (GIVIMP). *OECD Series on Testing and Assessment No. 286*. OECD Publishing, Paris. doi:10.1787/9789264304796-en
- Paur, H. R., Cassee, F. R., Teeguarden, J. et al. (2011). In-vitro cell exposure studies for the assessment of nanoparticle toxicity in the lung – A dialog between aerosol science and biology. *J Aerosol Sci* 42, 668-692. doi:10.1016/j.jaerosci.2011.06.005
- Pritchard, J. F., Jurima-Romet, M., Reimer, M. L. J. et al. (2003). Making better drugs: Decision gates in non-clinical drug development. *Nat Rev Drug Discov* 2, 542-553. doi:10.1038/nrd1131
- Rowe, C. R., Sheskey, P. J. and Quinn, E. M. (eds.) (2009). *Handbook of Pharmaceutical Excipients*. 6th edition. London, UK: Pharmaceutical Press. <http://pharmama.info/wp-content/uploads/2018/10/Excipients.pdf>
- Rushton, E. K., Jiang, J., Leonard, S. S. et al. (2010). Concept of assessing nanoparticle hazards considering nanoparticle dose-metric and chemical/biological response-metrics. *J Toxicol Environ Health A* 73, 445-461. doi:10.1080/15287390903489422
- Sauer, U. G., Vogel, S., Hess, A. et al. (2013). In vivo-in vitro comparison of acute respiratory tract toxicity using human 3D airway epithelial models and human A549 and murine 3T3 monolayer cell systems. *Toxicol In Vitro* 27, 174-190. doi:10.1016/j.tiv.2012.10.007
- Scherließ, R. (2011). The MTT assay as tool to evaluate and compare excipient toxicity in vitro on respiratory epithelial cells. *Int J Pharm* 411, 98-105. doi:10.1016/j.ijpharm.2011.03.053
- Schleh, C., Kreyling, W. G. and Lehr, C. M. (2013). Pulmonary surfactant is indispensable in order to simulate the in vivo situation. *Part Fibre Toxicol* 10, 6. doi:10.1186/1743-8977-10-6
- Schmid, O. and Stoeger, T. (2016). Surface area is the biologically most effective dose metric for acute nanoparticle toxicity in the lung. *J Aerosol Sci* 99, 133-143. doi:10.1016/j.jaerosci.2015.12.006



- Schmid, O. and Cassee, F. R. (2017). On the pivotal role of dose for particle toxicology and risk assessment: Exposure is a poor surrogate for delivered dose. *Part Fibre Toxicol* 14, 52. doi:10.1186/s12989-017-0233-1
- Shen, J. and Burgess, D. J. (2016). In vitro-in vivo correlation for complex non-oral drug products: Where do we stand? *J Contol Release* 219, 644-651. doi:10.1016/j.jconrel.2015.09.052
- Silva, E. D. and Sørli, J. B. (2018). Animal testing for acute inhalation toxicity : A thing of the past ? *Appl In Vitro Toxicol* 4, 89-90. doi:10.1089/aivt.2017.0037
- Sivars, K. B., Sivars, U., Hornberg, E. et al. (2018). A 3D human airway model enables prediction of respiratory toxicity of inhaled drugs in vitro. *Toxicol Sci* 162, 301-308. doi:10.1093/toxsci/kfx255
- Strickland, J., Clippinger, A. J., Allen, D. et al. (2018). Status of acute systemic toxicity testing requirements and data uses by U.S. regulatory agencies. *Regul Toxicol Pharmacol* 94, 183-196. doi:10.1016/j.yrtph.2018.01.022
- Sørli, J. B., Da Silva, E., Bäckman, P. et al. (2016). A proposed in vitro method to assess effects of inhaled particles on lung surfactant function. *Am J Respir Cell Mol Biol* 54, 306-311. doi:10.1165/rcmb.2015-0294MA
- United Nations (2017). GHS Classification. Part 3: Health Hazards. 115-116. http://www.unece.org/leadadmin/DAM/trans/danger/publi/ghs/ghs_rev02/English/03e_part3.pdf
- Upadhyay, S. and Palmberg, L. (2018). Air-liquid interface: Relevant in vitro models for investigating air pollutant-induced pulmonary toxicity. *Toxicol Sci* 164, 21-30. doi:10.1093/toxsci/kfy053
- Wiemann, M., Sauer, G. U., Vennemann, A. et al. (2018). In vitro and in vivo short-term pulmonary toxicity of differently sized colloidal amorphous SiO₂. *Nanomaterials* 8, 160. doi:10.3390/nano8030160
- Woodcock, J. and Woosley, R. (2008). The FDA critical path initiative and its influence on new drug development. *Annu Rev Med* 59, 1-12. doi:10.1146/annurev.med.59.090506.155819

Conflict of interest

The authors declare no conflict of interest.

Acknowledgements

Julia Metz and Marius Hittinger were financially supported by the BMBF project AeroSafe (031L0128C). Katharina Knoth, Marius Hittinger, Markus Limberger, Horst Zimmer and Henrik Groß were involved in the ZIM project NanOK. We thank Jak Masters for his help in proofreading the manuscript.

Metz et al.:

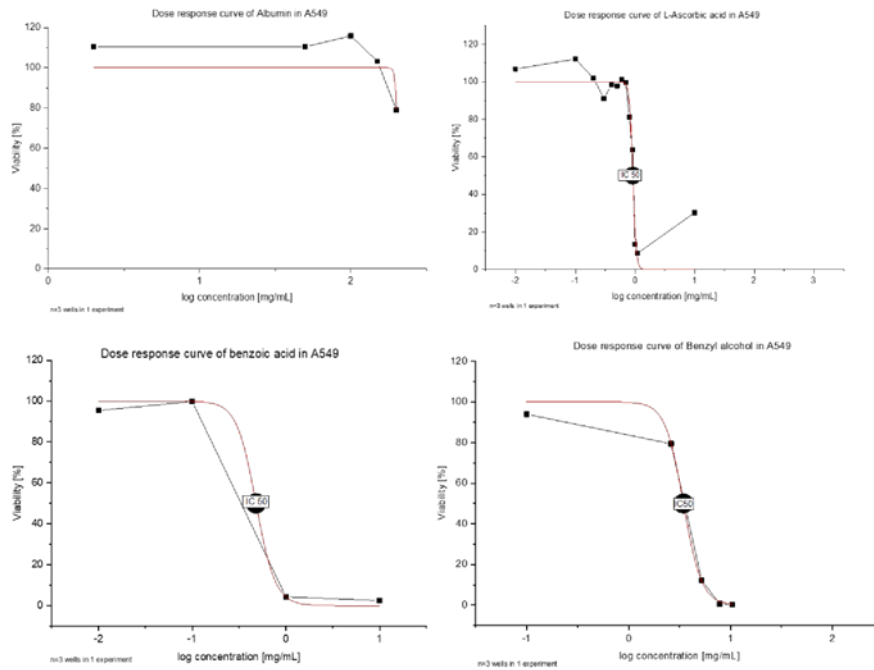
Safety Assessment of Excipients (SAFE) for Orally Inhaled Drug Products

Supplementary Data

Dose response curves for the IC50 calculation *in vitro*

As a general survey, Fig. S1 (A549) and Fig. S2 (Calu-3) summarise the dose response curves of the tested excipients. By testing different concentrations of the test substances, the cell viability was determined via MTT assays to limit the range of the IC50. Subsequently, the curves were generated with the software Origin®Pro 2019 by applying sigmoidal fits which were used for the IC50 calculation *in vitro*. The description "n=3 wells in 1 experiment" explains that the mean of three wells per concentration is shown. Some experiments were applied to confirm the data which increases the number of wells by 3 for each additional experiment.

Dose response with IC50 calculation in A549 cells:

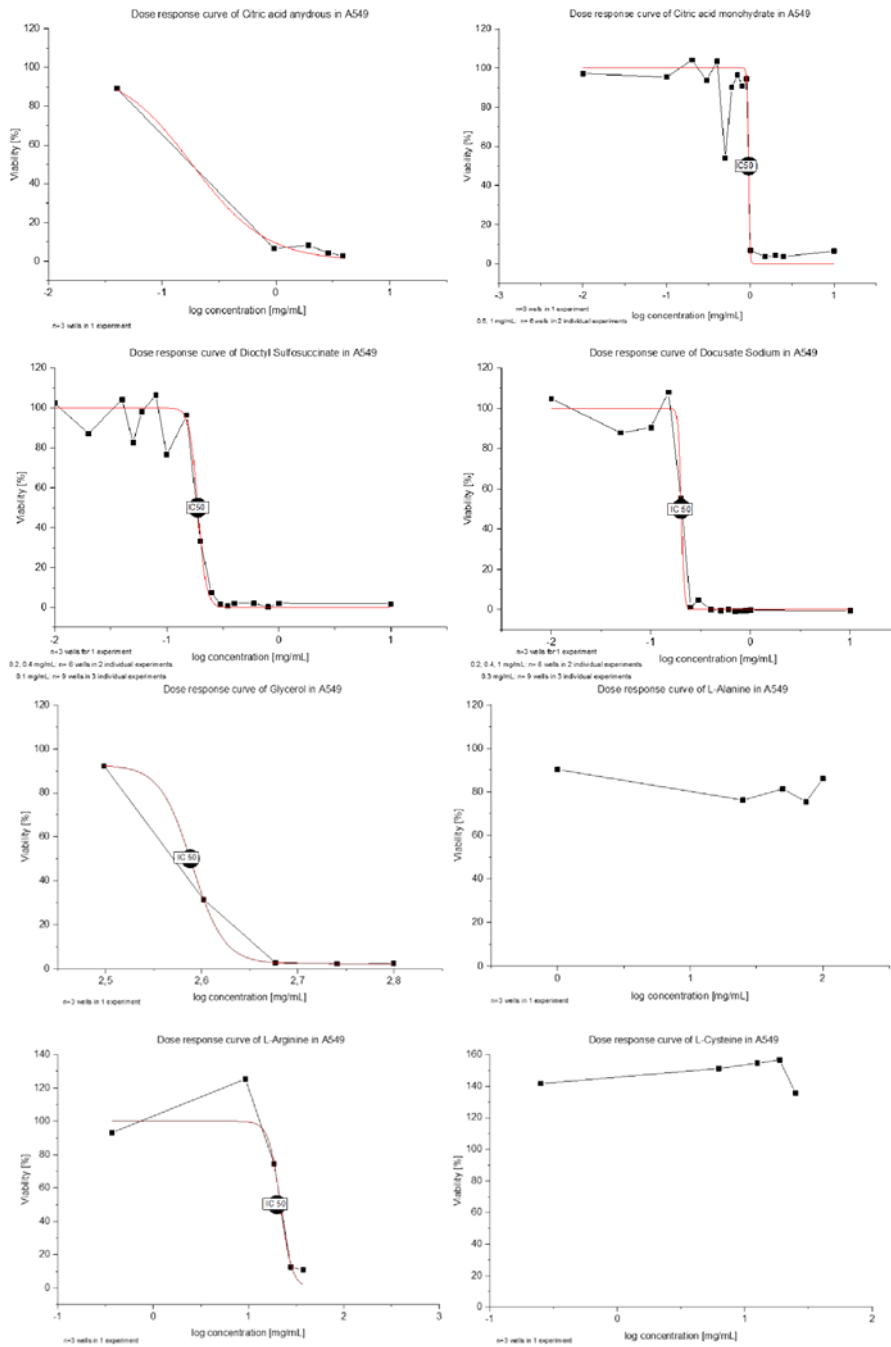


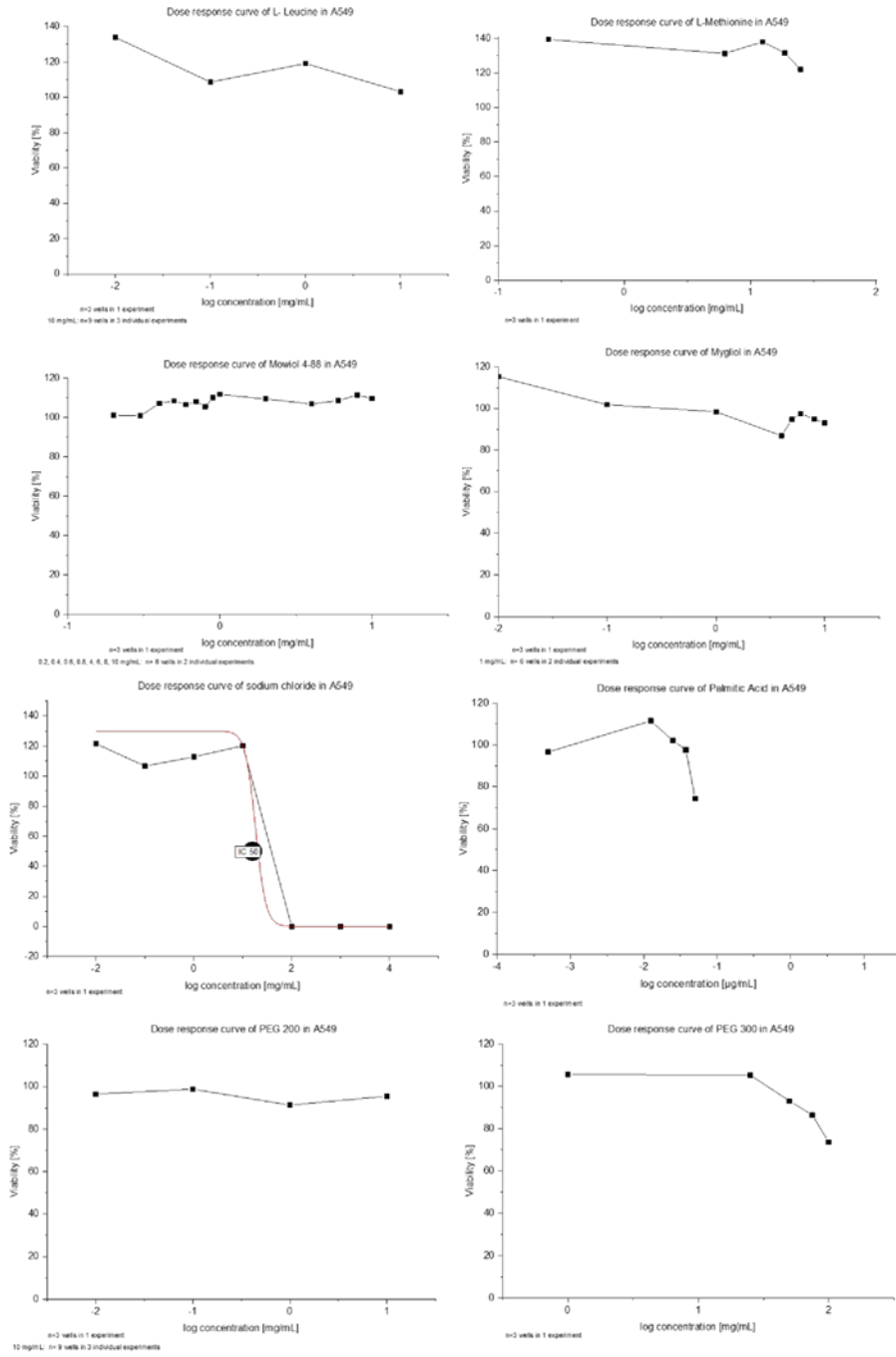
doi:10.14573/altex.1910231s

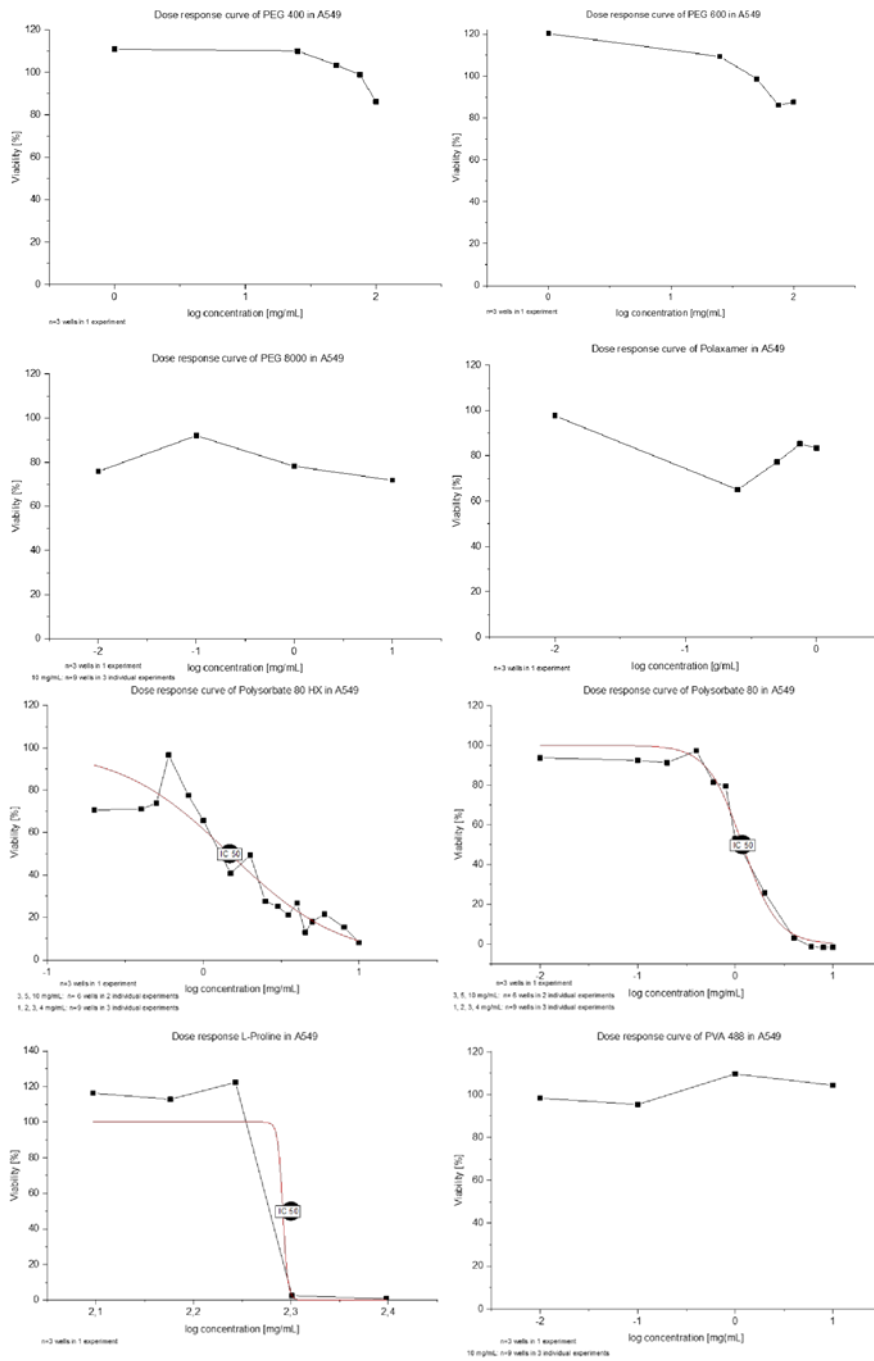
ALTEX 37(x), SUPPLEMENTARY DATA

This is an Open Access article distributed under the terms of the Creative Commons Attribution 4.0 International license (<http://creativecommons.org/licenses/by/4.0/>), which permits unrestricted use, distribution and reproduction in any medium, provided the original work is appropriately cited.

1







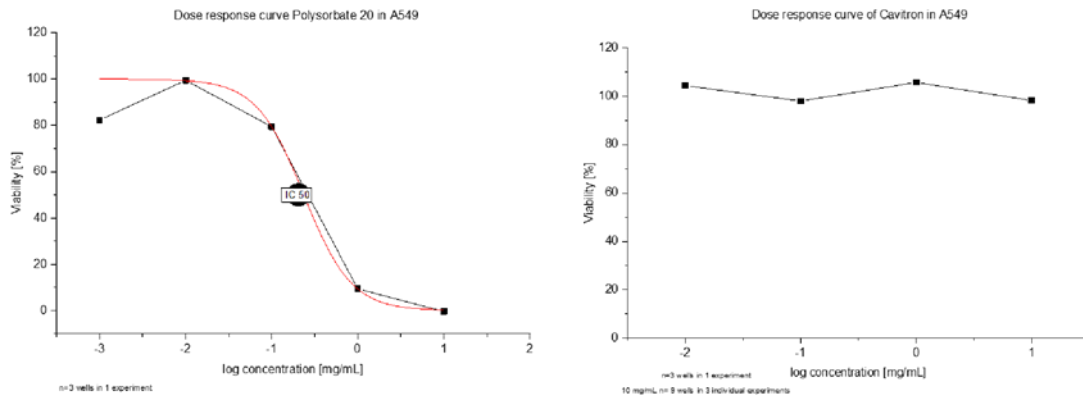
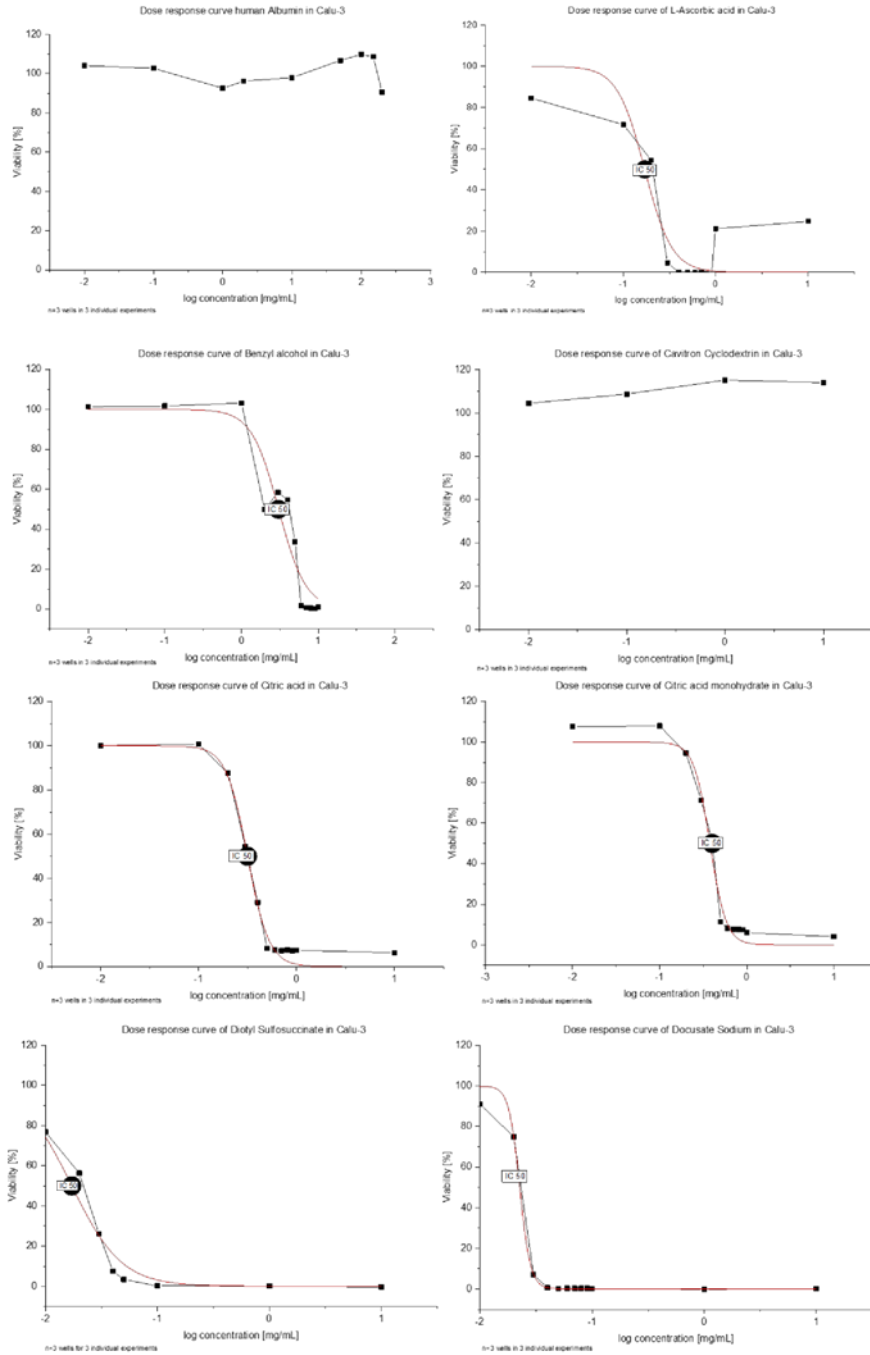
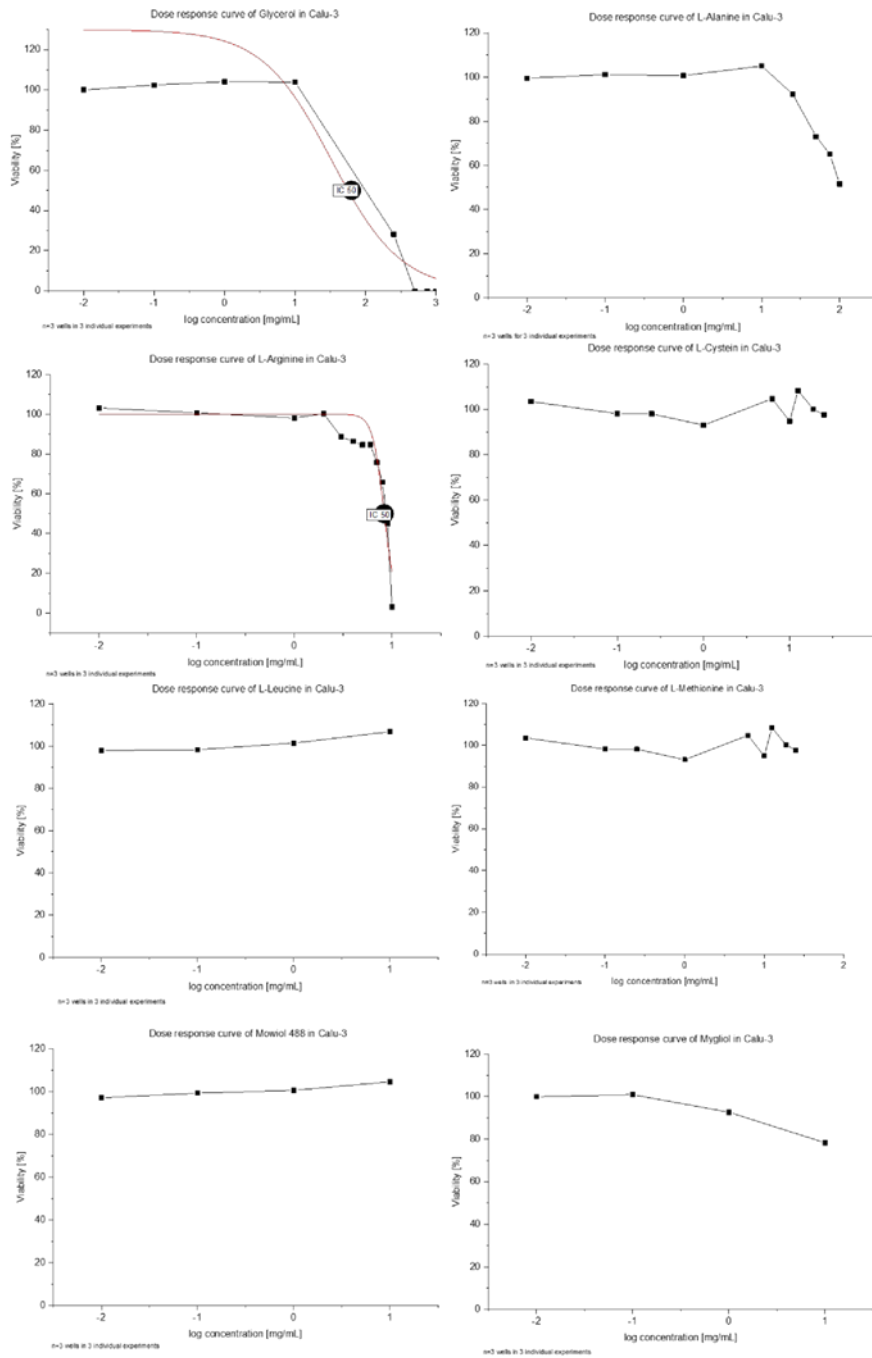
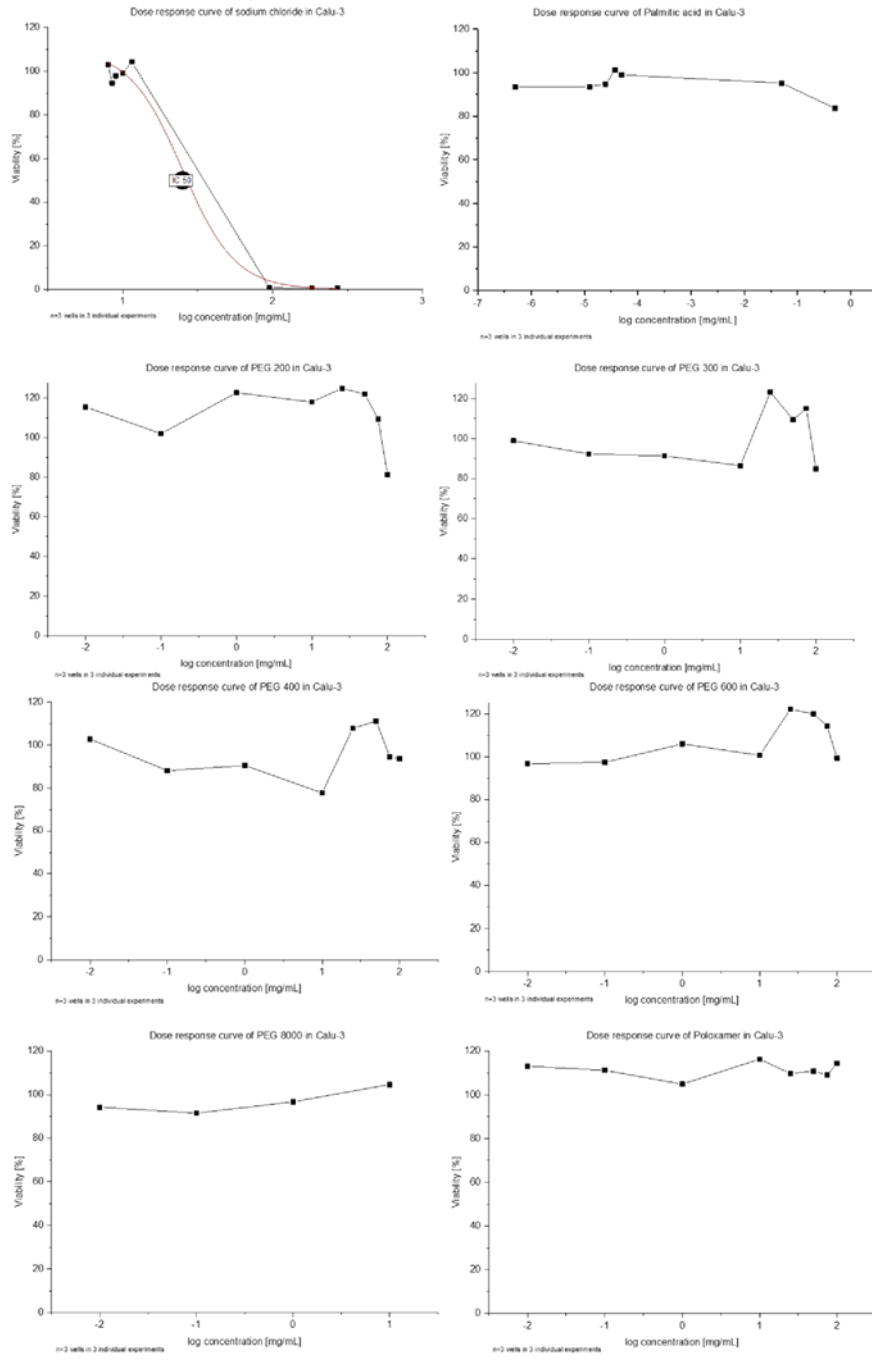


Fig. S1: Dose response and IC50 calculation of different excipients tested in A549 cells.

Dose response curves with IC50 calculation in Calu-3 cells:







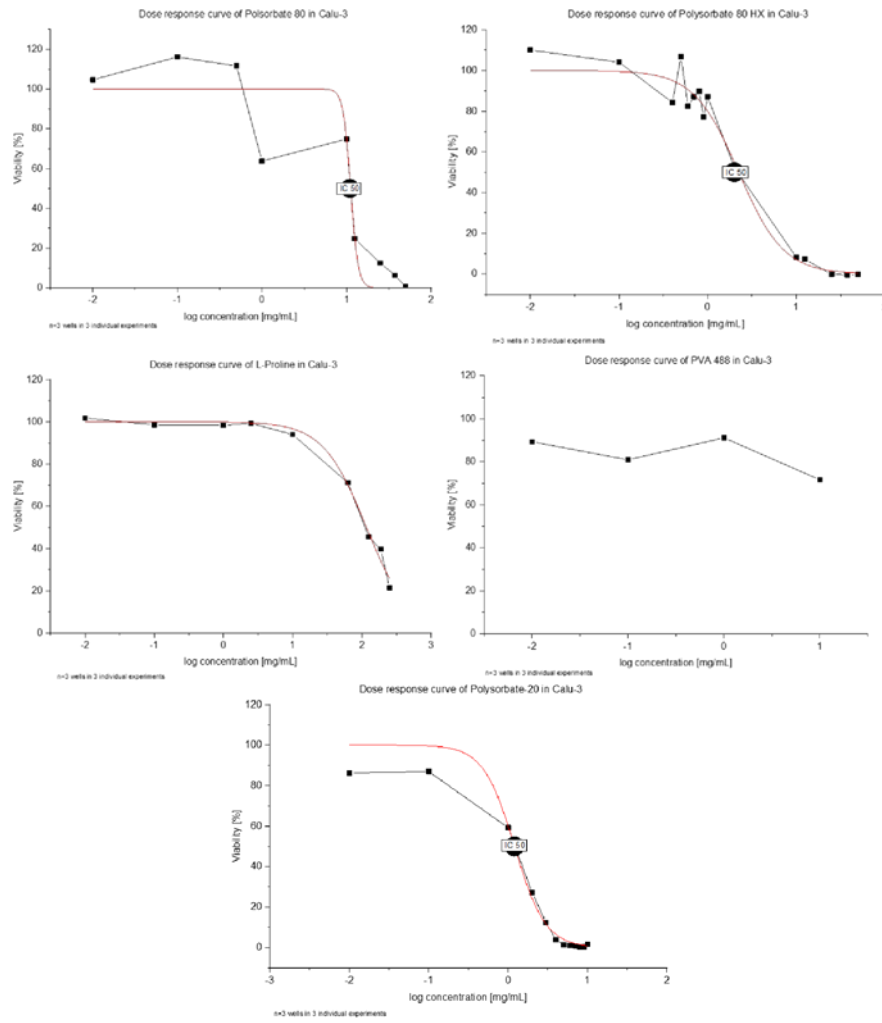


Fig. S2: Dose response and IC50 calculation of different excipients tested in Calu-3 cells.

Comparison between IC50 and GHS classification (LD50)

Tab. S1 lists the tested excipients with the corresponding GHS classification based on the pulmonary – or rather oral - LD50 values. This classification was used initially for the IVVC, but was rejected due to the recalculation of the corresponding concentration applied *in vivo*.

Tab. S1: List of excipients with their associated oral and pulmonary GHS classification based on the related LD50

Substance	CAS number	LD50 <i>in vivo</i> oral	GHS classification acute toxicity oral	LD50 <i>in vivo</i> pulmonal	GHS classification acute toxicity pulmonal
Albumin from human serum	70024-90-7 FDA:9048468	GHS: Pre-Registration, no classification available GESTIS: no toxicity data available Handbook of pharm. Excipients: >12.5 g/kg (rat, monkey) ICE: no toxicity data available	Category 5	Pre-Registration, no classification available GESTIS: no toxicity data available Handbook of pharm. Excipients: no toxicity data available ICE: no toxicity data available	not available missing LD50
Benzoic acid	65-85-0	GHS: 2250 mg/kg bw (mouse) GESTIS: 1700 mg/kg Handbook of pharm. Excipients: 2 g/kg (cat, dog), 1.94 (mouse, rat) ICE: [1700-2742 mg/kg], n=5, median=2360 mg/kg	Category 4-5	GHS: > 12200 mg/m ³ air (rat, 4h, inhalation: dust) GESTIS: no toxicity data available Handbook of pharm. Excipients: no toxicity data available ICE: no toxicity data available	Category 5
Benzyl alcohol	100-51-6	GHS: 1.55 mL/kg bw (rat) GESTIS: 1230 mg/kg Handbook of pharm. Excipients: 1.36 g/kg (mouse), 1.23 g/kg (rat) ICE: [1230-3120 mg/kg], n=3, median=1230 mg/kg	Category 4	GHS: >4178 mg/m ³ air (rat, 4h, inhalation: aerosol) GESTIS: > 4178 mg/L (4 h, inhalation: aerosol) Handbook of pharm. Excipients: no toxicity data available ICE: no toxicity data available	Category 1 (gases classification) Category 5 (vapours classification) Category 5 (dusts classification)
Citric acid monohydrate	5949-29-1	GHS: no toxicity data available GESTIS: no toxicity data available Handbook of pharm. Excipients: no toxicity data available ICE: no toxicity data available	not available missing LD50	GHS: no toxicity data available GESTIS: no toxicity data available Handbook of pharm. Excipients: no toxicity data available ICE: no toxicity data available	not available missing LD50
Citric acid anhydrous	77-92-9	GHS: Pre-Registration, no classification available GESTIS: 3000 mg/kg (GESTIS) Handbook of pharm. Excipients: 5.04 g/kg (mouse), 3.0 g/kg (rat) ICE: [3000-11700 mg/kg], n=5, median=6730 mg/kg	Category 5	GHS: Pre-Registration, no classification available GESTIS: no toxicity data available Handbook of pharm. Excipients: no toxicity data available ICE: no toxicity data available	not available missing LD50
Docusate sodium	577-11-7	GHS: > 3 000 mg/kg bw (rat) GESTIS: no toxicity data available Handbook of pharm. Excipients: 2.64 g/kg (mouse), 1.9 g/kg (rat)	Category 5	GHS: 20 mg/L (rat, 96h, inhalation: aerosol) GESTIS: no toxicity data available Handbook of pharm. Excipients: no	Category 2 (gases classification) Category 4

Substance	CAS number	LD50 <i>in vivo</i> oral	GHS classification acute toxicity oral	LD50 <i>in vivo</i> pulmonal	GHS classification acute toxicity pulmonal
		ICE: [1320-4200 mg/kg], n=9, median=2100 mg/kg		toxicity data available ICE: no toxicity data available	(vapours classification) Category 5 (dusts classification)
Glycerol	56-81-5	GHS: 27 mg/kg bw (rat) GESTIS: 12600 mg/kg (rat) Handbook of pharm. Excipients: 7.75 g/kg (guinea pig), 4.1 g/kg (mouse), 27 g/kg (rabbit), 5.57-12.6 g/kg (rat) ICE: [5570-27650 mg/kg], n=12, median=17102.5 mg/kg	Category 2 (GHS) Category 5	GHS: 4655 mg-min/L (rat, 7h, inhalation: vapour) GESTIS: no toxicity data available Handbook of pharm. Excipients: no toxicity data available ICE: no toxicity data available	Category 5
L(+)-Ascorbic acid	50-81-7	GHS: Pre-Registration, no classification available GESTIS: 11900 mg/kg (rat) Handbook of pharm. Excipients: 3.37 g/kg (mouse), 11.9 g/kg (rat) ICE: [11900-11900 mg/kg], n=2, median=11900 mg/kg	Category 5	GHS: Pre-Registration, no classification available GESTIS: no toxicity data available Handbook of pharm. Excipients: no toxicity data available ICE: no toxicity data available	not available missing LD50
L-Alanine	56-41-7	GHS: > 5110 mg/kg bw (rat) GESTIS: no toxicity data available Handbook of pharm. Excipients: no toxicity data available ICE: no toxicity data available	Category 5	GHS: no toxicity data available GESTIS: no toxicity data available Handbook of pharm. Excipients: no toxicity data available ICE: no toxicity data available	not available missing LD50
L-Arginine	74-79-3	GHS: 5110 mg/kg bw (rat) GESTIS: no toxicity data available Handbook of pharm. Excipients: no toxicity data available ICE: no toxicity data available	Category 5	GHS: no toxicity data available GESTIS: no toxicity data available Handbook of pharm. Excipients: no toxicity data available	not available missing LD50
L-Cysteine	52-90-4	GHS: 5.85 g/kg bw (rat) GESTIS: no toxicity data available Handbook of pharm. Excipients: no toxicity data available ICE: [1890-1890 mg/kg], n=2, median=1890 mg/kg	Category 5	GHS: no toxicity data available GESTIS: no toxicity data available Handbook of pharm. Excipients: no toxicity data available ICE: no toxicity data available	not available missing LD50
L-Methionine	63-68-3	GHS: > 10 000 mg/kg bw (rat) GESTIS: 36000 mg/kg (rat) Handbook of pharm. Excipients: 36 g/kg (rat) ICE: [36000-36000 mg/kg], n=2, median=36000 mg/kg	Category 5	GHS: > 5.25 mg/L air (analytical) (rat, 4h inhalation: dust) GESTIS: no toxicity data available Handbook of pharm. Excipients: no toxicity data available ICE: no toxicity data available	Category 5
L-Proline	147-85-3	GHS: > 5110 mg/kg bw (rat) GESTIS: no toxicity data available Handbook of pharm. Excipients: no toxicity data available ICE: no toxicity data available	Category 5	GHS: no toxicity data available GESTIS: no toxicity data available Handbook of pharm. Excipients: no toxicity data available ICE: no toxicity data available	not available missing LD50
Palmitic acid	57-10-3	GHS: >5 000 mg/kg bw (rat) GESTIS: > 10000 mg/kg (rat)	Category 5	GHS: > 0.162 mg/L (rat, 4h, inhalation: vapour)	Category 1-5

Substance	CAS number	LD50 <i>in vivo</i> oral	GHS classification acute toxicity oral	LD50 <i>in vivo</i> pulmonal	GHS classification acute toxicity pulmonal
		Handbook of pharm. Excipients: no toxicity data available ICE: 10000 mg/kg		GESTIS: no toxicity data available Handbook of pharm. Excipients: no toxicity data available ICE: no toxicity data available	
Poloxamer 188 (Kolliphor® 188)	/	GHS: Pre-Registration, no classification available GESTIS: no toxicity data available Handbook of pharm. Excipients: 15 g/kg (mouse), 9.4 g/kg (rat) ICE: no toxicity data available	Category 5	GHS: Pre-Registration, no classification available GESTIS: no toxicity data available Handbook of pharm. Excipients: no toxicity data available ICE: no toxicity data available	not available missing LD50
Polyethylene glycol 200 (PEG 200)	25322-68-3	GHS: Pre-Registration, no classification available GESTIS: no toxicity data available Handbook of pharm. Excipients: 34 g/kg (mouse), 28.0 g/kg (rat), 19.9 g/kg (rabbit) ICE: no toxicity data available	Category 5	GHS: Pre-Registration, no classification available GESTIS: no toxicity data available Handbook of pharm. Excipients: no toxicity data available ICE: no toxicity data available	not available missing LD50
Polyethylene glycol 300 (PEG 300)		GHS: Pre-Registration, no classification available GESTIS: no toxicity data available Handbook of pharm. Excipients: 27.5 g/kg (rat), 17.3 g/kg (rabbit), 19.6 g/kg (guinea pig) ICE: no toxicity data available	Category 5		
Polyethylene glycol 400 (PEG 400)		GHS: Pre-Registration, no classification available GESTIS: no toxicity data available Handbook of pharm. Excipients: 28.9 g/kg (mouse), 26.8 g/kg (rabbit), 15.7 g/kg (guinea pig) ICE: no toxicity data available	Category 5		
Polyethylene glycol 600 (PEG 600)		GHS: Pre-Registration, no classification available GESTIS: no toxicity data available Handbook of pharm. Excipients: 47 g/kg (mouse), 38.1 g/kg (rat) ICE: no toxicity data available	Category 5		
Polysorbate 80 (Tween-80)	9005-65-6	GHS: Pre-Registration, no classification available GESTIS: no toxicity data available Handbook of pharm. Excipients: 25 g/kg (mouse) ICE: no toxicity data available	Category 5	GHS: Pre-Registration, no classification available GESTIS: no toxicity data available Handbook of pharm. Excipients: no toxicity data available ICE: no toxicity data available	not available missing LD50
Polysorbate 80 (HX2)					
Polysorbate 20	9005-64-5	GHS: 36700 mg/kg bw (rat)	Category 5	GHS: > 5.1 mg/L (rat, 4h, inhalation):	Category 2

Substance	CAS number	LD50 <i>in vivo</i> oral	GHS classification acute toxicity oral	LD50 <i>in vivo</i> pulmonal	GHS classification acute toxicity pulmonal
(Tween 20)		GESTIS: no toxicity data available Handbook of pharm. Excipients: 37 g/kg (rat), 18 g/kg (hamster) ICE: no toxicity data available		aerosol) GESTIS: no toxicity data available Handbook of pharm. Excipients: no toxicity data available ICE: no toxicity data available	(gases classification) Category 3-5 (vapours classification) Category 5 (dusts classification)
Sodium chloride	7647-14-5	GHS. 3550 mg/kg be (rat) GESTIS: 3000 mg/kg (rat) Handbook of pharm. Excipients: 4.09 g/kg (mouse), 3 g/kg (rat) ICE: no toxicity data available	Category 5	GHS: >42 mg/l (rat, 1h, inhalation: aerosol) GESTIS: no toxicity data available Handbook of pharm. Excipients: no toxicity data available ICE: no toxicity data available	Category 2 (gases classification) Category 5 (vapours classification) Category 5 (dusts classification)

Correlation of the IC50 of A549 and Calu-3 cells

For the evaluation of the cellular variations between A549 and Calu-3 a regression analysis was performed including the IC50 of the substances for which an IC50 calculation was possible (benzyl alcohol, citric acid monohydrate, citric acid anhydrous, docusate Sodium, L(+)-Ascorbic acid, L-Arginine, Polysorbate 80 (Tween-80), Polysorbate 80 (HX2) and Polysorbate 20 (Tween 20)). A positive slope of the regression line of 0.88 ± 0.36 was obtained by performing a correlation analysis with a R^2 of 0.46 (Fig.S3). In sum, a point to point correlation is not given.

When comparing both data sets (IC50 A549 & Calu-3) by their *in vitro* hazard class (Sauer et. al 2013, A549), we find similar results (11/15 hits) and no preference for lower/higher IC50 values for A549/Calu-3 (Tab. S2).

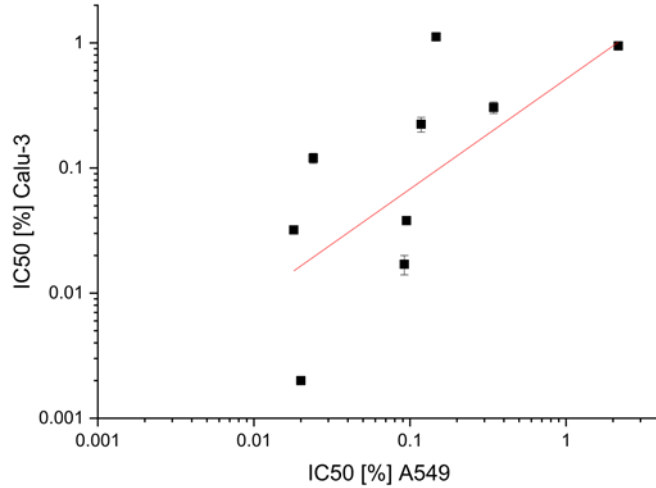


Fig. S3: Regression analysis of IC50 [%] in vitro in Calu-3 cells vs. IC50 [%] in A549

A linear regression was performed with the Software Origin®Pro 2019. The values for the regression analysis are: Slope: 0.88 ± 0.36 , Pearson R: 0.68; coefficient of determination (COD, R^2): 0.46; Correlation R^2 : 0.38.

Tab. S2: Comparison of IC50 data

Substance	IC50			
	<i>In vitro</i> hazard class			
	1	2	3	4
	< 0.1 mg/mL	0.1-1 mg/mL	1-10 mg/mL	> 10 mg/mL
	< 0.01%	0.01-0.1%	0.1%-1%	>1%
Albumin from human serum				A549 & Calu-3
Benzyl alcohol			A549 & Calu-3	
Citric acid monohydrate		A549 & Calu-3		
Citric acid anhydrous		A549 & Calu-3		
Docusate Sodium	Calu-3	A549		
L(+)-Ascorbic acid		A549 & Calu-3		
L-Alanine				A549 & Calu-3
L-Arginine		Calu-3	A549	
Polyethylene glycol 200 (PEG 200)				A549 & Calu-3
Polyethylene glycol 300 (PEG 300)				A549 & Calu-3
Polyethylene glycol 400 (PEG 400)				A549 & Calu-3
Polyethylene glycol 600 (PEG 600)				A549 & Calu-3
Polysorbate 80 (Tween-80)			A549	Calu-3
Polysorbate 80 (HX2)			A549 & Calu-3	
Polysorbate 20 (Tween 20)		A549	Calu-3	
IC50 (Calu 3 > A549)	2			
IC50 (A549 > Calu-3)	2			
Same range	11			

4.3 Modulating the Barrier Function of Human Alveolar Epithelial (hAELVi) Cell Monolayers as a Model of Inflammation

Reference

Modulating the Barrier Function of Human Alveolar Epithelial (hAELVi) Cell Monolayers as a Model of Inflammation

Julia Katharina Metz, Birgit Wiegand, Sabrina Schnur, Katharina Knoth, Nicole Schneider-Daum, Henrik Groß, Glenn Croston, Torsten Michael Reinheimer, Claus-Michael Lehr and Marius Hittinger

ATLA 2021 (1)1-16. doi:10.1177/0261192920983015

Original publication is reprinted from ATLA, 2021: *Modulating the Barrier Function of Human Alveolar Epithelial (hAELVi) Cell Monolayers as a Model of Inflammation*; Julia Katharina Metz, Birgit Wiegand, Sabrina Schnur, Katharina Knoth, Nicole Schneider-Daum, Henrik Groß, Glenn Croston, Torsten Michael Reinheimer, Claus-Michael Lehr and Marius Hittinger-*ATLA 2021, (1), 1-16. doi: 10.1177/0261192920983015*

For all articles published in the SAGE journal ATLA, copyright is retained by the authors.

Co-author statement in connection with submission of PhD thesis of Julia Metz

Related to: *`Vorläufiger Leitfaden und vorläufige Vorgaben für die Erstellung, Einreichung und Veröffentlichung von kumulativen Dissertationsschriften, Beschluss des Promotionsausschusses vom 06.12.2018`*

Paper title: Modulating the Barrier Function of Human Alveolar Epithelial (hAELVi) Cell Monolayers as a Model of Inflammation

- Published
- Accepted
- Submitted
- In preparation

Place of publication: ATLA 2021 (1)1-16. doi:10.1177/0261192920983015

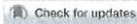
Has the article/manuscript been used in other PhD or doctoral dissertations?

- No Yes If yes, please specify:

List of authors: Julia Katharina Metz, Birgit Wiegand, Sabrina Schnur, Katharina Knoth, Nicole Schneider-Daum, Henrik Groß, Glenn Croston, Torsten Michael Reinheimer, Claus-Michael Lehr and Marius Hittinger

Specification of the contributions:

Julia Katharina Metz conceived and planned the experiments. Julia Katharina Metz carried out the data collection of the proinflammatory hAELVi stimulation (TEER measurements and transport experiments) and the statistical data interpretation. Birgit Wiegand helped with the TEER measurements. Sabrina Schnur and Katharina Knoth supported the routine cell culture. Nicole Schneider-Daum helped with the cultivation conditions of the hAELVi cells. Julia Katharina Metz, Henrik Groß, Glenn Croston, Torsten Michael Reinheimer, Claus-Michael Lehr and Marius Hittinger contributed to the interpretation of the results. Julia Metz took the lead in writing the manuscript. All authors provided critical feedback and helped shape the research, analysis, and manuscript.



Research Article

Modulating the Barrier Function of Human Alveolar Epithelial (hAELVi) Cell Monolayers as a Model of Inflammation

Julia Katharina Metz^{1,2}, Birgit Wiegand¹, Sabrina Schnur^{1,2}, Katharina Knoth¹, Nicole Schneider-Daum³, Henrik Groß¹, Glenn Croston⁴, Torsten Michael Reinheimer⁵, Claus-Michael Lehr^{2,3} and Marius Hittinger^{1,6}

Alternatives to Laboratory Animals
1–16

© The Author(s) 2021

Article reuse guidelines:

sagepub.com/journals-permissions

DOI: 10.1177/0261192920983015

journals.sagepub.com/home/atd



Abstract

The incidence of inflammatory lung diseases such as acute respiratory distress syndrome (ARDS) remains an important problem, particularly in the present time with the Covid-19 pandemic. However, an adequate *in vitro* test system to monitor the barrier function of the alveolar epithelium during inflammation and for assessing anti-inflammatory drugs is urgently needed. Therefore, we treated human Alveolar Epithelial Lentivirus-immortalised cells (hAELVi cells) with the pro-inflammatory cytokines TNF- α (25 ng/ml) and IFN- γ (30 ng/ml), in the presence or absence of hydrocortisone (HC). While TNF- α and IFN- γ are known to reduce epithelial barrier properties, HC could be expected to protect the barrier function and result in an anti-inflammatory effect. We investigated the impact of anti-inflammatory/inflammatory treatment on transepithelial electrical resistance (TEER) and the apparent permeability coefficient (P_{app}) of the low permeability marker sodium fluorescein (NaFlu). After incubating hAELVi cells for 48 hours with a combination of TNF- α and IFN- γ , there was a significant decrease in TEER and a significant increase in the P_{app} . The presence of HC maintained the TEER values and barrier properties, so that no significant P_{app} change was observed. By using hAELVi cells to study anti-inflammatory drugs *in vitro*, the need for animal experiments could be reduced and pulmonary drug development accelerated.

Keywords

alveolar epithelium, ARDS, hydrocortisone, paracellular permeability, TEER, Three Rs

Introduction

The alveolar epithelium of the lung forms the ‘air–blood barrier’, and is essential for the maintenance of lung function, including gas exchange, and immune responses after infection and lung injury.¹ Acute respiratory distress syndrome (ARDS) and acute lung injury (ALI) are examples of conditions that occur when the alveolar epithelium is damaged. This damage results in hypoxaemia, limited ventilation perfusion in the lung, decreased respiratory supply and oedema formation, with a mortality of up to 50%.^{2–4} With Covid-19 continuing to be a major health issue, the incidence of ARDS and ALI are significant concerns.⁵ ARDS and ALI are most commonly caused by viral or bacterial infections that trigger an inflammatory response by the immune system.⁶ In addition to neutrophils and dendritic

cells, alveolar macrophages play a major role in such an immune response to persistent infection in the respiratory region of the lung.⁷ Alveolar pathogens interact with toll-

¹ PharmBioTec GmbH, Saarbrücken, Germany

² Department of Pharmacy, Saarland University, Saarbrücken, Germany

³ Helmholtz Institute for Pharmaceutical Research Saarland (HIPS), Saarbrücken, Germany

⁴ Croston Consulting, San Diego, CA, USA

⁵ Department of Non-Clinical Development, Ferring Pharmaceuticals A/S, Copenhagen, Denmark

⁶ 3RProducts Marius Hittinger, Blieskastel, Germany

Corresponding author:

Marius Hittinger, PharmBioTec GmbH, Science Park I, Campus D 1.1, 66123 Saarbrücken, Germany.

Email: m.hittinger@pharmbiotec.de

like receptors (TLRs) of the resident macrophages⁸ which then secrete pro-inflammatory cytokines (such as IL-1 β , IL-6, IL-8 and TNF- α) to activate the penetration of neutrophils into the alveolar space leading to a high-protein oedema.^{9,10} This breakdown of the epithelial barrier has diverse consequences for cell communication, epithelial connection with the extracellular matrix (ECM), and the destruction of tight junctions (TJs).¹⁰ TJs are essential for the formation and maintenance of the epithelial cell barrier, and control the permeability of dissolved substances of various sizes and charges.¹¹ This paracellular permeability is based on the interaction of transmembrane, peripheral and cytoskeletal proteins. Claudins represent the main family of transmembrane proteins that ensure a regulated exchange of substances between cells, and they are responsible for controlled paracellular diffusion. Other junctional plaque components that are associated with the transmembrane proteins — for example, the zonula occludens 1 (ZO-1) protein — interact with the junctional membrane proteins F-actin and microtubules to regulate the contractility of the actomyosin cytoskeleton.^{12–14} The parameters of the resulting TJ permeability are defined by various complex cellular mechanisms. The main TJ regulators are phosphoinositide 3-kinase (PI3K)/serine and threonine kinase (Akt kinase), mitogen-activated protein kinase (MAPK), Rho-associated kinase (ROCK) and protein kinase C (PKC)-related signalling pathways, which can interact with each other in a network to change the phosphorylation of TJ proteins in response to infection in the microenvironment of the epithelial cells.¹⁵ For example, as a result of an infection, the production of the pro-inflammatory cytokine TNF- α is essential for the expression of inflammatory genes, cell viability, and for the initiation of immune cell responses.¹⁶ Through activation of the NF- κ B signalling pathway, TNF- α opens the TJs by interacting with the Claudin-5 (Cldn-5) protein.¹¹ In combination with IFN- γ , TNF- α increases the permeability of the epithelial barriers over the MLC/MLCK pathway, and induces the rearrangement of Cldn-2 and Cldn-3 to Cldn-4.^{17,18}

The complexity of these intracellular processes is one factor impeding the development of new therapies for ARDS/ALI. Experiments on animals are still the most common choice for testing drugs, as these animal models attempt to simulate the course of the diseases *in vivo*. The most widely used respiratory/inflammatory animal models in drug research are based on experiments that involve exposure to pro-inflammatory compounds, such as the aspiration of 0.1–0.5 M hydrochloric acid or treatment with lipopolysaccharide (LPS). These experiments are normally performed on mice.¹⁹ In addition, ventilator-induced lung injury (VILI) has great clinical importance, as it simulates ARDS *in vivo* by the mechanical disruption of the animal's epithelial barrier.²⁰ Overall, these methods are used to induce different inflammatory processes in respiratory epithelia, leading to various symptoms of ARDS/ALI, such

as the intrapulmonary release of cytokines and the breakdown of the air–blood barrier in the alveolar space.^{19,21} However, besides the ethical concerns and economic limitations of performing animal experiments, the development of adequate *in vivo* models for testing new therapies is complicated by a range of species differences, including: TLR expression; the structure of the mononuclear phagocyte system; the chemokines and receptors involved; and the overall size of the lung.²¹

Therefore, suitable *in vitro* methods for the simulation of ALI/ARDS are still urgently needed. In compliance with the Three Rs principles (in particular, *replacement*), and to overcome the challenges resulting from species differences, the further development and optimisation of human cell-based *in vitro* systems are required. Gordon et al.²² summarised the available *in vitro* models for simulating the lung, divided into those representing the central airway (e.g. Calu-3, 16HBE14o-, NCI-H441, BEAS-2B and primary cells) and those representing the peripheral airway, such as A549 cells.²² The latter model is commonly used for the investigation of pro-inflammatory effects after LPS stimulation²³ and hypoxia.²¹ However, the main disadvantages of a A549 cell-based model in the simulation of ARDS/ALI is their inability to form TJs, leading to a high paracellular permeability without the ability to evaluate transepithelial electrical resistance (TEER).²⁴ Complex multicellular test systems consisting of epithelial cells (e.g. primary cells, A549, Calu-3, BEAS-2B or CFTE29o- cells), macrophages and dendritic cells are suitable for investigating pulmonary fibrosis or the efficacy of anti-inflammatory drugs *in vitro*.^{25,26} These sophisticated cell culture models can be used as part of lung-on-a-chip systems,²⁶ with a more physiological reconstitution of the lung being feasible, but they still lack standardised end-user formats.²⁷

Commercially available 3-D human airway models like EpiAirway™ (MatTek Life Sciences) and MucilAir™ (Epithelix Sàrl) are now being used for respiratory safety assessments.^{28,29} These cell culture systems represent the airway epithelium of the bronchi and not the alveolar epithelium of the deep lung. Therefore, the EpiAlveolar™ model (MatTek Life Sciences) is suitable for the *in vitro* simulation of the alveolar region, which can be used, for example, to mimic pulmonary fibrosis development after nanoparticle exposure.³⁰ Epithelial monolayers are perhaps of limited use for modelling inflammatory processes, due to the lack of complex immune cell communication.³¹ In the current study, this limitation was addressed by combining primary human alveolar macrophages with primary epithelial type I-like cells from the same donor.³² However, while such a primary cell culture model probably most closely reflects human epithelial responses, it is not commercially available and it is not very practical to implement, due to limited access to human lung tissue.

For use as an alternative to primary human alveolar cells, human Alveolar Epithelial Lentivirus-immortalised cells (hAELVi cells) have been recently developed and characterised. These cells were originally derived from primary human cells and have pneumocyte type I characteristics, with functional TJs characterised by a high TEER.³³ Based on this new cell line, the present study aims to establish an *in vitro* test system for pulmonary inflammatory studies. The inflammatory response is observed through changes in the barrier properties of the hAELVi cells after stimulation with the pro-inflammatory cytokines TNF- α and IFN- γ . By measuring the TEER and P_{app} of the hAELVi cell barrier, we demonstrate how hAELVi cells react to pro-inflammatory cytokine stimulation (TNF- α and IFN- γ) at different time points (0, 24 and 48 hours), in the presence or absence of fetal calf serum (FCS) and the anti-inflammatory glucocorticoid, hydrocortisone (HC). To provide a useful model for *in vivo* conditions, experimental conditions were optimised to clearly show any HC-mediated amelioration of TEER decreases and P_{app} increases that were occurring as a result of inflammatory stimulation.

Materials and methods

Culture of the hAELVi cells

The human cell line, hAELVi, was obtained from InSCREENeX GmbH (Braunschweig, Germany) and cultured in Small Airway Epithelial Cell Growth Medium™ (SAGM™; Lonza, Basel, Switzerland) supplemented with 1% v/v fetal calf serum (FCS; South American origin, Superior; Biochrom, Berlin, Germany) and 1% v/v antibiotics (Gibco™ penicillin (10,000 U/ml)/streptomycin (10,000 μ g/ml); Fisher Scientific, Waltham, MA, USA). For the HC-free conditions, no HC from the supplement kit (Lonza) nor FCS were added to the medium. Otherwise, the concentration of HC in SAGM™ was 400–600 ng/ml when prepared according to the manufacturer's instructions. For the routine cell culture, the cells were passaged once a week and grown in parallel in either HC-free or HC-containing medium (both without FCS). The cells were detached with 0.05% trypsin-EDTA (Gibco™; Fisher Scientific) for 5 minutes at 37°C. As hAELVi cells cultured in the presence of HC and FCS have a faster growth rate, 1.5×10^5 cells and 3×10^5 cells were seeded per T75 cm² flask in SAGM with HC/FCS and SAGM without HC/FCS, respectively. The effects of FCS as media supplement on a successful stimulation were primarily investigated, in order to omit FCS when possible, with the goal of generating a non-animal product-based model in line with the Three Rs principles.

For the inflammation experiments, 1×10^5 hAELVi cells per 1.12 cm² were seeded in the Transwell® filter devices (Cat. No. 3460; Corning, New York, NY, USA)

without media supplementation (i.e. in SAGM only). The pore size of the Transwell filter devices used was 0.4 μ m, which is optimised for transport and permeability studies.³⁴ Cell counting was performed with a LUNA™ Automated Cell Counter (Logo Biosystems, Anyang-si, South Korea). All plastic devices were pre-coated with a 1% v/v fibronectin-collagen solution (Corning and Sigma-Aldrich, Darmstadt, Germany, respectively) solution.³³ The hAELVi cells were maintained in a humidified atmosphere with 5% v/v CO₂ at 37°C, from passage number 29 to 41.

TEER measurements

The transepithelial electrical resistance (TEER) of the hAELVi cells was measured every 48 hours in the Transwell inserts, in order to evaluate barrier formation and integrity. During the measurements, the cells were placed on a heating plate at 37°C to avoid stress-related temperature variations that might affect the TEER. The TEER values were determined with a chopstick electrode connected to an EVOM² epithelial volt-ohmmeter (World Precision Instruments, Sarasota, FL, USA). The chopstick electrode was cleaned and sterilised by soaking in 70% v/v isopropanol for 5 minutes, at the start of each session. The EVOM² was also calibrated with a reference resistance of 1000 Ω , prior to any measurements being taken. Between measurements of the different experimental groups, the electrode was cleaned with $1 \times$ Dulbecco's Phosphate-Buffered Saline (DPBS; no Calcium (CaCl₂), no Magnesium (MgCl₂); Fisher Scientific) to prevent any carry-over of the cytokines. After the TEER measurement, a medium change was carried out. To avoid damage to the cells, the medium was first discarded from the basolateral compartment of the Transwell system, followed by removal from the apical side. Then, 0.5 ml of fresh medium was gently pipetted first into the apical compartment, and 1.5 ml of fresh medium were pipetted into the basolateral compartment. The hAELVi cells on the Transwell filters were maintained in a humidified atmosphere with 5% CO₂ at 37°C.

Stimulation process

Based on the correlation of intestinal TEER values and intact barrier properties that was previously reported by Srinivasan et al.,³⁵ the hAELVi cells were stimulated with cytokines when TEER values of $> 800 \Omega \cdot \text{cm}^2$ were obtained (this being indicative of tight barrier formation). In preliminary experiments, hAELVi cells were stimulated apically and basolaterally with TNF- α (Fisher Scientific). A stock solution of 5 μ g/ml TNF- α was initially prepared with $1 \times$ DPBS without CaCl₂ or MgCl₂ and stored at -20°C. The stimulation was carried out with TNF- α at concentrations of 50 ng/ml apically and 17 ng/ml

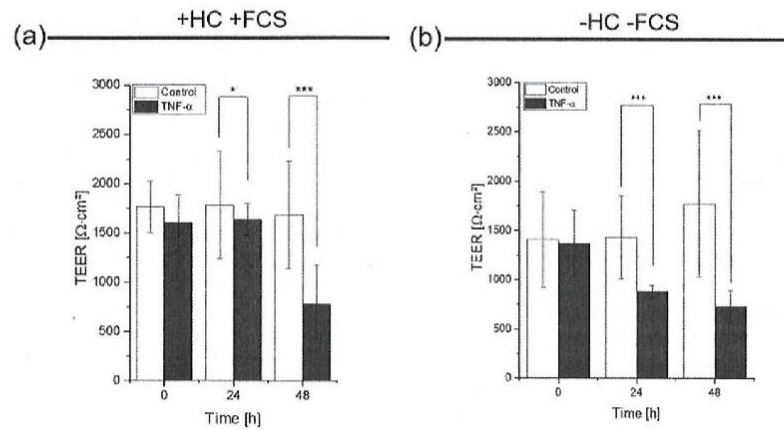


Figure 1. The effects of HC and FCS on the TEER values of hAELVi cells after TNF- α stimulation. The TEER values of hAELVi cells 0, 24 and 48 hours after stimulation with TNF- α (50 ng/ml and 17 ng/ml in the apical and basolateral compartments, respectively) under different culture conditions: (a) SAGM with HC and FCS; (b) SAGM without HC or FCS. Values represent the mean \pm SD for $n = 6$, in three individual experiments; * $p < 0.05$ and *** $p < 0.001$ versus defined test group (two-sample t-test) after 24 or 48 hours indicates a significant difference. HC = hydrocortisone; FCS = fetal calf serum; TNF- α = tumour necrosis factor alpha; TEER = transepithelial electrical resistance; SAGM = Small Airway Epithelial Cell Growth Medium; SD = standard deviation.

basolaterally, in SAGM without HC or FCS. For preparation of the apical working solution, 40 μl of the 5 $\mu\text{g}/\text{ml}$ TNF- α stock were added to 4 ml of SAGM -HC/-FCS and 500 μl of this solution transferred to the apical compartment for the treatment. For the basolateral working solution, 40 μl of the 5 $\mu\text{g}/\text{ml}$ TNF- α stock were added to 12 ml of SAGM -HC/-FCS and 1.5 ml of this solution transferred to the basolateral compartment. After 24 and 48 hours, the TEER was determined again without an additional medium change. It should be noted that TNF- α was not present during the transport studies during the optimisation experiments.

After optimising the protocol, inflammation of the hAELVi cells was induced by exposing one group to 25 ng/ml TNF- α , another group to 30 ng/ml IFN- γ (Fisher Scientific), and a third one to both cytokines in a 'cocktail' (at these same concentrations) in SAGM with or without HC. The stock of IFN- γ was prepared in sterile and purified water at a concentration of 0.1 mg/ml and stored at -20°C . A further dilution was performed to obtain 1 $\mu\text{g}/\text{ml}$ in Hanks' Balanced Salt Solution (HBSS; Gibco; Fisher Scientific), from which 210 μl were diluted in 7 ml SAGM with or without HC and FCS to obtain the working concentration of 30 ng/ml. In all experiments, SAGM +/-HC, SAGM +/-FCS, all without any cytokine addition, were used as the control group.

The hAELVi cells on the Transwell filters were maintained in a humidified atmosphere with 5% CO_2 at 37°C . The TEER was measured pre-treatment (0 hours), and after 24 and 48 hours; a transport study with sodium fluorescein was performed after 48 hours.

Transport studies and calculation of the apparent permeability coefficient (P_{app})

In addition to the TEER experiments, apparent permeability coefficients (P_{app}) were determined to assess potential damage to the barrier after stimulation with the cytokines. After 48 hours of stimulation, the TEER values of the hAELVi cells were measured in the Transwell plate. Thereafter, the cells were incubated in HBSS for 30 minutes, 500 μl apically and 1.5 ml basolaterally, in a humidified atmosphere with 5% CO_2 at 37°C . For the preliminary experiments, in which TNF- α was used alone for the stimulation experiments, the cytokine was not present during the transport studies. However, for the optimised experiments with 25 ng/ml TNF- α and 30 ng/ml IFN- γ , the cytokines were present during the transport studies. The TEER values were measured after 48 hours of stimulation (the TEER values are presented in Figures 1, 3 and 5) and after the transport studies (Figures 2, 4 and 6), in order to check the effectiveness of the barrier properties during the experiments. After assessing the TEER values of the cells in HBSS, 0.5 ml of fresh HBSS with 10 $\mu\text{g}/\text{ml}$ sodium fluorescein (NaFlu; Merck, Darmstadt, Germany) was added to the apical compartment, and 1.5 ml HBSS without NaFlu added to the basolateral compartment. To obtain time 0 readings, 20 μl and 200 μl aliquots were immediately taken from the apical and basolateral compartments, respectively, and transferred to a 96-well plate. After 20, 40, 60 and 90 minutes, 200 μl were taken from only the basolateral compartments; after 120 minutes, 20 μl were taken from the apical compartments and a further 200 μl from each

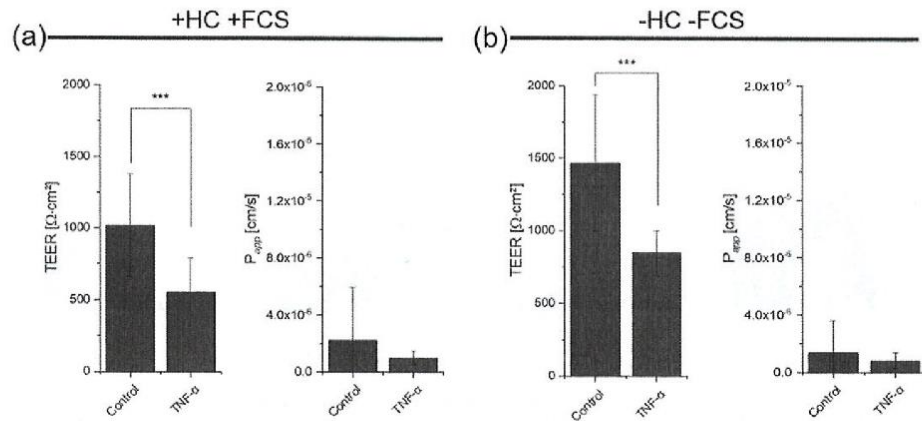


Figure 2. The effects of HC and FCS on the TEER and P_{app} values of hAELVi cells after TNF- α stimulation for 48 hours. The TEER values and the calculated P_{app} values of hAELVi cells after 48 hours of stimulation with TNF- α (50 ng/ml and 17 ng/ml in the apical and basolateral compartments, respectively) under different culture conditions: (a) SAGM with HC and FCS; (b) SAGM without HC or FCS. For the transport studies to determine the P_{app} values, cells were transferred to HBSS with no added TNF- α . Values represent the mean \pm SD for $n = 6$, in three individual experiments; $^{***}p < 0.001$ versus unstimulated control (two-sample t-test) indicates a significant difference. HC = hydrocortisone; FCS = fetal calf serum; TNF- α = tumour necrosis factor alpha; TEER = transepithelial electrical resistance; P_{app} = apparent permeability coefficient; HBSS = Hanks' Balanced Salt Solution; SD = standard deviation.

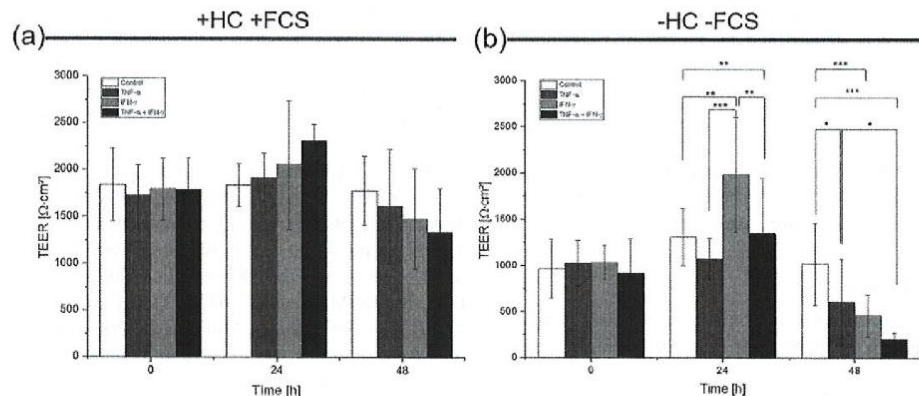


Figure 3. The effects of HC and FCS on the TEER values of hAELVi cells after TNF- α and IFN- γ stimulation. The TEER values of hAELVi cells 0, 24 and 48 hours after stimulation with either 25 ng/ml TNF- α , 30 ng/ml IFN- γ , or the two cytokines combined at these same concentrations, in: (a) SAGM with HC and FCS; (b) SAGM without HC or FCS. Values represent the mean \pm SD for (a) $n = 3$, in three individual experiments and (b) $n = 3$, in five individual experiments; $^*p < 0.05$, $^{**}p < 0.01$ and $^{***}p < 0.001$ versus defined test group (one-way ANOVA with Bonferroni post-hoc test) after 24 and 48 hours indicates significant difference. HC = hydrocortisone; FCS = fetal calf serum; TNF- α = tumour necrosis factor alpha; IFN- γ = interferon-gamma; TEER = transepithelial electrical resistance; SAGM = Small Airway Epithelial Cell Growth Medium; SD = standard deviation; ANOVA = analysis of variance.

basolateral compartment. During the transport study, the Transwell plate was placed on a 35 rpm shaker (Heidolph, Germany) at 37°C, and protected from the light. For the fluorescence measurements, the 20 μl apical compartment samples were diluted in 180 μl HBSS in a 96-well plate, and the 200 μl samples from the basolateral compartments were transferred to the plate without further dilution. To

replace the medium lost and maintain the total volume throughout the study, 20 μl and 200 μl of HBSS were added after sampling, to the apical and basolateral compartments, respectively. The fluorescence of the samples was quantified with a plate reader (Synergy2; Biotek, Winooski, VT, USA) at a wavelength of 485 nm (emission) and 528 nm (excitation). The TEER of the hAELVi cells was measured

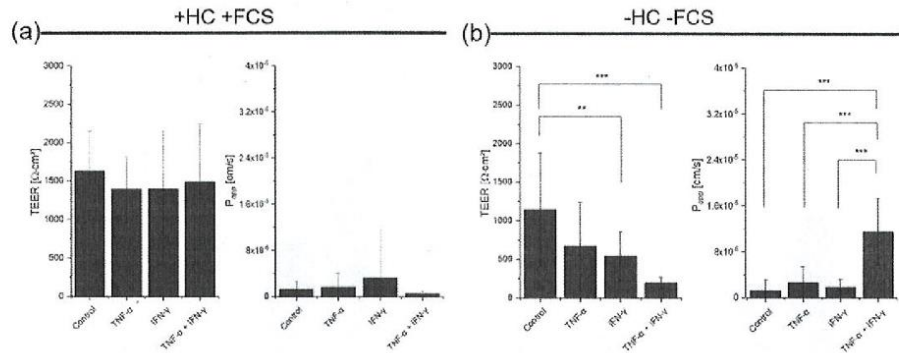


Figure 4. The effects of HC and FCS on the TEER and P_{app} values of hAELVi cells after TNF- α and IFN- γ stimulation for 48 hours. The TEER values and the calculated P_{app} of hAELVi cells after 48 hours of stimulation with either 25 ng/ml TNF- α , 30 ng/ml IFN- γ , or the two cytokines combined at these same concentrations, in: (a) SAGM with HC and FCS; (b) SAGM without HC or FCS. For the transport studies to determine the P_{app} values, cells were transferred to HBSS with no added cytokines. Values represent the mean \pm SD for (a) $n = 3$, in three individual experiments and (b) $n = 3$, in five individual experiments; $*p < 0.01$ and $***p < 0.001$ versus defined test group (one-way ANOVA with Bonferroni post-hoc test) indicates significant difference. HC = hydrocortisone; FCS = fetal calf serum; TNF- α : tumour necrosis factor alpha; IFN- γ : interferon-gamma; TEER = transepithelial electrical resistance; P_{app} = apparent permeability coefficient; HBSS = Hanks' Balanced Salt Solution; SAGM = Small Airway Epithelial Cell Growth Medium; SD = standard deviation; ANOVA = analysis of variance.

at the end of each experiment (the TEER values are presented in Figures 2, 4 and 6).

The P_{app} was determined by means of a calibration curve and calculated by using the formula shown³⁶:

$$P_{app} = \left(\frac{1}{AC_0} \right) \times \left(\frac{dQ}{dt} \right)$$

where, A = area, C_0 = initial concentration of sodium fluorescein, Q = amount of sodium fluorescein that permeated across the Transwell membrane, t = time.

Statistical analysis

The data are presented as the mean \pm standard deviation (SD), indicating the number of independent replicates (n). The data were statistically analysed by a one-way analysis of variance (ANOVA) followed by the Bonferroni post-hoc test (specified in the figure legends), and by a two-sampled t -test for comparisons of specific test groups. The p values are marked if there was a significant difference compared to the defined test group ($*p < 0.05$, $**p < 0.01$ and $***p < 0.001$). The statistics were performed with Origin[®]Pro 2019.

Results

Stimulation with TNF- α decreases the TEER of hAELVi cells, but does not increase paracellular permeability of sodium fluorescein (NaFlu)

TNF- α can rearrange actin-myosin contractility through the activation of the NF- κ B pathway, resulting in an impaired epithelial barrier formation.¹⁷ Therefore, two

experiments were performed, in order to investigate the effect of TNF- α on epithelial barrier formation in hAELVi cells. The parameters that were determined were: TEER values, to evaluate changes in epithelial barrier formation³⁵; and P_{app} values, which represent a marker for paracellular permeability, which consequently increases with decreasing TEER values.^{37,38}

Once TEER values above 1000 $\Omega \cdot \text{cm}^2$ were reached (see *Supplementary Figures S4 and S5*), hAELVi cells were stimulated in preliminary experiments with TNF- α (50 ng/ml and 17 ng/ml in the apical and basolateral compartments, respectively) for 24 and 48 hours. In the presence of HC and FCS in SAGM (SAGM +HC/+FCS), a decrease in the TEER was observed 24 hours after exposure to TNF- α ($p < 0.05$), and this was even more marked after 48 hours ($p < 0.001$; Figure 1a). In the absence of HC and FCS (SAGM -HC/-FCS), after TNF- α stimulation a significant reduction in the TEER, as compared to the control group, was observed after both 24 and 48 hours ($p < 0.001$; Figure 1b). The TEER values shown in Figure 1 were measured before stimulation (0 hours), and after 24 and 48 hours of stimulation in SAGM +HC/+FCS or SAGM -HC/-FCS, before the transport studies were performed.

After TNF- α stimulation for 48 hours, transport studies with the tracer molecule sodium fluorescein (NaFlu) were performed in order to assess paracellular permeability by calculating P_{app} values. The TEER values presented in Figure 2 were measured on completion of the transport studies. Upon stimulation by TNF- α for 48 hours, hAELVi cells previously cultured in SAGM +HC/+FCS (Figure 2a), showed a significant reduction ($p < 0.001$) in TEER values, from 1019 \pm 359 $\Omega \cdot \text{cm}^2$ in the control

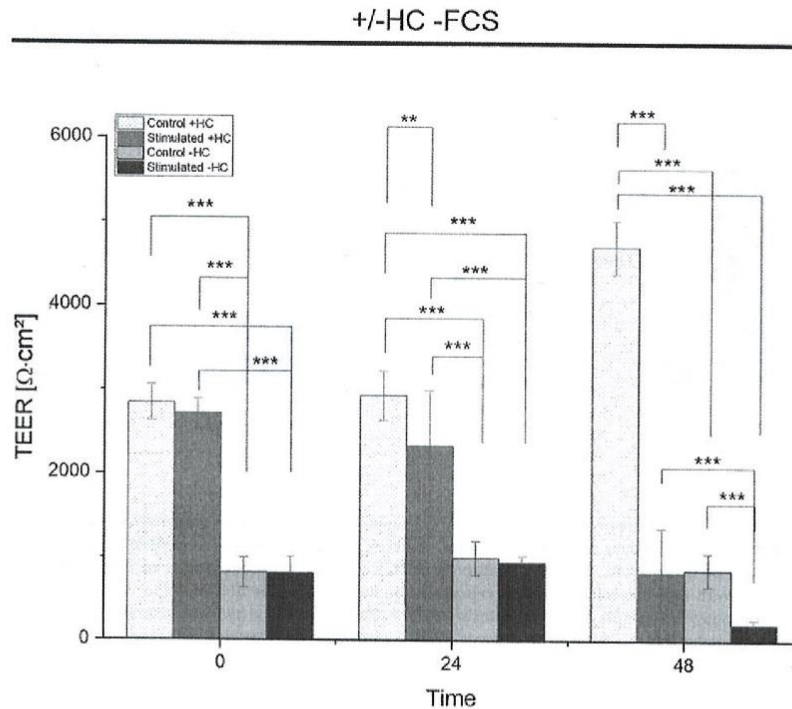


Figure 5. The contribution of FCS to the protective effect HC/FCS supplementation during combined TNF- α and IFN- γ stimulation of hAELVi cells. The TEER values of hAELVi cells 0, 24 and 48 hours after stimulation with a combination of 25 ng/ml TNF- α and 30 ng/ml IFN- γ , in SAGM with or without HC, both in the absence of FCS. Values represent the mean \pm SD for $n = 3$, in four individual experiments; ** $p < 0.01$ and *** $p < 0.001$ versus defined test group (one-way ANOVA with Bonferroni post-hoc test) indicates significant difference. HC = hydrocortisone; FCS = fetal calf serum; TNF- α = tumour necrosis factor alpha; IFN- γ = interferon-gamma; TEER = transepithelial electrical resistance; SAGM = Small Airway Epithelial Cell Growth Medium; SD = standard deviation.

group to $553 \pm 236 \Omega \cdot \text{cm}^2$ in the stimulated group. However, the corresponding P_{app} values for the control and the stimulated group were not significantly different ($2.23 \times 10^{-6} \pm 3.70 \times 10^{-6} \text{ cm/s}$ and $1.02 \times 10^{-6} \pm 4.68 \times 10^{-7} \text{ cm/s}$, respectively).

The same trend was observed in the absence of HC and FCS (SAGM -HC/-FCS), where stimulation of hAELVi cells with TNF- α significantly reduced ($p < 0.001$) TEER values from $1466 \pm 472 \Omega \cdot \text{cm}^2$ in the control group to $846 \pm 153 \Omega \cdot \text{cm}^2$ in the stimulated group, whereas the P_{app} of NaFlu did not change significantly (Figure 2b). It is clear that TNF- α causes a moderate loss of barrier function, leading to a slight but significant drop in the TEER ($p < 0.001$). This is more pronounced in the absence of HC and FCS in the medium. The permeability of the paracellular transport marker NaFlu was, however, not significantly affected by this moderate change in barrier function. A more pronounced disruption of the cellular barrier would have been required in order to instigate a more significant effect on barrier permeability.

Synergistic effects of TNF- α and IFN- γ reduced the TEER and increased the paracellular permeability of NaFlu

As stimulation with TNF- α alone was not sufficient to mediate a significant increase in paracellular transport activity, as determined by the P_{app} , IFN- γ treatment — either alone or in combination with TNF- α — was included in subsequent experiments. This would also investigate whether these cytokines would act synergistically to bring about a reduction in epithelial barrier properties.^{17,39}

Once a TEER above $1000 \Omega \cdot \text{cm}^2$ was reached (see *Supplementary Figures S7 and S8*), the stimulation experiments with either 25 ng/ml TNF- α , 30 ng/ml IFN- γ , or TNF- α and IFN- γ combined in a cytokine ‘cocktail’, were performed. The TEER of hAELVi cells cultured in HC and FCS (SAGM +HC/+FCS) did not show a significant decrease in any group (Figure 3a). In contrast, when hAELVi cells were cultured in HC and FCS depleted SAGM (SAGM -HC/-FCS; Figure 3b), a significant decrease in TEER was achieved after a 48-hour stimulation

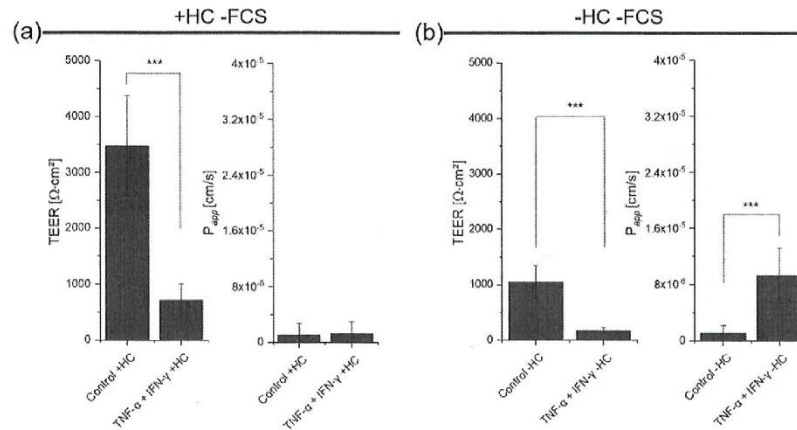


Figure 6. The contribution of FCS to the protective effect HC/FCS supplementation during combined TNF- α and IFN- γ stimulation of hAELVi cells for 48 hours. The TEER values of hAELVi cells after 48 hours of stimulation with a combination of 25 ng/ml TNF- α and 30 ng/ml IFN- γ , in SAGM with or without HC, both in the absence of FCS. For the transport studies to determine the P_{app} values, cells were transferred to HBSS with added cytokines. Values represent the mean \pm SD for $n = 3$, in four individual experiments; *** $p < 0.001$ versus defined test group (two-sample t -test) indicates significant difference. HC = hydrocortisone; FCS = fetal calf serum; TNF- α = tumour necrosis factor alpha; IFN- γ = interferon-gamma; TEER = transepithelial electrical resistance; P_{app} = apparent permeability coefficient; HBSS = Hanks' Balanced Salt Solution; SAGM = Small Airway Epithelial Cell Growth Medium; SD = standard deviation.

with TNF- α alone ($p < 0.05$), IFN- γ alone ($p < 0.001$), and both in combination ($p < 0.001$). The TEER values presented in Figure 3 were measured before stimulation (0 hours), and after 24 and 48 hours of stimulation in SAGM +HC/+FCS or -HC/-FCS, before the transport studies were performed.

The significant reduction in TEER shown in Figure 3b raised the question as to whether stimulation with TNF- α alone, IFN- γ alone, or both in combination, would increase the permeability of NaFlu. Therefore, we performed transport studies to calculate the P_{app} of the stimulated hAELVi cells (Figure 4). When hAELVi cells were stimulated in SAGM +HC/+FCS, no significant changes in TEER values were observed (as shown in Figure 3a). This finding was also reflected in the permeability characteristics, with no significant changes apparent in the P_{app} (Figure 4a). However, this changed dramatically in the absence of HC and FCS (Figure 4b). A significant change in the TEER values was noted between the groups stimulated with IFN- γ ($541 \pm 313 \Omega \cdot \text{cm}^2$, $p < 0.01$) or IFN- γ + TNF- α ($195 \pm 74 \Omega \cdot \text{cm}^2$, $p < 0.001$), as compared to the unstimulated control ($1145 \pm 729 \Omega \cdot \text{cm}^2$). These results suggested that TNF- α and IFN- γ had a synergistic effect on the reduction of TEER, as stimulation with TNF- α alone did not have a significant impact ($669 \pm 570 \Omega \cdot \text{cm}^2$), and IFN- γ stimulation alone mediated a less significant effect. The cytokine cocktail also had the greatest impact on permeability, with

the P_{app} increasing significantly compared to the control group ($1.14 \times 10^{-5} \pm 5.8 \times 10^{-6}$ cm/s for the control group; $1.27 \times 10^{-6} \pm 1.85 \times 10^{-6}$ cm/s for the stimulated group). Stimulation with the cocktail also resulted in a significant increase in the P_{app} , as compared to the groups stimulated with TNF- α and IFN- γ alone (Figure 4b, $p < 0.001$). The TEER values presented in Figure 4 were measured after the transport studies were performed.

Hydrocortisone maintains barrier properties independently of FCS supplementation

From the experiments carried out to investigate the potential synergistic effects of the cytokine cocktail, it was clear that stimulation with combined TNF- α and IFN- γ significantly decreased the integrity of the epithelial barrier in the absence of HC and FCS (Figure 4b). It was also apparent that the presence of HC and FCS during the cytokine exposure ameliorated the detrimental effects on the barrier properties (Figure 4a). The contribution of FCS to the protective effect of this HC/FCS supplementation was investigated by omitting FCS completely from the medium during the cytokine exposure. This was with the overall aim of generating a non-animal product-based model in line with Three Rs principles.

The hAELVi cells were cultured in SAGM without FCS, in the presence or absence of HC (i.e. SAGM +HC/-FCS

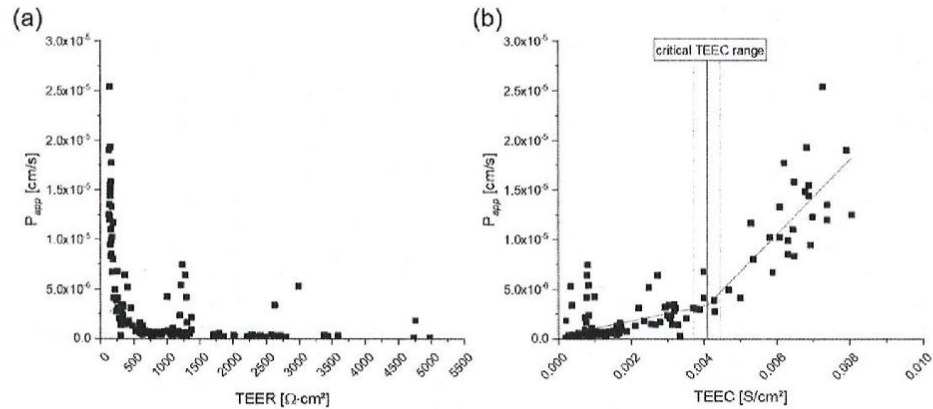


Figure 7. The relationship between electrical resistance and increased permeability of NaFlu to calculate the critical transepithelial electrical conductance (TEEC). (a) All the collected data points were plotted on the graph, regardless of the culture conditions and stimulation parameters. With decreasing TEER values, the P_{app} increases. (b) By taking the reciprocal value of the TEER, the transepithelial electrical conductance (TEEC) value was obtained and plotted against the P_{app} value. A sharp increase in P_{app} was observed after the 'critical TEEC' (marked by the vertical line; vertical dashed lines indicate the standard error). To calculate the exact value of the critical TEEC, a piece-wise linear fitting (PWLF) of the curve was performed (with Origin Pro 2019 software). By using this fitting procedure, the critical TEEC was calculated to be 0.0041 S/cm^2 and the P_{app} to be $3 \times 10^{-6} \text{ cm/s}$. By taking the reciprocal value of the critical TEEC, a TEER of $245 \pm 20 \text{ } \Omega \cdot \text{cm}^2$ was then calculated. When this critical point is exceeded, the permeability rises sharply. Fit parameters: $n = 144$ data points, $R^2 = 0.83$, Origin script: if $(x < x3) \gamma = (\gamma1*(x3 - x) + \gamma3*(x - x1)) / (x3 - x1)$; else $\gamma = (\gamma3*(x2 - x) + \gamma2*(x - x3)) / (x2 - x3)$. NaFlu = sodium fluorescein; TEER = transepithelial electrical resistance; P_{app} = apparent permeability coefficient; TEEC = transepithelial electrical conductivity.

and -HC/-FCS), until a TEER value above $1000 \text{ } \Omega \cdot \text{cm}^2$ was reached (see *Supplementary Figure S8*). The cells were then stimulated with a cytokine cocktail of $25 \text{ ng/ml TNF-}\alpha$ and $30 \text{ ng/ml IFN-}\gamma$ in SAGM +HC/-FCS or SAGM -HC/-FCS, and the TEER was measured after 24 and 48 hours, prior to performing the transport studies. These TEER values, as well as the values obtained before stimulation (0 hours), are presented in Figure 5.

Without HC added, in the absence of FCS, a significant decrease of TEER was observed after 48 hours to $< 300 \text{ } \Omega \cdot \text{cm}^2$, as compared to the control with $849 \pm 196 \text{ } \Omega \cdot \text{cm}^2$ ($p < 0.001$). Interestingly, the presence of HC in the unstimulated control groups resulted in increasing TEER values, from $2927 \pm 295 \text{ } \Omega \cdot \text{cm}^2$ at the 24-hour time-point, to $4701 \pm 196 \text{ } \Omega \cdot \text{cm}^2$ after 48 hours. Cytokine stimulation reduced the TEER significantly, from $4701 \pm 196 \text{ } \Omega \cdot \text{cm}^2$ to $822 \pm 528 \text{ } \Omega \cdot \text{cm}^2$ at this 48-hour time-point ($p < 0.001$), even in the presence of HC. No FCS dependency was identified, but TEER is clearly enhanced by the addition of HC (Figure 5).

In the presence of HC, stimulation with the inflammatory cytokines did not lead to a significant increase in the P_{app} value (Figure 6a, right). In the absence of HC (Figure 6b), the TEER was significantly decreased ($p < 0.001$) following the 48-hour exposure to inflammatory cytokines, when compared with the unstimulated control ($175 \pm 56 \text{ } \Omega \cdot \text{cm}^2$ versus $1048 \pm 294 \text{ } \Omega \cdot \text{cm}^2$, respectively).

The corresponding calculation of the P_{app} (Figure 6b, right) shows that the permeability of cytokine-stimulated hAELVi cells cultured without HC was significantly higher than that of the unstimulated control group ($9.30 \times 10^{-6} \pm 3.89 \times 10^{-6} \text{ cm/s}$ versus $1.08 \times 10^{-6} \pm 1.07 \times 10^{-6} \text{ cm/s}$; $p < 0.001$). The TEER values presented in Figure 6 were measured after the transport studies were performed. Overall, these results suggest that hAELVi cells can mimic *in vitro* the reduction in epithelial barrier integrity induced by lung inflammation. $\text{TNF-}\alpha$ and $\text{IFN-}\gamma$ in combination appeared to reduce barrier properties (TEER) and increase cell permeability (P_{app}). Hydrocortisone acted as expected from clinical findings, in that it functioned as an anti-inflammatory drug and contributed to the maintenance of the barrier function in hAELVi cell *in vitro* cultures. FCS did not seem to influence these findings, and therefore its use could be avoided when using this *in vitro* model.

The relationship between electrical resistance and increased permeability

These studies demonstrated that stimulation with the pro-inflammatory cytokines, $\text{TNF-}\alpha$ and $\text{IFN-}\gamma$, reduced the barrier function of hAELVi cells. Increased paracellular permeability was observed at lower TEER values, in the absence of HC.

In principle, data points in the function of TEER and P_{app} follow a hyperbolic function ($1/x$), and this can be seen in Figure 7a. All of the collected data points were plotted on this graph, regardless of the culture conditions or the stimulation parameters. From this graph, it was clear that with decreasing TEER values the P_{app} increased.

An inverse function leads to a linear relation, and thus the reciprocal of the TEER values were calculated and plotted against the corresponding P_{app} values (see Figure 7b). The TEER is defined as the epithelial resistance (Ω) multiplied by the measurement area (cm^2). The reciprocal of resistance is electrical conductivity — more specifically in this case, it is the transepithelial electrical conductance (TEEC; conductivity (S) per measurement area; S/cm^2). The inverse plot follows a straight line up to a certain point (the ‘critical TEEC’), after which the permeability increases abruptly. This is indicated by the vertical line in the graph in Figure 7b, with the vertical dashed lines indicating the standard error. A sharp increase in P_{app} was observed after this ‘critical TEEC’ point.

To calculate the exact value of the critical TEEC, a piece-wise linear fitting (PWLFF) of the curve was performed. By using this fitting procedure, the critical TEEC was calculated to be $0.0041 \pm 3.63 \times 10^{-4} \text{ S}/\text{cm}^2$ and the P_{app} to be $3 \times 10^{-6} \text{ cm}/\text{s}$. By taking the reciprocal value of the ‘critical TEEC’, it was then possible to calculate a TEER value of $245 \pm 20 \Omega\text{-cm}^2$. Thus, for hAELVi cells, a reduction in TEER to a range lower than $245 \pm 20 \Omega\text{-cm}^2$ will lead to a significantly increased permeability to NaFlu ($p < 0.001$, Figures 4b and 6b).

Discussion

hAELVi cells represent a simple in vitro model for the simulation of inflammation

Major interstitial lung diseases (ILDs), such as idiopathic pulmonary fibrosis (IPF), acute interstitial pneumonia (AIP), or the mostly aetiologically unclear ARDS, illustrate the heterogeneity of the life-threatening consequences initiated by inflammatory irregularities of the lung.^{40,41} ARDS results from bilateral pulmonary infiltrates, hypoxaemia and diffuse alveolar damage.¹⁰ The alveolar epithelium is mainly responsible for the normal lung fluid balance and, thus, for the avoidance of oedema.⁴² As soon as the cells lose their barrier function, this fluid balance is disturbed and liquids can accumulate in the interstitial tissue or directly in the alveoli themselves.^{10,43} To avoid lung oedema, it is essential that the physiological integrity of the epithelial barrier is maintained, and this is mostly mediated by the TJs and interacting proteins.⁴⁴

To develop therapeutic options for the recovery of impaired TJs and barrier function, an appropriate test model is essential. Therefore, in this study, we tried to simulate a state of cell barrier property impairment by

using simple *in vitro* methods. The hAELVi cells used here are particularly suitable for this purpose, since this immortalised cell line demonstrates strong barrier properties expressed by type I pneumocytes with associated stable TEER values, both in liquid–liquid and air–liquid culture conditions. Despite the great potential of hAELVi cells for the development of a stable barrier, the barriers formed by these cells have an increased range of TEER values (from 1000–7000 $\Omega\text{-cm}^2$, see *Supplementary Figures S4–S8*). EDTA was used as control, as a TJ opener, to decrease TEER values to $< 500 \Omega\text{-cm}^2$, leading to P_{app} values of $1 \times 10^{-5} \text{ cm}/\text{s}$.³³ Overall, hAELVi cells can form a tight barrier with corresponding high TEER values and thus they can provide an additional read-out in inflammation studies, as compared to non-barrier forming cell lines, such as A549.³⁵

TNF- α decreases the TEER of hAELVi cells, but does not increase the paracellular permeability of NaFlu

The stimulation of hAELVi cells with the pro-inflammatory cytokine TNF- α was tested first with 50 ng/ml TNF- α in the apical compartment (modelling the cytokine release from tissue macrophages)⁴⁵ and with 17 ng/ml in the basolateral compartment (simulating the systemic inflammation by activated neutrophils and monocytes).⁴⁶ Here, a significant reduction in the TEER was observed, but an effective opening of the TJs, demonstrated by a constant P_{app} value, was not observed. TNF- α alone significantly decreased the TEER by up to $500 \Omega\text{-cm}^2$, as seen in Figures 1a and 3b. Whether the barrier function was subsequently reduced depended heavily on the initial TEER value of the hAELVi cells (Figure 1b *versus* Figure 3b). The higher the initial TEER of the cell barrier before stimulation, the less likely it was to exhibit increased permeability. In this preliminary experiment, we were able to show a significant decrease in TEER after stimulation with TNF- α , but not a significant increase in paracellular permeability. In future experiments, further tracer molecules of different molecular weights could be tested, in addition to NaFlu.^{47,48}

The most appropriate concentration of TNF- α to use in *in vitro* assays is often debated. TNF- α is released from stimulated leucocytes and is a key mediator of inflammation.⁴⁹ Among other pro-inflammatory cytokines (e.g. IFN- γ , IL-1 β , IL-6, IL-8), TNF- α leads to increased epithelial permeability.^{50,51} This effect has been extensively investigated *in vitro* by using the intestinal epithelial cell line Caco-2. A time- and concentration-dependent significant decrease in the TEER of Caco-2 cells arose from TNF- α stimulation from 1 ng/ml to 100 ng/ml and remained stable within this concentration range.^{50,52} Comparing this experimental concentration range to that found in ARDS patients, TNF- α has been detected at 932.6 pg/ml in bronchoalveolar lavage (BAL) samples, seven days after diagnosis.⁵³

Such an increase in cytokine level leads to a reduced barrier function, by downregulating aPKC (atypical protein kinase C), which is mainly responsible for the maintenance of cell polarity through the phosphorylation of the myosin light chains (MLCs).⁵⁴ Consequently, TNF- α induces NF- κ B activation, resulting in the upregulation of myosin light chain kinase (MLCK) expression, causing cytoskeletal contraction and permeable TJs.^{55,56}

While TNF- α stimulation has been reported to increase the permeability of the intestinal epithelium, we did not observe this effect in hAELVi cells (see Figures 1 and 2). The barrier function of human lung epithelial cells (HLECs) in comparison to that of Caco-2 cells is more robust against stimulation with cytokines (such as TNF- α and IFN- γ), with the difference attributed to the mitochondrial energy state during acute inflammation.⁵⁷ This might explain the increased robustness of barrier properties exhibited by hAELVi cells after TNF- α stimulation and explain why an additional inflammatory mediator (IFN- γ) was necessary.

TNF- α and IFN- γ synergistically increase the paracellular permeability of NaFlu

It was not possible to consistently increase the permeability of the hAELVi barrier by using TNF- α alone as a pro-inflammatory mediator. Therefore, further experiments were carried out to assess the synergistic effects of co-stimulation with TNF- α and IFN- γ to decrease the barrier properties of hAELVi cells.

IFN- γ is mainly secreted by lymphocytes and dendritic cells, activating macrophages and triggering increased TJ permeability.⁵⁶ A time- and concentration-dependent decrease in TEER of up to 50% was observed with the intestinal epithelial cell line T84 after stimulation with 1–100 ng/ml IFN- γ ,⁵⁸ which was in line with a similar study involving TNF- α stimulation.⁵⁰ Mice infected with H1N1 have shown an increase in BAL fluid IFN- γ levels of up to 200 pg/ml.⁵⁹ Analysis of serum from severe acute respiratory syndrome (SARS) patients does not indicate an increase in IFN- γ concentration, which suggests that symptoms are not triggered by circulating IFN- γ .⁶⁰ Nevertheless, in *in vitro* experiments with T84 cells, Watson et al. observed impaired barrier function (TEER < 300 Ω ·cm²) after stimulation with 10 ng/ml IFN- γ for 48 hours, but an increased in P_{app} value was only evident at concentrations of 10–100 ng/ml (i.e. 10 ng/ml was at the extreme lower end of the concentration range needed to successfully increase the P_{app}). Therefore, in the present work, a stimulatory concentration of 30 ng/ml IFN- γ was used.⁶¹ IFN- γ inhibits the Wnt signalling pathway to stop proliferation, and can trigger apoptosis, MLC and MLCK phosphorylation, as well as the release of intercellular adhesion molecule-1 (ICAM-1), to instigate rearrangement of actin components and the opening of TJs.⁶² IFN- γ can open TJs

by activating the NF- κ B pathway, which is related to the hypoxia-inducible factor-1 (HIF-1) in T84 intestinal epithelial cells.⁶³

Representing the bronchial epithelium, Calu-3 cells rearrange occludin and ZO-1 proteins in TJs through the epidermal growth factor receptor (EGFR) dependent MAPK/ERK 1/2 pathway, to increase permeability after IFN- γ stimulation. For hAELVi cells, this effect was observed in the reduction of TEER after 48 hours of IFN- γ stimulation (Figure 4), but without a significant increase in permeability (as shown for the Calu-3 cells). As co-stimuli, TNF- α and IFN- γ were shown to induce a significant TEER reduction after a 48-hour stimulation of Calu-3 cells,⁶⁴ similar to the results obtained with hAELVi cell stimulation in the present study (see Figures 3 and 4). The hAELVi cells were co-stimulated with TNF- α and IFN- γ , in order to determine whether these two cytokines would exert any synergistic effects on TJ opening (explained in more detail in the literature).^{17,56,65} The co-stimulation of hAELVi cells in the current study showed a significant increase of permeability after 48 hours (see Figure 4), demonstrating increased susceptibility to the cytokine cocktail than primary bronchial cells.⁶⁶ In addition, Figure 7 demonstrates that hAELVi cells behave as a permeability barrier to NaFlu in a similar manner to the bronchial epithelial cell line 16HBE14o- analysed in Ehrhardt et al.,⁶⁷ particularly with regard to their paracellular activity and the culture method used. The observation that low TEER correlates with high P_{app} values enables the evaluation of the different transport rates of potential new drugs, depending on their molecular weight.⁶⁸

The balance between inflammatory reactions and apoptosis

The activation of NF- κ B signalling protects cells against the initiation of apoptosis after exposure to inflammatory stimuli.⁶⁹ Pro-inflammatory cytokines, such as TNF- α , IFN- γ and IL-1 β , can increase Fas-mediated apoptosis in ARDS patients, and this has been simulated *in vitro* in NHBE cells, resulting in the loss of barrier properties in the alveolar space.^{70,71} In HT29 epithelial cells, pro-inflammatory cytokines cannot individually induce apoptosis, but IFN- γ can increase the susceptibility of TNF- α triggered apoptotic gene expression.^{72,73} Additionally, TNF- α and IFN- γ can upregulate the expression of the TNF-related apoptosis inducing ligand (TRAIL), which induces cell-specific apoptotic pathways by caspase-8 activation. Alternatively, and directly dependent on the incoming stimuli, the NF- κ B pathway can initiate proliferation and survival of intestinal as well as airway epithelial cells.^{74,75}

A change in morphology was observed in hAELVi cells cultured without HC or FCS, as stimulation led to the cells becoming more rounded (see *Supplementary Figures*

S1–S3). To clarify, if these are signs of apoptosis, the consequences of stimulating hAELVi cells with the pro-inflammatory TNF- α and IFN- γ must be examined more closely in further studies, to evaluate the balance between initiating events of the NF- κ B pathway and the activation of potential apoptotic processes. Such studies would involve cell viability measurements (for example, the MTT assay), dUTP nick-end labelling (TUNEL) assay or caspase activity detection.

The cytokine-dependent increase in paracellular permeability of NaFlu in the absence of hydrocortisone is independent of fetal calf serum supplementation

In addition to the effects of pro-inflammatory cytokines discussed so far, the influence of HC and FCS in the stimulation studies was determined. The aim was to determine the optimal culture conditions that would cause an effective reduction in the barrier function of hAELVi cells, in order to simulate inflammation *in vitro*. hAELVi cells are normally cultured with 1% FCS³³ to support proliferation and cell attachment, and to promote strong growth conditions.⁷⁶ By omitting FCS from the culture medium, the new culture conditions contributed to an indirect reduction in animal use, according to the Three Rs principles.⁷⁷ FCS supplementation provided no benefit in terms of increased permeability of the stimulated model (see Figures 4 and 6), and thus the new culture conditions eliminated the need for animal-derived products.

The addition of HC to various cell cultures has been shown to increase cell proliferation and extend the utility of cell lines, especially young cultures.⁷⁸ This is also the case with the routine culture of hAELVi cells. HC is usually used as supplement of Lonza's SAGM. It was shown that HC absence is an immensely important factor in the successful induction of a significant increase in permeability after stimulation, as observed in Figure 5. hAELVi cells are usually kept under cortisone-supplemented conditions during routine cell culture, which is the same as for primary isolated lung cells.³² The cells keep their barrier function for some days in culture, even in the absence of HC, but this absence is necessary for their use as an inflammatory model. The TEER was significantly decreased after TNF- α and IFN- γ stimulation, regardless of the presence or absence of HC, but a significant increase in the P_{app} of stimulated hAELVi cells could only be achieved in the absence of HC (Figure 6b). This effect has also been observed in relation to the TJ properties of endothelial cells, especially in the blood–brain barrier (BBB).⁷⁹ TNF- α stimulation of hCMEC/D3 cells significantly decreased the TEER, which could be limited by the addition of HC.⁷⁹ Permeability also decreased after HC supplementation.⁷⁹ Glucocorticoids, including HC and dexamethasone,

upregulate the expression of TJ proteins of endothelial cells, increasing the stability of the basal lamina as a result of increased levels of integrin α 1, occludin, ZO-1⁸⁰ as well as VE-cadherin.⁸¹ Drasler et al. investigated the anti-inflammatory effect of a reduced secretion of IL-8, after the methylprednisolone treatment of a multicellular human alveolar model consisting of macrophage, dendritic and epithelial cells.²⁵ In June 2020, dexamethasone was reported to reduce by one-third the 28-day mortality of Covid-19 patients with severe disease progression that were undergoing intensive mechanical ventilation.⁸² Future studies should determine whether improved barrier properties in our inflammation model, as characterised by a higher TEER (up to 5000 Ω -cm²; see Figure 5a), could be mediated and stabilised by treatment with corticosteroids such as dexamethasone or methylprednisolone. In our experiments, hAELVi cells that were cultured with HC clearly showed a more stable and robust barrier formation over time than the cells cultured without HC (see Figures 4 and 5, and *Supplementary Figures S4–S8*).

Evaluation of the test system

The TEER can serve as a simple starting point to draw conclusions about the inflammatory response of hAELVi cells. However, the TEER depends on many factors, such as the number of cell layers (e.g. one cell layer or multi-layer), cytotoxic effects and media composition (e.g. the presence of HC).^{83–85} The effects of these external influences on TEER values must therefore be evaluated in further studies. By examining the reciprocal relationship between TEER and TEEC (transepithelial electrical conductance), we were able to calculate a 'critical' TEER range of $245 \pm 20 \Omega$ -cm². Below this range, the cellular barrier of hAELVi cells exhibits increased permeability to NaFlu (see Figure 7). Consequently, assays with hAELVi cells could detect the anti-inflammatory potential of a compound by using the TEER or cell permeability parameters. Particular caution is recommended for compounds that interact with ions (e.g. EDTA) or are cytotoxic, as both cases will lead to a reduced TEER and increased barrier permeability.⁴⁷

The nature of the cell barrier during inflammation should be characterised by using histology, immunofluorescence (ZO-1, occludin) and transmission electron microscopy (TEM), in addition to TEER and P_{app} measurements. Further studies of inflamed hAELVi cells should evaluate whether treatment with different anti-inflammatory drugs, such as other glucocorticoids or anti-inflammatory substances (such as curcumin),⁸⁶ can lead to the regeneration of the inflamed alveolar epithelium. The precise signalling pathways involved in these pro-inflammatory stimuli (NF- κ B *versus* apoptosis) have not yet been investigated in hAELVi cells. To further reproduce lung physiology *in vitro*, coculture with macrophages (e.g. THP-1M or

monocyte-derived macrophages) should be considered. Kletting et al. established a coculture system of hAELVi and THP-1M cells, which can be used as a functional barrier model⁸⁷ and should be tested for its potential to study lung inflammation.

Future testing may include a combination of hAELVi cells with macrophage-based assays. Rather than measuring cytokine release from immune cells by ELISA (or indirectly by PCR), supernatants could be added to hAELVi cells and the presence of inflammatory cytokines evaluated by TEER and/or P_{app} measurements. This approach would reduce the complexity of the methods, as compared to coculture systems, and permit faster screening by simple *in vitro* readouts.

Conclusions

The present study established a simple *in vitro* test system that simulates the impaired barrier function of the alveolar epithelium that occurs during inflammation. These cells produced a stable barrier, which is essential for *in vitro* inflammation studies and anti-inflammatory drug testing strategies. Co-stimulation with IFN- γ and TNF- α in the absence of HC induced a significant increase in the paracellular permeability of NaFlu. In order to optimise and standardise this *in vitro* system, further studies should investigate potential cytotoxic effects, and the minimum effective cytokine and HC concentrations.

Overall, the generation of inflamed hAELVi cells provides a first step in the development of an *in vitro* system to test new therapeutic options for the treatment of ARDS, ALI and other causes of pulmonary inflammation, thus accelerating the discovery of new therapeutics for such conditions while reducing the need for animal experiments.

Acknowledgement

We thank Oya Paugh for her help in proofreading the manuscript.

Declaration of conflicting interests

The author(s) declared the following potential conflicts of interest with respect to the research, authorship, and/or publication of this article: TMR is employed by Ferring Pharmaceuticals A/S; GC was sponsored by Ferring Pharmaceuticals A/S.

Ethical approval

Ethics approval was not required for this research article.

Funding

The author(s) disclosed receipt of the following financial support for the research, authorship, and/or publication of this article: Julia Metz and Marius Hittinger were financially supported by the BMBF project AeroSafe (03IL0128C). Katharina Knoth, Marius Hittinger and Henrik Groß were involved in the ZIM project NanOK. The first experiments were sponsored by Ferring Pharmaceuticals A/S.

Informed consent

Informed consent was not required for this research article.

Supplemental material

Supplemental material for this article is available online.

References

1. Manicone AM. Role of the pulmonary epithelium and inflammatory signals in acute lung injury. *Expert Rev Clin Immunol* 2009; 1: 63–75.
2. Dushianthan A, Grocott MPW, Postle AD, et al. Acute respiratory distress syndrome and acute lung injury. *Postgrad Med J* 2011; 87: 612–622.
3. Hamacher J, Hadizamani Y, Borgmann M, et al. Cytokine-channel interactions in pulmonary inflammation. *Front Immunol* 2008; 8: 1644.
4. Villar J, Sulemanji D and Kacmarek RM. The acute respiratory distress syndrome: Incidence and mortality, has it changed? *Curr Opin Crit Care* 2014; 20: 3–9.
5. Shen C, Wang Z, Zhao F, et al. Treatment of 5 critically ill patients with COVID-19 with convalescent plasma. *JAMA* 2020; 323: 1582–1589.
6. Han S and Mallampalli RK. The acute respiratory distress syndrome: from mechanism to translation. *J Immunol* 2015; 194: 855–860.
7. Aggarwal NR, King LS and D'Alessio FR. Diverse macrophage populations mediate acute lung inflammation and resolution. *Am J Physiol Lung Cell Mol Physiol* 2014; 306: L709–L725.
8. Bhattacharya J and Westphalen K. Macrophage-epithelial interactions in pulmonary alveoli. *Semin Immunopathol* 2016; 38: 461–469.
9. Huang X, Xiu H, Zhang S, et al. The role of macrophages in the pathogenesis of ALI/ARDS. *Mediators Inflamm* 2018; 2018: 1264913.
10. Herrero R, Sanchez G and Lorente JA. New insights into the mechanisms of pulmonary edema in acute lung injury. *Ann Transl Med* 2018; 6: 32–32.
11. Wittekindt OH. Tight junctions in pulmonary epithelia during lung inflammation. *Pflugers Arch Eur J Physiol* 2017; 469: 135–147.
12. Koval M. Tight junctions, but not too tight: fine control of lung permeability by claudins. *Am J Physiol Lung Cell Mol Physiol* 2009; 297: 217–218.
13. Zihni C, Mills C, Matter K, et al. Tight junctions: from simple barriers to multifunctional molecular gates. *Nat Rev Mol Cell Biol* 2016; 17: 564–580.
14. Citi S. The mechanobiology of tight junctions. *Biophys Rev* 2019; 11: 783–793.
15. González-Mariscal L, Tapia R and Chamorro D. Crosstalk of tight junction components with signaling pathways. *Biochim Biophys Acta Biomembr* 2008; 1778: 729–756.

16. Mazzone E and Cuzzocrea S. Role of TNF- α in lung tight junction alteration in mouse model of acute lung inflammation. *Respir Res* 2007; 8: 1–19.
17. Capaldo CT and Nusrat A. Cytokine regulation of tight junctions. *Biochim Biophys Acta* 2010; 1788: 864–871.
18. Youakim A and Ahdieh M. Interferon- γ decreases barrier function in T84 cells by reducing ZO-1 levels and disrupting apical actin. *Am J Physiol Liver Physiol* 2017; 276: G1279–G1288.
19. Proudfoot AG, McAuley DF, Griffiths MJD, et al. Human models of acute lung injury. *Dis Model Mech* 2011; 4: 145–153.
20. Beitler JR, Malhotra A and Thompson TB. Ventilator-induced lung injury. *Clin Chest Med* 2016; 37: 633–646.
21. Matute-Bello G, Frevert CW and Martin TR. Animal models of acute lung injury. *Am J Physiol Cell Mol Physiol* 2008; 295: L379–L399.
22. Gordon S, Daneshian M, Bouwstra J, et al. Non-animal models of epithelial barriers (skin, intestine and lung) in research, industrial applications and regulatory toxicology. *ALTEX* 2015; 32: 327–378.
23. Wang L, Taneja R, Wang W, et al. Human alveolar epithelial cells attenuate pulmonary microvascular endothelial cell permeability under septic conditions. *PLoS One* 2013; 8: e55311.
24. Ren H, Birch NP and Suresh V. An optimised human cell culture model for alveolar epithelial transport. *PLoS One* 2016; 11: 1–22.
25. Drasler B, Karakocak BB, Tankus EB, et al. An inflamed human alveolar model for testing the efficiency of anti-inflammatory drugs in vitro. *Front Bioeng Biotechnol* 2020; 8: 1–21.
26. Castellani S, Di Gioia S, di Toma L, et al. Human cellular models for the investigation of lung inflammation and mucus production in cystic fibrosis. *Anal Cell Pathol* 2018; 15: Article ID 3839803.
27. Junaid A, Mashaghi A, Hankemeier T, et al. An end-user perspective on organ-on-a-chip: assays and usability aspects. *Curr Opin Biomed Eng* 2017; 1: 15–22.
28. Balogh Sivars K, Sivars U, Hornberg E, et al. A 3D human airway model enables prediction of respiratory toxicity of inhaled drugs in vitro. *Toxicol Sci* 2018; 162: 301–308.
29. Neilson L, Mankus C, Thorne D, et al. Development of an in vitro cytotoxicity model for aerosol exposure using 3D reconstructed human airway tissue; application for assessment of e-cigarette aerosol. *Toxicol In Vitro* 2015; 29: 1952–1962.
30. Barosova H, Maione AG, Septiadi D, et al. Use of EpiAlveolar lung model to predict fibrotic potential of multiwalled carbon nanotubes. *ACS Nano* 2020; 14: 3941–3956.
31. Zscheppang K, Berg J, Hedtrich S, et al. Human pulmonary 3D models for translational research. *Biotechnol J* 2018; 13: 1–12.
32. Hittinger M, Mell NA, Huwer H, et al. Autologous co-culture of primary human alveolar macrophages and epithelial cells for investigating aerosol medicines. Part II: evaluation of IL-10-loaded microparticles for the treatment of lung inflammation. *Altern Lab Anim* 2016; 44: 349–360.
33. Kuehn A, Kletting S, De Souza Carvalho-Wodarz C, et al. Human alveolar epithelial cells expressing tight junctions to model the air–blood barrier. *ALTEX* 2016; 33: 251–260.
34. Fisher Scientific. *Permeable supports selection guide*, http://www.corning.com/catalog/cls/documents/selection-guides/Selection_Guide_CLS-CC-027_Permeable_Supports.pdf (2015, accessed 18 November 2020).
35. Srinivasan B, Kolli AR, Esch MB, et al. TEER measurement techniques for in vitro barrier model systems. *J Lab Autom* 2015; 20: 107–126.
36. Elbert KJ, Schäfer UF, Schäfers HJ, et al. Monolayers of human alveolar epithelial cells in primary culture for pulmonary absorption and transport studies. *Pharm Res* 1999; 16: 601–608.
37. Molenda N, Urbanova K, Weiser N, et al. Paracellular transport through healthy and cystic fibrosis bronchial epithelial cell lines — Do we have a proper model? *PLoS One* 2014; 9: e100621.
38. Gaillard PJ and De Boer AG. Relationship between permeability status of the blood–brain barrier and in vitro permeability coefficient of a drug. *Eur J Pharm Sci* 2000; 12: 95–102.
39. Dörfel MJ and Huber O. Modulation of tight junction structure and function by kinases and phosphatases targeting occludin. *J Biomed Biotechnol* 2012; 2012: 303–313.
40. Faverio P, De Giacomo F, Sardella L, et al. Management of acute respiratory failure in interstitial lung diseases: overview and clinical insights. *BMC Pulm Med* 2018; 18: 1–13.
41. Kojicic M, Festic E and Gajic O. Acute respiratory distress syndrome: insights gained from clinical and translational research. *Bosn J Basic Med Sci* 2009; 9: S59–S68.
42. Matthay MA, Folkesson HG and Clerici C. Lung epithelial fluid transport and the resolution of pulmonary edema. *Physiol Rev* 2002; 82: 569–600.
43. Zemans RL and Matthay MA. Bench-to-bedside review: the role of the alveolar epithelium in the resolution of pulmonary edema in acute lung injury. *Crit Care* 2004; 8: 469–477.
44. Ohta H, Chiba S, Ebina M, et al. Altered expression of tight junction molecules in alveolar septa in lung injury and fibrosis. *Am J Physiol Lung Cell Mol Physiol* 2012; 302: 193–205.
45. Herold S, Mayer K and Lohmeyer J. Acute lung injury: how macrophages orchestrate resolution of inflammation and tissue repair. *Front Immunol* 2011; 2: 1–13.
46. Grommes J and Soehnlein O. Contribution of neutrophils to acute lung injury. *Mol Med* 2011; 17: 293–307.
47. Deli MA. Potential use of tight junction modulators to reversibly open membranous barriers and improve drug delivery. *Biochim Biophys Acta Biomembr* 2009; 1788: 892–910.
48. Linnankoski J, Mäkelä J, Palmgren J, et al. Paracellular porosity and pore size of the human intestinal epithelium in tissue and cell culture models. *J Pharm Sci* 2010; 99: 2166–2175.

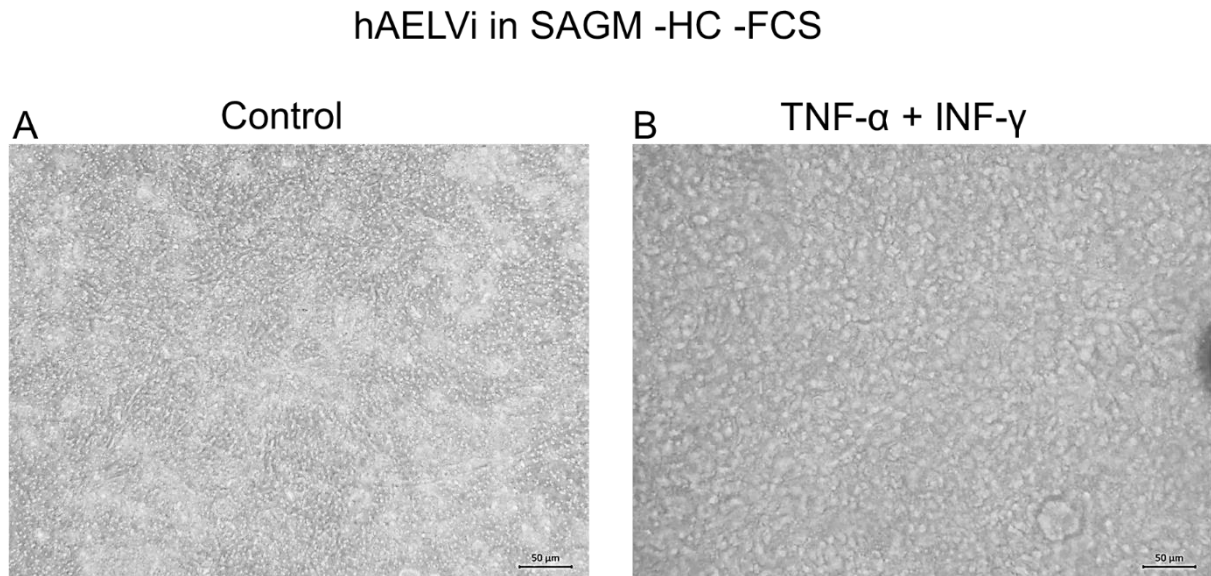
49. Mukhopadhyay S, Hoidal JR and Mukherjee TK. Role of TNF α in pulmonary pathophysiology. *Respir Res* 2006; 7: 1–9.
50. Ma TY, Iwamoto GK, Hoa NT, et al. TNF- α -induced increase in intestinal epithelial tight junction permeability requires NF- κ B activation. *Am J Physiol* 2011; 1: 367–376.
51. Moldoveanu B, Otmishi P, Jani P, et al. Inflammatory mechanisms in the lung. *J Inflamm* 2009; 2: 1–11.
52. Cui W, Li LX, Sun CM, et al. Tumor necrosis factor alpha increases epithelial barrier permeability by disrupting tight junctions in Caco-2 cells. *Braz J Med Biol Res* 2010; 43: 330–337.
53. Park WY, Goodman RB, Steinberg KP, et al. Cytokine balance in the lungs of patients with acute respiratory distress syndrome. *Am J Respir Crit Care Med* 2001; 164: 1896–1903.
54. Mashukova A, Wald FA and Salas PJ. Tumor necrosis factor alpha and inflammation disrupt the polarity complex in intestinal epithelial cells by a posttranslational mechanism. *Mol Cell Biol* 2011; 31: 756–765.
55. Ma TY, Boivin MA, Ye D, et al. Mechanism of TNF- α modulation of Caco-2 intestinal epithelial tight junction barrier: role of myosin light-chain kinase protein expression. *Am J Physiol Gastrointest Liver Physiol* 2005; 288: 422–430.
56. Al-Sadi R, Boivin M and Ma T. Mechanism of cytokine modulation of epithelial tight junction barrier. *Front Biosci* 2009; 14: 2765–2778.
57. Julian MW, Bao S, Knoell DL, et al. Intestinal epithelium is more susceptible to cytopathic injury and altered permeability than the lung epithelium in the context of acute sepsis. *Int J Exp Pathol* 2011; 92: 366–376.
58. Boivin MA, Roy PK, Bradley A, et al. Mechanism of interferon- γ -induced increase in T84 intestinal epithelial tight junction. *J Interf Cytokine Res* 2009; 29: 45–54.
59. Liu B, Bao LL, Wang L, et al. Anti-IFN- γ therapy alleviates acute lung injury induced by severe influenza A (H1N1) pdm09 infection in mice. *J Microbiol Immunol Infect*. Epub ahead of print 12 November 2019, DOI: 10.1016/j.jmii.2019.07.009.
60. Zhang Y, Li J, Zhan Y, et al. Analysis of serum cytokines in patients with severe acute respiratory syndrome. *Infect Immun* 2004; 72: 4410–4415.
61. Watson CJ, Hoare CJ, Garrod DR, et al. Interferon- γ selectively increases epithelial permeability to large molecules by activating different populations of paracellular pores. *J Cell Sci* 2005; 118: 5221–5230.
62. Andrews C, McLean MH and Durum SK. Cytokine tuning of intestinal epithelial function. *Front Immunol* 2018; 9: 1270.
63. Yang S, Yu M, Sun L, et al. Interferon- γ -induced intestinal epithelial barrier dysfunction by NF- κ B/HIF-1 α pathway. *J Interf Cytok Res* 2014; 34: 195–203.
64. Petecchia L, Sabatini F, Usai C, et al. Cytokines induce tight junction disassembly in airway cells via an EGFR-dependent MAPK/ERK1/2-pathway. *Lab Invest* 2012; 92: 1140–1148.
65. Coyne CB, Vanhook MK, Gambling TM, et al. Regulation of airway tight junctions by proinflammatory cytokines. *Mol Biol Cell* 2002; 13: 4100–4109.
66. Pohl C, Hermanns MI, Uboldi C, et al. Barrier functions and paracellular integrity in human cell culture models of the proximal respiratory unit. *Eur J Pharm Biopharm* 2009; 72: 339–349.
67. Ehrhardt C, Kneuer C, Fiegel J, et al. Influence of apical fluid volume on the development of functional intercellular junctions in the human epithelial cell line 16HBE14o-: implications for the use of this cell line as an *in vitro* model for bronchial drug absorption studies. *Cell Tissue Res* 2002; 308: 391–400.
68. Bur M, Huwer H, Lehr CM, et al. Assessment of transport rates of proteins and peptides across primary human alveolar epithelial cell monolayers. *Eur J Pharm Sci* 2006; 28: 196–203.
69. Baichwal VR and Baeuerle PA. Apoptosis: Activate NF- κ B or die? *Curr Biol* 1997; 7: 94–96.
70. Lee KS, Choi YH, Kim YS, et al. Evaluation of bronchoalveolar lavage fluid from ARDS patients with regard to apoptosis. *Respir Med* 2008; 102: 464–469.
71. Nakamura M, Matute-Bello G, Liles WC, et al. Differential response of human lung epithelial cells to Fas-induced apoptosis. *Am J Pathol* 2004; 164: 1949–1958.
72. Ossina NK, Cannas A, Powers VC, et al. Interferon- γ modulates a p53-independent apoptotic pathway and apoptosis-related gene expression. *J Biol Chem* 1997; 272: 16351–16357.
73. Wright K, Kolios G, Westwick J, et al. Cytokine-induced apoptosis in epithelial HT-29 cells is independent of nitric oxide formation. Evidence for an interleukin-13-driven phosphatidylinositol 3-kinase-dependent survival mechanism. *J Biol Chem* 1999; 274: 17193–17201.
74. Begue B, Wajant H, Bambou JC, et al. Implication of TNF-related apoptosis-inducing ligand in inflammatory intestinal epithelial lesions. *Gastroenterol* 2006; 130: 1962–1974.
75. Braithwaite AT, Marriott HM and Lawrie A. Divergent roles for TRAIL in lung diseases. *Front Med* 2018; 5: 1–8.
76. Gstraunthaler G, Lindl T and Van Der Valk J. A plea to reduce or replace fetal bovine serum in cell culture media. *Cytotechnology* 2013; 65: 791–793.
77. Russell WMS and Burch RL. *The principles of humane experimental technique*. London: Methuen, 1959, 238 pp.
78. Rosner BA and Cristofalo VJ. Hydrocortisone: a specific modulator of *in vitro* cell proliferation and aging. *Mech Ageing Dev* 1979; 9: 485–496.
79. Förster C, Burek M, Romero IA, et al. Differential effects of hydrocortisone and TNF α on tight junction proteins in an *in vitro* model of the human blood–brain barrier. *J Physiol* 2008; 586: 1937–1949.
80. Förster C, Kahles T, Kietz S, et al. Dexamethasone induces the expression of metalloproteinase inhibitor TIMP-1 in the murine cerebral vascular endothelial cell line cEND. *J Physiol* 2007; 580: 937–949.

81. Blecharz KG, Drenckhahn D and Förster CY. Glucocorticoids increase VE-cadherin expression and cause cytoskeletal rearrangements in murine brain endothelial cEND cells. *J Cereb Blood Flow Metab* 2008; 28: 1139–1149.
82. The RECOVERY Collaborative Group. Effect of dexamethasone in hospitalized patients with COVID-19: preliminary report. *N Engl J Med* 2020, Published online 17 Jul 2020. DOI: 10.1056/NEJMoa2021436.
83. Shuler L and Hickman JJ. TEER measurement techniques for *in vitro* barrier model systems. *J Lab Autom* 2015; 20: 107–126.
84. Chen S, Einspanier R and Schoen J. Transepithelial electrical resistance (TEER): a functional parameter to monitor the quality of oviduct epithelial cells cultured on filter supports. *Histochem Cell Biol* 2015; 144: 509–515.
85. Kielgast F, Schmidt H, Braubach P, et al. Glucocorticoids regulate tight junction permeability of lung epithelia by modulating claudin 8. *Am J Respir Cell Mol Biol* 2016; 54: 707–717.
86. Patel VJ, Biswas Roy S, Mehta HJ, et al. Alternative and natural therapies for acute lung injury and acute respiratory distress syndrome. *Biomed Res Int* 2018; 2018: 2476824.
87. Kletting S, Barthold S, Repnik U, et al. Co-culture of human alveolar epithelial (hAELVi) and macrophage (THP-1) cell lines. *ALTEX* 2018; 35: 211–222.

Supplementary information

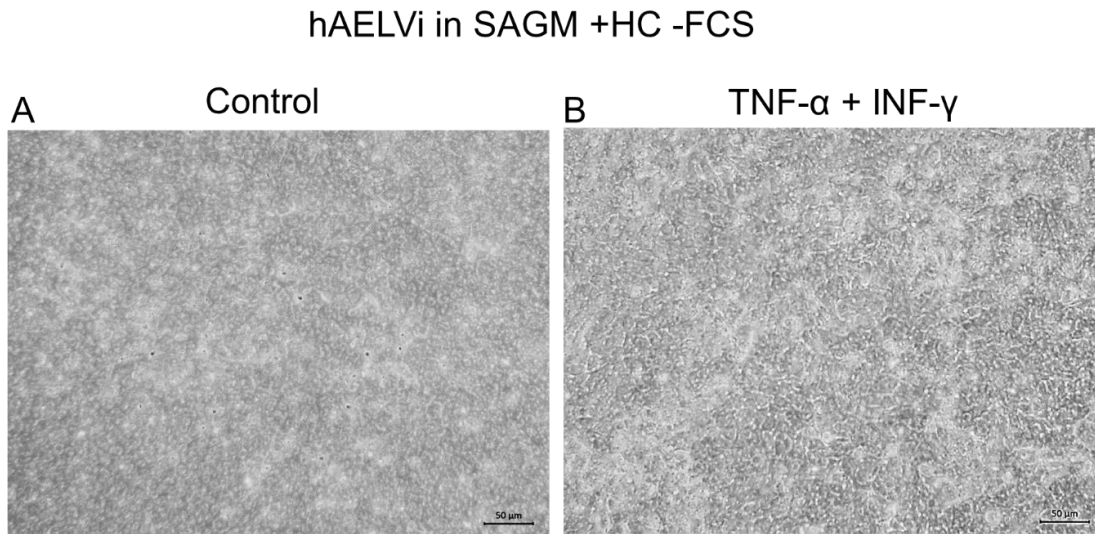
List of abbreviations used: HC = hydrocortisone; FCS = fetal calf serum; TNF- α = tumour necrosis factor-alpha; INF- γ = interferon-gamma; TEER = transepithelial electrical resistance; SAGM = Small Airway Epithelial Cell Growth Medium™

Figure S1. Light microscopy images of hAELVi cells cultured in SAGM without HC or FCS.



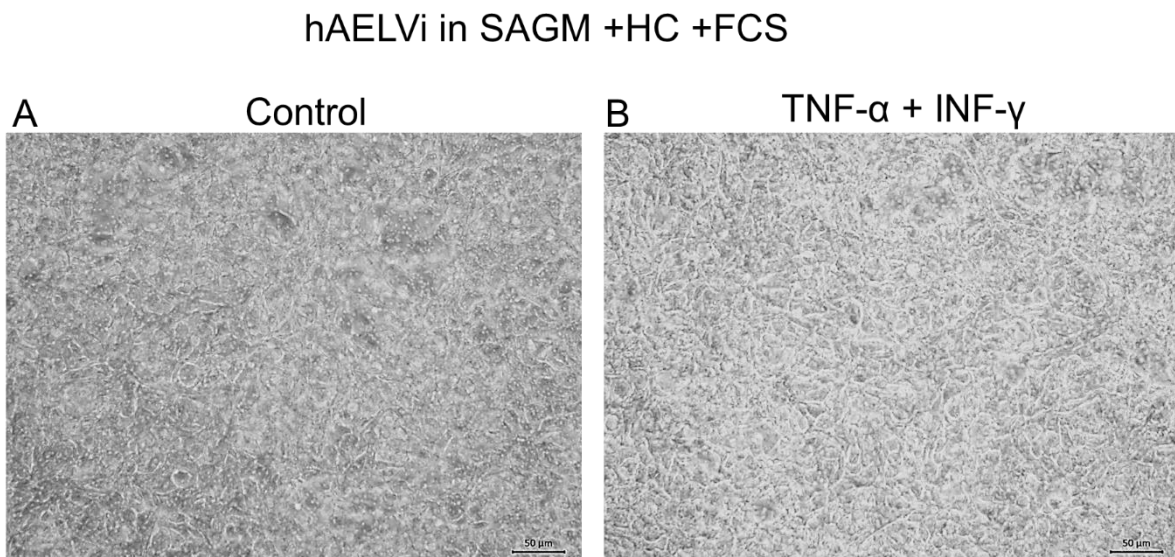
Light microscopy images of: (a) an unstimulated hAELVi cell control, showing regular cell morphology on Transwell inserts; (b) hAELVi cells stimulated with combined 25 ng/ml TNF- α and 30 ng/ml INF- γ , showing a changed morphology in comparison to the unstimulated control (the cells were rounder in shape and showed the first morphological signs of apoptosis). These cells were cultured in the absence of HC and FCS. It should be noted that hAELVi cells cultured +HC/+FCS and +HC/-FCS did not show any morphological anomalies, either before or after cytokine stimulation.

Figure S2. Light microscopy images of hAELVi cells cultured in SAGM with HC and without FCS.



Light microscopy images of: (a) an unstimulated hAELVi cell control, showing regular cell morphology on Transwell inserts; (b) hAELVi cells stimulated with combined 25 ng/ml TNF- α and 30 ng/ml INF- γ , which did not affect the morphology of the cells. These cells were cultured in presence of HC, and the absence of FCS.

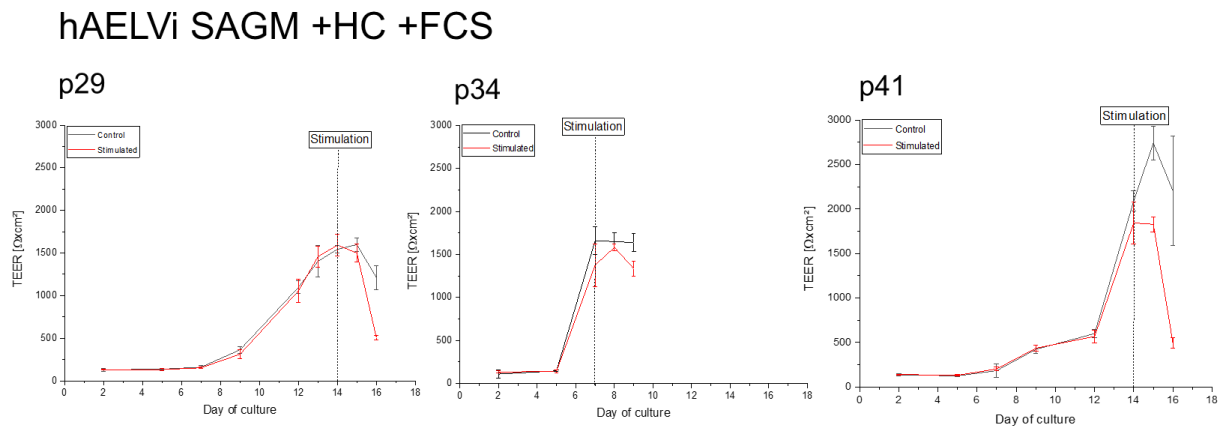
Figure S3. Light microscopy images of hAELVi cells cultured in SAGM with HC and FCS.



Light microscopy images of: (a) an unstimulated hAELVi cell control, showing regular cell morphology on Transwell inserts; (b) hAELVi cells stimulated with combined 25 ng/ml TNF- α and 30 ng/ml INF- γ , which did not affect the morphology of the cells. These cells were cultured in presence of HC and FCS.

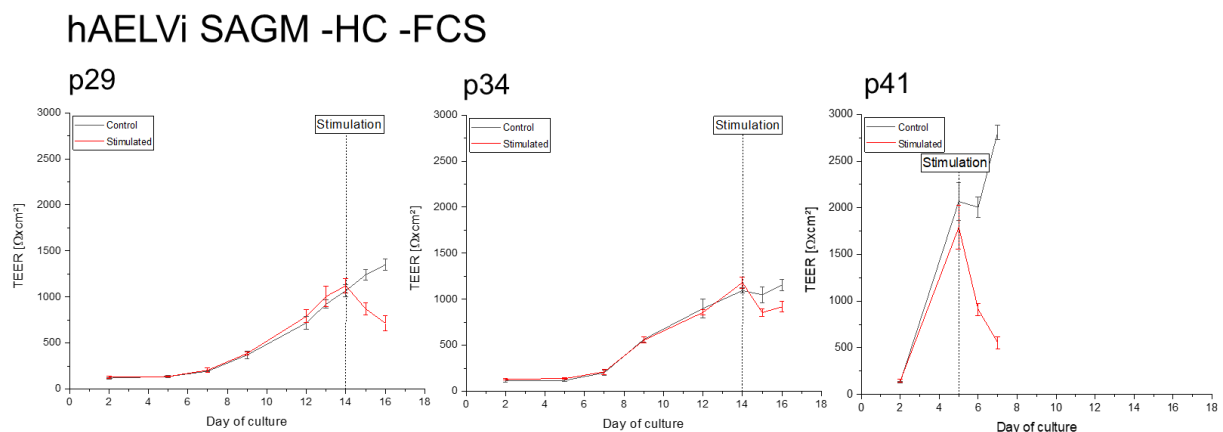
Figures S4–S8 show the TEER of hAELVi cells according to the different passages, and in culture conditions (with and without HC and FCS). When considering the change in TEER values over the hAELVi cell culture period, it becomes obvious that the TEER values reached and the temporal generation of the cell barrier varies significantly, which can be attributed to both the addition of HC and effect of the passage number.

Figure S4. Passage-dependent change in TEER over an extended culture period, for hAELVi cells cultured in SAGM with HC and FCS.



The TEER was measured three times a week followed by a medium change. When a TEER of up to $1000 \Omega\text{-cm}^2$ was reached, the cells were stimulated with $\text{TNF-}\alpha$ (50 ng/ml and 17 ng/ml in the apical and basolateral compartments, respectively). In passage 29 (p29) and passage 41 (p41), stimulation with $\text{TNF-}\alpha$ was performed on day 14; passage 34 (p34) was stimulated on day 7 (indicated by the dotted line). The TEER was measured 24 and 48 hours after stimulation. $n = 6$ wells for the control group and $n = 6$ wells for the stimulation group.

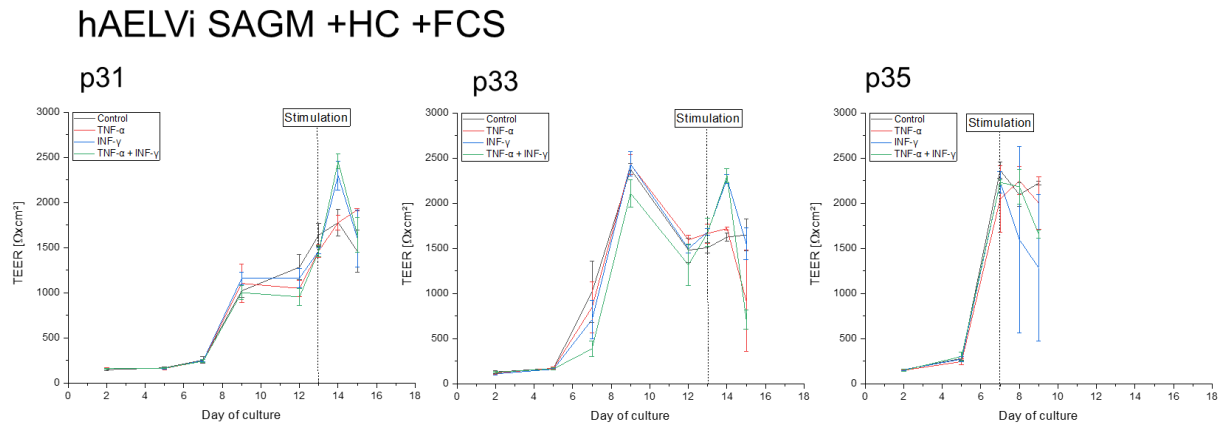
Figure S5: Passage-dependent change in TEER over an extended culture period, for hAELVi cells cultured in SAGM without HC or FCS.



The TEER was measured three times a week followed by a medium change. When a TEER of up to $1000 \Omega\text{-cm}^2$ was reached, the cells were stimulated with $\text{TNF-}\alpha$ (50 ng/ml and 17 ng/ml in the apical and basolateral compartments, respectively). In passage 29 (p29) and passage 34 (p34), stimulation with $\text{TNF-}\alpha$ was performed on day 14; passage 41 (p41) was stimulated on day 5 (indicated by the dotted line). The TEER

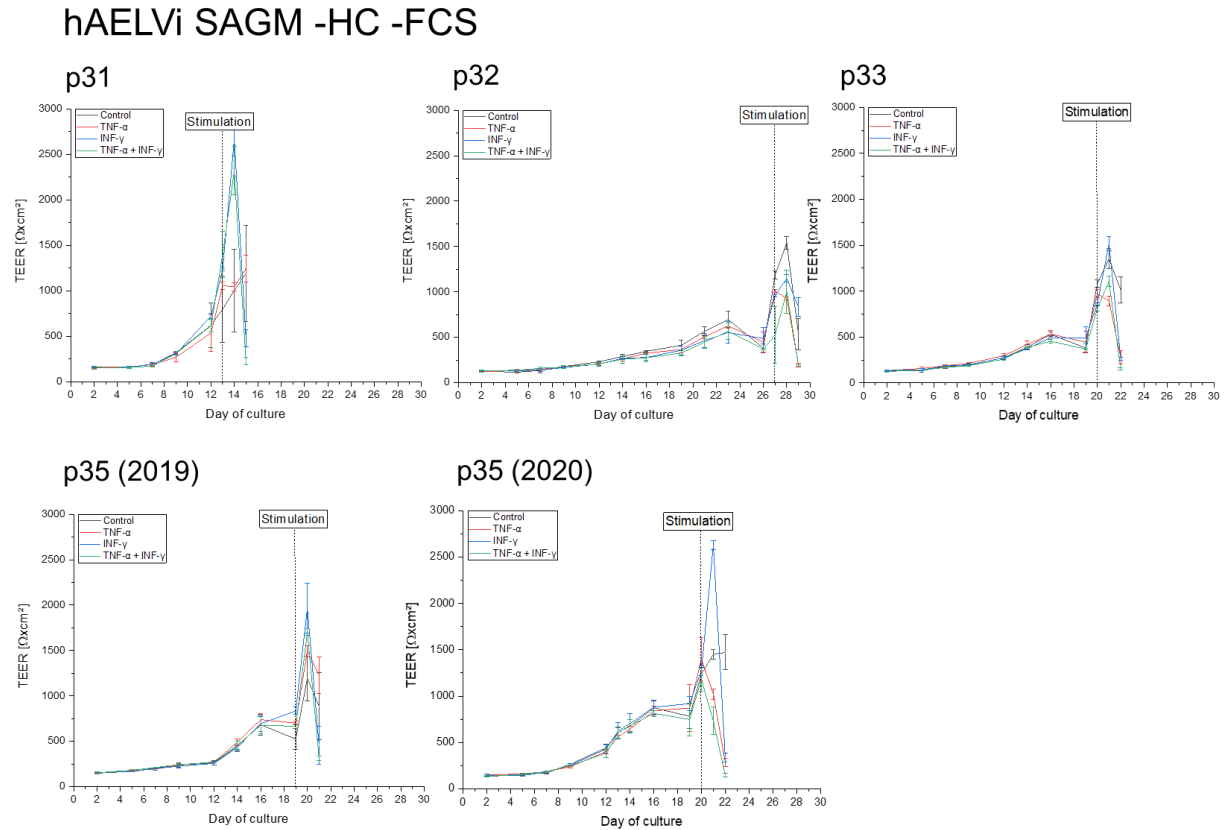
was measured 24 and 48 hours after stimulation. $n = 6$ wells for the control group and $n = 6$ wells for the stimulation group.

Figure S6. Passage-dependent change in TEER over an extended culture period, for hAELVi cells cultured in SAGM with HC and FCS.



The TEER was measured three times a week followed by a medium change. When a TEER of up to $1000 \Omega \cdot \text{cm}^2$ was reached, the cells were stimulated with $25 \text{ ng/ml TNF-}\alpha$ and $30 \text{ ng/ml IFN-}\gamma$. In passage 31 (p31) and passage 33 (p33), stimulation was performed on day 13; passage 35 (p35) was stimulated on day 7 (indicated by the dotted line). The TEER was measured 24 and 48 hours after stimulation. $n = 3$ wells for the control group and $n = 3$ wells for the stimulation group.

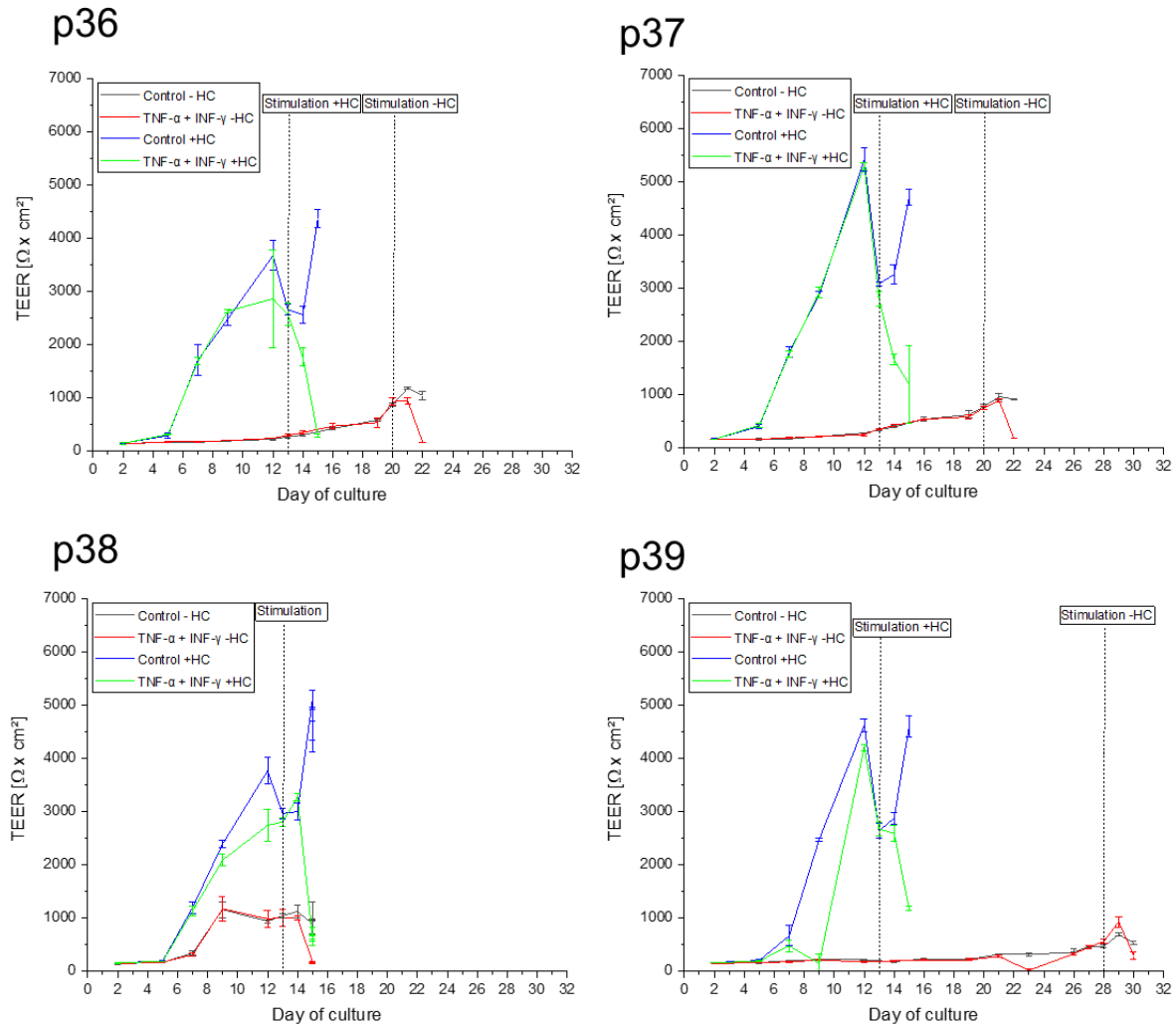
Figure S7. Passage-dependent change in TEER over an extended culture period, for hAELVi cells cultured in SAGM without HC or FCS.



The TEER was measured three times a week followed by a medium change. When a TEER of up to 1000 $\Omega \cdot \text{cm}^2$ was reached, the cells were stimulated with 25 ng/ml TNF- α and 30 ng/ml IFN- γ . The dotted line indicates the day of stimulation. The TEER was measured 24 and 48 hours after stimulation. $n = 3$ wells for the control group and $n = 3$ wells for the stimulation group.

Figure S8. Passage-dependent change in TEER over an extended culture period, for hAELVi cells cultured in SAGM with or without HC, in the absence of FCS.

hAELVi SAGM –HC/+HC -FCS



The TEER was measured three times a week followed by a medium change. When a TEER of up to $1000 \Omega \cdot \text{cm}^2$ was reached, the cells were stimulated with 25 ng/ml TNF- α and 30 ng/ml IFN- γ . The dotted line indicates the day of stimulation. The TEER was measured 24 and 48 hours after stimulation. $n = 3$ wells for the control group and $n = 3$ wells for the stimulation group.

5. Discussion

The work presented in this thesis contributes to the development of an *in vitro* test strategy in order to reduce or to replace animal experiments for a safety assessment of orally inhaled drug products according to the Three Rs principle. It was demonstrated that a more complex experimental structure does not necessarily lead to a better *in vivo* predictability of inflammatory reactions, not least because of missing data for a useful comparison. Consequently, at present, a step-by-step approach, which considers various aspects successively, is the most sensible tactic for the realization of an *in vitro* safety assessment. The protocol for a safety assessment established in this thesis involves a) examining the cytotoxicity categorized by the IC50 value, and b) analysing the effects on inflammatory reactions on the epithelial barrier. Although this is a good starting point for a comprehensive test strategy, many issues which arose during this dissertation, remain to be investigated further to achieve a final regulatory acceptance. These include unanswered questions such as, how can we close the gap to the missing *in vitro* comparability of useful *in vivo* data; how important is the *in vitro* simulation of the complex physiology of the lung and the exposure routes with corresponding deposition mechanisms to reach a better correlation; to what extent do non-cellular barriers play a role; and how can a standardized *in vitro* test strategy be offered in the future, addressing all these issues obtained under 'Good-Laboratory-Practice' (GLP) according to the OECD GIVIMP¹ guidelines. To address these challenges, some relevant aspects are discussed in more detail below.

5.1 Complexity of an *in vitro* system has (still) no influence on an officially accepted alternative method

In the first study, a complex experimental setup was chosen to achieve a physiological pollen deposition on the MucilAirTM system combined with the Dry powder chamber (VPC) of Vitrocell® systems. In addition, the protective and anti-inflammatory effect of an ointment formulation was investigated via the release of IL-8 after bacterial lipopolysaccharides (LPS) stimulation. An increased IL-8 release was obtained after 24 hours LPS simulation mimicking *in vitro* the human inflammation processes after an infection, but no verified *in vitro* - *in vivo* correlation (IVIVC) could be derived from these results. In 2019, Fizeşan *et al.* used a 3D tetraculture with Ea.hy 926, THP-1M, HMC-1 and A549 in combination with the VitrocellTMCloud System to exposed silver particles and nanowires. With this setup, they were able to provide a near complete overview of the particle exposition by analysing the cytotoxicity, RT-PCR of pro-inflammatory and stress response markers, characterisation of the exposed particles, ROS production, and the cytokine and chemokine secretion in comparison to LPS stimulation. They found that

the pro-apoptotic gene CASP7 and the NF κ B pathway were triggered after particle exposition,² which seems to simulate the *in vivo* situation for an inflammatory reaction.³ This very detailed study of Fizeşan *et al.* includes a data set larger than the data set obtained in the pollen exposure study performed in this dissertation, but they still could not provide any further information about a successful implementation of validation, standardization, or IVIVC. A year later, a 3D microfluidic lung-on-a-chip model of the alveolar epithelium (HPAEpiCs) co-cultivated with microvascular endothelium (HPMECs) was able to successfully simulate an increased release of inflammatory cytokines (IL-8, MCP-1, IL-1 β , and TNF- α) after benzopyrene (BaP) exposition as an example of the human exposition to environmental pollution.⁴ Even these results from a more advanced microfluid device do not provide data that leads convincingly in the direction of a valid IVIVC. Overall, a lot of well performed studies leave some open questions due to a lack of an *in vitro in vivo* correlation. Here, the question arises why the development of pulmonary *in vitro* methods simulating the respiratory system is so far advanced but not able to correlate *in vitro* with *in vivo*.

In 2015, Forbes *et al.* summarized several reasons for this still missing IVIVC. The main challenges are the *in vitro* simulation of aerosol deposition, absorption, dissolution, permeation and binding to the surrounding lung tissue and the resulting systemic availability, all of which are prerequisites for determining the effectiveness or toxicity of the inhaled substance.⁵ The *in vivo* analysis of deposited inhaled substance is performed, for example, with single-photon emission computed tomography (SPECT)⁶ or by pharmacokinetic and pharmacodynamic profiles.^{5,7} However, not many *in vitro* studies are published which thematise the pharmacokinetic/dynamic investigations of the deposit substances in the lung. There are some *in silico* methods that combine, for example, computational fluid dynamics (CFD) and physiologically- based pharmacokinetic (PBPK) modelling, show promising success in predictability, but they must still be validated against *in vivo* results.^{8,9} Apart from the pharmacokinetic/dynamic issue, the comparison of the *in vitro* – *in vivo* dosimetry is still in discussion, especially regarding the cytotoxicity of nanomaterials.¹⁰ Addressing this issue, Loret *et al.* used a compatible dose metrics system for the *in vitro* prediction of cytotoxicity of nanomaterials. Figure 1 shows the intersection of the dose metrics which should be used for the interpretation of *in vitro* (ALI, LLI) and *in vivo* (inhalation, instillation) to obtain a high predictability of their results. Nevertheless, Loret *et al.* were not able to establish a model by using the different dose metrics which increases the predictability for every type of *in vitro* deposition. The reasons for this were that data-sets did not provide exact dose intervals and only one type of relatively harmless nanoparticles was tested which reduces the positive estimate.¹¹

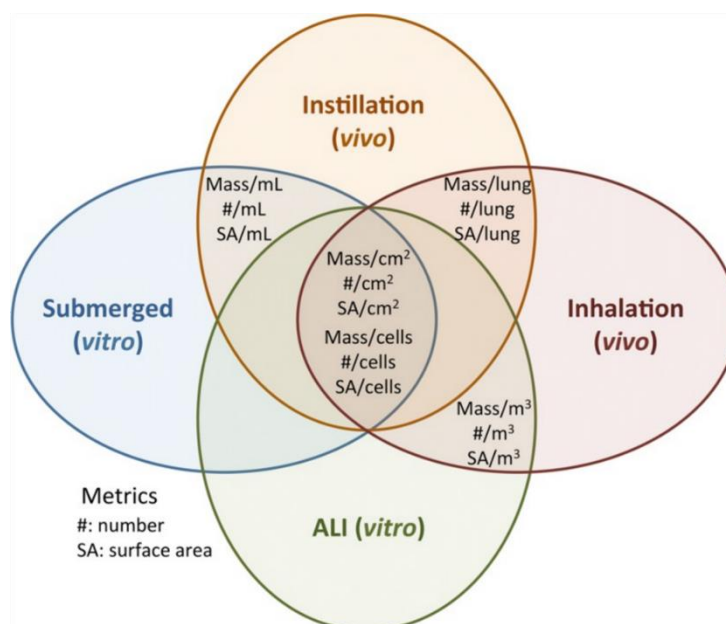


Figure 1: Intersections of dose metrics of the *in vitro* methods (ALI, LLI) and *in vivo* deposition (inhalation and instillation).

In the most cases, the doses of inhaled substance are expressed as mass/volume (mL) for LLI and instillation deposition, for ALI and inhalation mass/air volume (m³). For a better comparison of these different dose metrics, the tissue surface, or the number of the cells (#/cells) and mass doses for the surface area (SA/cells) are the most suitable dose metric, especially for nanoparticles lung deposition. *Adapted from Loret et al 'Predicting the in vivo pulmonary toxicity induced by acute exposure to poorly soluble nanomaterials by using advanced in vitro methods', copyright © 2018, The Author(s)*¹²

The aforementioned explanations demonstrate that even with a more complex experimental setup, such as described in the first study in this dissertation, no evidently improved *in vivo* predictability could be achieved. Therefore, a reduction of the complexity is required in order to continue with simple monolayers in a stepwise approach to evaluate first the cytotoxicity, and second, the inflammation reactions *in vitro*. One approach that specifically addresses a stepwise test strategy during a risk assessment is the framework of adverse outcome pathways (AOPs) connecting key events (KEs) and adverse outcomes (AOs) after a substance exposure which is also supported by the OECD.¹³

5.2 An AOP-based approach is the most reliable way to perform an *in vitro* safety assessment

Taking a closer look at the successful story of alternative methods for skin sensitization, we see that the OECD recommends several guidelines to confirm the incidence of a skin sensitisation potential of substances. The *in vitro/in chemico* guidelines TG 442C (Direct Peptide Reactivity Assay, DPRA) address the covalent binding to proteins as the first key event (KE1) of skin sensitization, followed by the TG 442D investigating the KE2 keratinocyte activation

(ARENrf2 Luciferase test method) and the TG 442E describing the KE3 dendritic cell activation (h-CLAT, U-Sens™, IL-8 Luc assay).^{14–16} This breakdown in different KE under the application of the AOP approach results in a diverse test strategy to rule out all possible consequences of substance exposure. This stepwise approach applied for skin sensitization should be transferred to those AOPs necessary for a respiratory safety assessment. The specific AOPs are illustrated by Clippinger *et al.* as a result from a workshop of the PETA International Science Consortium Ltd., and the U.S. National Toxicology Program (NTP) Interagency Center for the Evaluation of Alternative Toxicological Methods (NICEATM) in 2018. As a result, the main respiratory AOs occurring after substance exposure are listed in the categories target site exposure, molecular initiating key events (MIEs), tissue/organ KEs, and the organism/population KEs (Figure 2).¹⁷

Target Site Exposure	Molecular Initiating Events	Cellular Key Events	Tissue / Organ Key Events	Organism / Population Responses
<ul style="list-style-type: none"> • Solubility • Vapor pressure • Particle size, density, distribution • Mass transfer coefficient • Chemical reactivity • ADME • Breathing mode, rate and volume 	<ul style="list-style-type: none"> • Oxidation of cellular molecules • Acetylcholinesterase inhibition • Cytochrome C oxidase inhibition • DNA/protein alkylation • Modulation of ion channels • Receptor binding e.g., <ul style="list-style-type: none"> • Activation of EGFR • Activation of TRPA1 receptor • Activation of glucocorticoid receptor • Activation/inhibition of G protein coupled receptors • Inhibition of muscarinic acetylcholine receptors • Inhibition of NMDA receptors • Binding to hormone receptor 	<ul style="list-style-type: none"> • ROS formation • Antioxidant (e.g., glutathione) depletion • Inhibition of energy (ATP) production • Cytotoxicity • Collagen deposition • Increased mucous production • Cytoskeleton disruption • Cytokine/chemokine production • Surfactant depletion • Modulation of signal transduction pathways • Inhibition of nucleotide synthesis • Protein modification • Modulation of protein synthesis • Effects on the blood • Vitamin interference 	<ul style="list-style-type: none"> • Cell proliferation • Inflammatory response • Cell transformation • Squamous cell metaplasia • Loss of epithelial barrier function • Reduced ciliary beat frequency • Goblet (mucous) cell hyperplasia, metaplasia, and proliferation • Respiratory failure • Tracheitis • Bronchiolitis • Alveolitis • Pulmonary edema • Bronchoconstriction • Alveolar distention • Smooth muscle remodeling • Change in lung mechanics (resistance, compliance, pressure-volume curves, FEV1) 	<ul style="list-style-type: none"> • Systemic toxicity • Acute lethality • Target organ effects (e.g., hepatotoxicity) • Airway hyperreactivity • Chemical narcosis

Figure 2: List of adverse outcomes (AOs) categorized in the related key events (KE) applying the adverse outcome pathway (AOP) approach after inhalation of materials which an *in vitro* test strategy should be able to simulate.

The target site exposure (TSE) involves, inter alia, the circumstances of ADME properties, the chemical reactivity, and the physicochemical properties of the inhaled material. The molecular initiating event (MIE) is mainly characterised by a potential receptor binding. After the signal enters the cell, different processes were triggered, such as the production of reactive oxygen species (ROS), cytokine release and protein modification. These events impact the overall lung key event resulting mostly in diseases as alveolitis or bronchitis. The organism response leads to systemic toxicity effects and, in the worst case, to acute lethality. *Adapted from Clippinger et al. Pathway-based predictive approaches for non-animal assessment of acute inhalation toxicity, © 2018 The Author(s). Published by Elsevier Ltd.*¹⁷

Part of the discussed AOPs are listed in the database ‘AOP Wiki’ which is hosted by the Society for the Advancement of Adverse Outcome Pathways (SAAOP) under the guidance of the OECD. The wiki includes all categorized AOs related to the specific KE.¹⁸

Applying the OECD advice for implementing the AOP framework in the development of guidelines,¹⁹ Vinken and Blaauboer discussed the cytotoxic effects of a chemical substance exposed to different cell lines *in vitro*. They proposed that the *in vitro* cytotoxicity should be evaluated by testing two assays related to two KEs. One KE is the mitochondrial damage which can be measured by a MTT assays to calculate the IC50 value.²⁰ Following this interpretation, the categorization of various pharmaceutical excipients tested on lung epithelial cells proposed in this dissertation on the basis of the IC50 in the *SAFE* classification can be regarded as the 1st cellular KE in an AOP-based test strategy. To complete this KE of cytotoxicity, plasma membrane damage should be examined as the second KE using a LDH assay.²⁰ The AOP framework can also be used to some extent for the categorization of the 3rd study of this thesis, which deals with the consequences of inflammatory reactions on epithelial cells. According to Villeneuve *et al.* in 2018, the increased release of pro-inflammatory cytokines is one of the three KE in inflammation, next to the activation of tissue resident cells and leukocyte recruitment or activation, whereby the endpoint of the AOP is declared as lung fibrosis or emphysema.²¹ When trying to simulate the consequences of increased cytokine expression the question arises again of how to achieve the required complexity of the *in vitro* system. When studying inflammation process, different cell types, such as Th1/2 cells, macrophages (MDMs, MDCCs) and fibroblasts, are essential to reproduce the complete inflammatory AOP and should therefore be present in the applied test system.^{21,22} In this dissertation, an external stimulation with cytokines on the respiratory epithelial hAELVi cells was performed successfully, which could cover an initial part of the discussed AOP by Villeneuve *et al.* as one AO in the KE of an increased cytokine presence of TNF- α /INF- γ .

The stepwise approach of this dissertation also promotes the AOP framework. However, only two of countless KEs could be discussed partially. Further optimization and coordination are necessary to standardize more complex cell systems, for instance the microfluidic devices, which offer the possibility to cover concurrently several AOs resulting in an extensive and detailed test system for orally inhaled chemicals, particles, and drug products.

References

1. OECD. Guidance Document on Good In Vitro Method Practices (GIVIMP). 2018. doi: 10.1787/9789264304796-en.
2. Fizeşan I, Cambier S, Moschini E, et al. In vitro exposure of a 3D-tetraculture representative for the alveolar barrier at the air-liquid interface to silver particles and nanowires. *Part Fibre Toxicol* 2019; 16: 1–21. doi: 10.1186/s12989-019-0297-1.
3. Dong J, Ma Q. In vivo activation and pro-fibrotic function of NF- κ B in fibroblastic cells during pulmonary inflammation and fibrosis induced by carbon nanotubes. *Front Pharmacol* 2019; 10: 1–10. doi: 10.3389/fphar.2019.01140.
4. Zhang F, Liu W, Zhou S, et al. Investigation of Environmental Pollutant-Induced Lung Inflammation and Injury in a 3D Coculture-Based Microfluidic Pulmonary Alveolus System. *Anal Chem* 2020; 92: 7200–7208. doi: <https://doi.org/10.1021/acs.analchem.0c00759>
5. Forbes B, Bäckman P, Christopher D, et al. In Vitro Testing for Orally Inhaled Products: Developments in Science-Based Regulatory Approaches. *AAPS J* 2015; 17: 837–852. doi: 10.1208/s12248-015-9763-3.
6. Tay ZW, Chandrasekharan P, Zhou XY, et al. In vivo tracking and quantification of inhaled aerosol using magnetic particle imaging towards inhaled therapeutic monitoring. *Theranostics* 2018; 8: 3676–3687. doi: 10.7150/thno.26608
7. Zhou Y-F, Tao M-T, Wei H, et al. In Vivo Pharmacokinetic and Pharmacodynamic Profiles of Antofloxacin against *Klebsiella pneumoniae* in a Neutropenic Murine Lung Infection Model. *Antimicrob Agents Chemother* 2017; 61: 1–10. doi: 10.1128/AAC.02691-16
8. Walenga RL, Babiskin AH, Zhao L. In Silico Methods for Development of Generic Drug–Device Combination Orally Inhaled Drug Products. *CPT Pharmacometrics Syst Pharmacol* 2019; 8: 359–370. doi: 10.1002/psp4.12413
9. Longest WP, Bass K, Dutta R, et al. Use of computational fluid dynamics deposition modeling in respiratory drug delivery. *Expert Opin Drug Deliv* 2019; 16: 7–26. doi: 10.1080/17425247.2019.1551875
10. Schmid O, Cassee FR. On the pivotal role of dose for particle toxicology and risk assessment: exposure is a poor surrogate for delivered dose. *Part Fibre Toxicol* 2017; 14: 52. doi: 10.1186/s12989-017-0233-1
11. Loret T, Peyret E, Dubreuil M, et al. Air-liquid interface exposure to aerosols of poorly soluble nanomaterials induces different biological activation levels compared to exposure to suspensions. *Part Fibre Toxicol*; 13. 2016 Nov 3;13(1):58. doi: 10.1186/s12989-016-0171-3. doi: 10.1186/s12989-016-0171-3
12. Loret T, Rogerieux F, Trouiller B, et al. Predicting the in vivo pulmonary toxicity induced by acute exposure to poorly soluble nanomaterials by using advanced in vitro methods. *Part Fibre Toxicol* 2018; 15: 1–21. doi: 10.1186/s12989-018-0260-6
13. OECD (Organisation for Economic Cooperation and Development). ‘Users’ Handbook supplement to the Guidance Document for developing and assessing Adverse Outcome Pathways”, OECD Series on Adverse Outcome Pathways, No. 1, OECD Publishing, Paris’. *Organ Econ Co-operation Dev Publ*. doi: 10.1787/5jlv1m9d1g32-en
14. OCDE (Organisation for Economic Cooperation and Development). Test Guideline No. 442C In Chemo Skin Sensitisation. 2020. doi: 10.1787/9789264229709-en
15. OECD (Organisation for Economic Cooperation and Development). Test No. 442D: in vitro skin sensitisation assays addressing the AOP key event on keratinocyte activation. 2018. doi: 10.1787/9789264229822-en.
16. OECD (Organisation for Economic Cooperation and Development). Test No. 442E: In Vitro Skin

- Sensitisation: In Vitro Skin Sensitisation assays addressing the Key Event on activation of dendritic cells on the Adverse Outcome Pathway for Skin Sensitisation. 2018.
doi: 10.1787/9789264264359-en
17. Clippinger AJ, Allen D, Behrsing H, et al. Pathway-based predictive approaches for non-animal assessment of acute inhalation toxicity. *Toxicol Vitro* 2018; 52: 131–145.
doi: 10.1016/j.tiv.2018.06.009
 18. Society for the Advancement of Adverse Outcome Pathways (SAAOP). AOP Wiki, https://aopwiki.org/info_pages/3 (2021, accessed 6 February 2021).
 19. Carusi A, Davies MR, De Grandis G, et al. Harvesting the promise of AOPs: An assessment and recommendations. *Sci Total Environ* 2018; 628–629: 1542–1556.
doi: 10.1016/j.scitotenv.2018.02.015
 20. Vinken M, Blaauboer BJ. In vitro testing of basal cytotoxicity: Establishment of an adverse outcome pathway from chemical insult to cell death. *Toxicol Vitro* 2017; 39: 104–110. doi: 10.1016/j.tiv.2016.12.004
 21. Villeneuve DL, Landesmann B, Allavena P, et al. Representing the process of inflammation as key events in adverse outcome pathways. *Toxicol Sci* 2018; 163: 346–352.
doi: 10.1093/toxsci/kfy047
 22. Drasler B, Karakocak BB, Tankus EB, et al. An Inflamed Human Alveolar Model for Testing the Efficiency of Anti-inflammatory Drugs in vitro. *Front Bioeng Biotechnol* 2020; 8: 1–21. doi: 10.3389/fbioe.2020.00987

6 Conclusion and Perspectives

The intention of this dissertation was to develop a test strategy for orally inhaled drug products employing the Three Rs principle. It was shown that more complex exposure systems combined with tissue-based cell systems, which simulate the lung physiology in an enhanced way, can be successfully implemented methodically. Nevertheless, no standardization or meaningful comparison with *in vivo* data could be obtained. For this reason, simpler cell systems were used in the studies conducted for this thesis to deal with separate adverse outcomes such as the cytotoxicity and, respectively, the inflammation effects of an inhaled substance. A successful correlation with human data could be achieved through the *SAFE* classification, which will facilitate an initial *in vitro* assessment of the hazard potential of a substance. Furthermore, a simple test system was developed which enables the identification of potential pro- or anti-inflammatory effects of substances on the epithelial barrier. Despite the successful establishment of separate methods to consider two relevant adverse outcomes, no uniform test strategy could be developed in this dissertation. Many challenges remain to be overcome on the way to an officially approved alternative method:

1. A standardisation of cellular based *in vitro* assays is required for the official acceptance of an *in vitro* test strategy for orally inhaled drugs. According to the OECD GIVIMP guideline, a high-quality management for the development of an alternative method is necessary. Therefore, all methods, apparatus, utilities, chemicals, and data interpretation must be validated and obtained under Good-Laboratory-Practice (GLP) conditions.
2. To ensure the accuracy of the alternative method, an *in vitro-in vivo* correlation (IVIVC) must be performed. Regarding the IVIVC, a number of important issues have not been resolved, e.g., to what data sets can an *in vitro* result correlate with, for example, *in vivo* mouse/rat/dog/human? Where can the developer find these *in vivo* data sets? Here, a more transparent policy of the agencies and the pharma industry is required.
3. To submit an established *in vitro* test strategy to the competent authority, many bureaucratic challenges must be overcome without any financial compensation for the applicant. This is a lengthy and costly process that can only be carried out by a few larger companies. The acceptance criteria for a verification of an *in vitro* test system should be simplified so that research institutes or academic researchers with fewer financial resources can also contribute to the development of alternative methods.

Despite these challenges, the development of alternative methods for the respiratory safety assessment is still being pushed forward, and with the combination of advanced *in vitro* and *in silico* methods, an overall picture of the substance effects can be obtained. A milestone in the next few years will probably be the evaluation and acceptance of the EpiAirway™ as an alternative method by the EURL ECVAM, which offers new opportunities for further developments. It should also be noted that public pressure can also contribute to the development of alternative methods, as it was shown on the example of the animal-free skin testing law. We need to ask ourselves to what extent are we prepared to accept reduced human safety in order to reduce animal experiments. And we must bear in mind that an *in vitro* model remains a model, or, to put it with René Magritte and his 1929 painting *La Trahison des images*:

‘The famous pipe. How people reproached me for it! And yet, could you stuff my pipe? No, it's just a representation, is it not? So if I had written on my picture "This is a pipe", I'd have been lying!´

7 Scientific Output

ARTICLES

Metz, J. K., Knoth, K., Groß, H., Lehr, C. M., Stäbler, C., Bock, U., Hittinger, M. (2018). *Combining MucilAirTM and Vitrocell® powder chamber for the in vitro evaluation of nasal ointments in the context of aerosolized pollen.*

Pharmaceutics, 10(2). DOI: 10.3390/pharmaceutics10020056

Metz, J. K., Scharnowske, L., Hans, F., Schnur, S., Knoth, K., Zimmer, H., Lehr, C. M.; Hittinger, M. (2020). *Safety assessment of excipients (SAFE) for orally inhaled drug products.*

Altex, 37(2), 275–286. DOI: 10.14573/altex.1910231

Metz, J. K.; Wiegand, B.; Schnur, S.; Knoth, K.; Schneider-Daum, N.; Groß, H.; Croston, G.; Reinheimer, T.M.; Lehr, C. M.; Hittinger, M. (2021). *Modulating the Barrier Function of Human Alveolar Epithelial (hAELVi) Cell Monolayers as a Model of Inflammation.*

ATLA, 1, 1-16. DOI: 10.1177/0261192920983015

ORAL PRESENTATIONS

hAELVi cells as an *in vitro* inflammation model

J. K. Metz, M. Hittinger

21st European Congress on Alternatives to Animal Testing (EUSAAT) October 2018, Linz, Austria

Establishment of an *in vitro* test strategy for safety assessment

J. K. Metz, M. Hittinger

AeroSafe Project Meeting, October 2019, Ludwigshafen, BASF, Germany

The potential of inflamed human Alveolar Epithelial Lentivirus immortalized (hAELVi) cells as an *in vitro* test system

J. K. Metz, M. Hittinger

11th annual Advances in Cell and Tissue Culture (ACTC), September 2020, virtual event

POSTER PRESENTATIONS

Cellular and non-cellular barriers influence the efficacy of pulmonary gene delivery- an *in vitro* study

J. K. Metz, G. Gehring, S. Andes, H. Yasar, X. Murgia, B. Loretz, N. Schneider-Daum, H. Groß, C.-M. Lehr, M. Hittinger

Doktorandentag, November 2017, Saarbrücken, Germany

Cellular and non-cellular barriers influence the efficacy of pulmonary gene deliver-an *in vitro* study

J. K. Metz, G. Gehring, S. Andes, H. Yasar, X. Murgia, B. Loretz, N. Schneider-Daum, H. Groß, C.-M. Lehr, M. Hittinger

22nd annual meeting, CRS Germany Local Chapter, March 2018, Halle, Germany

Optimizing physiologically relevant in vitro tests for the development of pulmonary gene delivery systems

J. K. Metz, G. Gehring, S. Andes, H. Yasar, X. Murgia, B. Loretz, N. Schneider-Daum, H. Groß, C.-M. Lehr, M. Hittinger

HIPS Symposium, June 2018, Saarbrücken, Germany

Immortalized human alveolar cells (hAELVi) for testing of antiinflammatory drugs

M. Hittinger, B. Wiegand, J. K. Metz, K. Knoth, R. Hendrix, B. Loretz, N. Schneider-Daum, H. Groß, C.-M. Lehr, T. Reinheimer, G. Croston

12th Conference and Workshop on Biological Barriers, August 2018, Saarbrücken, Germany

From Research to Industry – Drug Delivery at PharmBioTec GmbH

J. K. Metz, K. Knoth, B. Wiegand, S. Schnur, L. Scharnawske, V. Vogel, C.-M. Lehr, H. Groß, M. Hittinger

12th Conference and Workshop on Biological Barriers, August 2018, Saarbrücken, Germany

Specific targeting of human macrophages using aspherical microparticles as gene delivery system

T. Fischer, T. Tschernig, F. Drews, M. Simon, J. K. Metz, M. Schneider

12th Conference and Workshop on Biological Barriers, August 2018, Saarbrücken, Germany

Standardized exposure systems for an in vitro test strategy for orally inhaled drug products

L. Scharnawske, J. K. Metz, A. Buth, P. Carius, N. Schneider-Daum, U. Bock, J. Lichter, B. Blömeke, B. Birk, L. Ma-Hock, R. Landsiedel, N. L. Krutz, H. Groß, C.-M. Lehr, M. Hittinger

HIPS Symposium, June 2019, Saarbrücken, Germany

Safety assessment of compounds -an in chemico/in vitro test strategy for inhalable substances from chemical, consumer goods and pharmaceutical industry

B. Blömeke, U. Bock, J. Lichter, A. Buth, J. K. Metz, M. Hittinger, H. Groß, B. Birk, L. Ma-Hock, N. L. Krutz, C.-M. Lehr, R. Landsiedel

55th Congress of the European Societies of Toxicology, September 2019, Helsinki, Finland

Excipients for orally inhaled drug products - How can cell culture models facilitate drug development and replace animal experiments?

J. K. Metz, L. Scharnawske, F. Hans, K. Knoth, S. Schnur, H. Zimmer, M. Limberger, H. Groß, C.-M. Lehr, M. Hittinger

55th Congress of the European Societies of Toxicology, September 2019, Helsinki, Finland

Competence of cytokine-release in PMA differentiated THP1-cells – comparison of two methods

B. Birk, L. Ma-Hock, A. Verlohner, J. Keller, J. K. Metz, M. Hittinger, W. Wohlleben, B. van Ravenzwaay, R. Landsiedel

5th German Pharm-Tox Summit, 86th Annual Meeting of the German Society for Experimental and Clinical Pharmacology and Toxicology (DGPT), March 2020, Leipzig, Germany

The benefit of more complex in vitro assays for the prediction of safety aspects in drug formulation

J. K. Metz, L. Scharnawske, F. Hans, M. Keppel, C. Ruf, S. Schnur, U. Bock, J. Lichter, B. Blömeke, B. Birk, L. Ma-Hock, R. Landsiedel, K. Knoth, H. Groß, C.-M. Lehr, M. Hittinger

5th German Pharm-Tox Summit, 86th Annual Meeting of the German Society for Experimental and Clinical Pharmacology and Toxicology (DGPT), March 2020, Leipzig, Germany

8 Curriculum Vitae

PERSONAL DATA

Date/Place of birth: 23.11.1989 in Bad Bergzabern
 Citizenship: German

EDUCATION

05/2017 - 12/2020: Doctoral Thesis, Saarland University, Department of Biopharmaceutics and Pharmaceutical Technology, Department of Pharmacy, PharmBioTec Research & Development GmbH, Saarbrücken

Since 10/2019 Continuing education `Expert Toxicologists`, Helmholtz Zentrum München, Institute for molecular toxicology and pharmacology

09/2015 Master of Science, Biotechnology, Saarland University

10/2014 - 06/2015 Master Thesis, University Hospital Freiburg, Department of Exosomes and Tumour Biology

04/2013 - 09/2015 Master's degree in Biotechnology, Saarland University

10/2009 - 02/2013 Bachelor of Sciences, Applied Life Science, Hochschule Kaiserslautern

05/2009 Abitur, Albert-Schweitzer-Gymnasium, Kaiserslautern

INTERNSHIPS AND WORK EXPERIENCE

October 2020 - today Scientist, PharmBioTec Research & Development GmbH, Saarbrücken

Mai 2017 - today PhD student, PharmBioTec Research & Development GmbH, Saarbrücken

07/2016 - 04/2017 Medical Representative, physician and pharmacy related sales force, Biologische Heilmittel Heel GmbH

10/2015 - 06/2016 Medical Representative, physician related sales force, Quintiles Commercial Germany GmbH, Sanofi-Aventis, Deutschland GmbH

08/2011 - 10/2011 Internship, Leibniz- Institute for New Materials, Department for CVD, Bio surfaces, Saarland University

09/2009 - 10/2009 Internship, Institut für Biotechnologie und Wirkstoff Forschung e.V., Kaiserslautern

07/2007 - 08/2007 Internship, Facharbeit, Max-Planck-Institute for Biophysics, Department of Molecular Membrane Biology, MPI, Frankfurt/Main

9 Acknowledgments

In this last section of my dissertation, I would like to thank everyone who has helped and supported me during this time.

A big thank you goes to my 'Doktorvater' Prof. Dr. Claus-Michael Lehr, who improved my work with his scientific contributions and advice and by pointing out new perspectives. I am also incredibly grateful to him that he saw me as a full member of HIPS and that the laboratory doors were always open for me, even during the Corona period. I am sure that I can count on his support and advice even after my doctorate.

A huge thanks to Prof. Marc Schneider, who gave me the opportunity to present my results in his group meetings, for his input, which has always improved my scientific work, and for his understanding, even during hectic times. Thank you for giving me the opportunity to gain experience in internship supervision, for the 'adoption' in your work group, for invitations to the Christmas parties and the honest collaboration.

I am very thankful to the ladies at the office, for always getting everything sorted and organized. Thank you, Karin, Isabelle, and Sarah, for helping the doctoral students in so many ways, e.g., with personal delivery free of charge. You are the best!

I would like to thank the AeroSafe consortium, especially Udo, Jutta, Barbara, and Lan, for the exceptionally good cooperation and support in this project. I would like to thank Ferring Pharmaceuticals and Gleen Croston for their patience and support with the inflammation work, Team Nanok for their helpfulness and scientific input, Vitrocell and Team Bayer Vital GmbH for the incredibly good and reliable cooperation during our joint projects.

I would like to thank the members of HIPS & the BION Group, Nicole, Cristiane, Brigitta, Alberto, Patrick, Sara Nasr, Hanzey, Olga, Rebecca, Benedikt, Robert, Max, Kathrin, Eileen, Chiara, Pascal, Petra and Jana for their scientific support and helpfulness, for their patience with me when I used the laboratory equipment and for their open ears. I have always felt very welcome and will continue to do so in future.

A huge thank you goes to the Schneider working group, especially Marijas, Marcel, Alexandra, Enkeleda, Tamara, Karola, Joschi and Thorben. Thank you for the nice and funny times, for your willingness to help me in the laboratory, for making me part of your team, for the wonderful Christmas parties and the evenings in the Nauwieser Viertel, the Malle party, various PhD seminars and champagne on the terrace. Your friendly welcome gave me the opportunity

to meet Agnes, a great scientist, woman, and friend. Thank you, Agnes, for your encouragement, your unwavering support, and your friendship.

Dear Marius, I do not even know how to start. Thank you for 'picking me up from the street' and for giving me the opportunity to do my PhD in your work group. You not only promoted me scientifically, but also gave me the opportunity to develop personally. I thank you for your patience with me, for your honesty, friendly collaboration, your trust, and your support. Even if we both have completely different views (actually in everything), I enjoy my work and I am happy to work in your team.

I would like to thank the PBT management, Henrik, and Bianca, for their support and trust, thank Alex and Benni for the very good cooperation. I would like to thank the whole PBT team, especially Phillip, who made my daily business easier with his extraordinary willingness to help. Thanks to the analytics girls Saskia, Jacky and Mona for the gossip in the 'Schleuse' and my chemists Christopher, Marius and Ole for their patience and helpfulness, no matter how heavily their own workload was. I thank my former work colleagues, Lorenz and Carsten, for their 'chemical' support and helpfulness. I would like to thank my students, Lara, Fabian, Christopher, Miriam, Simon and Annika for the exceptionally good cooperation and their support.

A huge thank you goes to my 'Dragon-Cave' team, Sabrina, Katharina, and Edda. On some days, the work would have been too hard to bear without my girls. Thank you, Sabrina, for your support in the laboratory, especially with the cell culture and the hAELVis, for your helpfulness and your open ears. Thank you, Katharina for your encouragement, your understanding, your willingness to help, your correction of my paper / work and your friendship. Thank you two, that we have such a good and friendly working relationship. I hope that we can sip champagne together more often in the future.

Throughout the years I was studying and doing my PhD I was always supported by my family and friends. Thanks to Julia Petry for proofreading my work, your open ears, and your female support during all Petry family events. Thank you, Hans for giving us the opportunity to live in your house, for your understanding and your support over the years. Thanks to the Heltersberger / Horbacher clan, Oma, Mimi, Bernhard, Ilka, Michael, Anke, Peter and Lea, Armin, Steffi, Luisa and Niklas, the Bundenthaler family, as well as to my siblings Anna and Lukas, to Tatjana and Andrey for their encouragement, patience, understanding and interest in my work. Thanks to my best friends Sabrina, Jens, Simone and Ziggo, for the good encouragement, understanding and for one or the other great party.

Thanks to mom and dad, who not only supported me financially, but also always believed in me. Thank you for your trust, patience, encouragement, and support throughout the years. This PhD would never have been possible without you.

Finally, I would like to thank my life partner Denis. For his understanding, his unwavering support, his cooking skills, his friendship, and his love.